Wildfires for resilience in California's Sierra Nevada: fine-scale assessment at regional scales with airborne lidar

Caden Philip Chamberlain

A dissertation

submitted in partial fulfillment of the

requirements for the degree of

Doctor of Philosophy

University of Washington

2024

Reading Committee:

Van R. Kane, Chair

L. Monika Moskal

Malcolm P. North

Program Authorized to Offer Degree:

School of Environmental and Forest Science

University of Washington

Abstract

Wildfires for resilience in California's Sierra Nevada: fine-scale assessment at regional scales with airborne lidar

Caden Philip Chamberlain

Chair of the Supervisory Committee:

Van R. Kane

School of Environmental and Forest Sciences

Montane forest ecosystems in western North America hold significant ecological and social value. However, these valued forest ecosystems are at heightened risk in the modern era due to a warming climate and increasingly severe wildfires, droughts, and bark beetle outbreaks. In dry forest types, a history of fire exclusion, removal of Indigenous burning, and extensive logging have drastically altered forest structures and compositions over the past century, making the impacts of climate change and shifting disturbance regimes particularly severe. Fire played a vital ecological role in maintaining the resilience and adaptive capacity of dry forest ecosystems historically. As managers work to conserve dry forest landscapes in the 21st century, it is crucial to understand the contemporary role of wildfires in these ecosystems, and the extent to which wildfires themselves can be utilized as a management tool to increase resilience.

In this dissertation, I leveraged the high-resolution and synoptic coverage of airborne lidar to explore interactions between contemporary wildfires and dry forest ecosystems in California's Sierra Nevada. For chapter one, I developed a geospatial dataset delineating sites where a frequent and low- to moderate-severity fire regime has begun to reestablish in the modern era, then used lidar to compare multi-scale structural patterns between these sites and fire-excluded control sites. I found that contemporary fire-intact dry forest landscapes were characterized by distinct and heterogeneous structural patterns at the neighborhood- (1 ha) and site-level (100-1000 ha) and consistency in these patterns among sites, indicating a strong bottom-up shaping mechanism of contemporary wildfires in dry forests. For chapter two, I analyzed 35 recent wildfires spanning a gradient of biophysical conditions in the Sierra Nevada to (1) quantify the extent to which first-entry burns produced structural patterns that aligned with contemporary reference landscapes and (2) evaluate the environmental drivers of restorative fire effects. I found that moderate-severity patches – occurring primarily in close proximity to recent burns, during periods of moderate fire weather, and at higher elevations – aligned most closely with reference conditions, but that relatively large extents of first-entry burned areas will likely require additional fires or management to fully achieve restoration objectives. For chapter three, I used a bi-temporal airborne lidar dataset to evaluate the resistance of forest structures during fire and drought within a partially-restored active-fire landscape in Yosemite National Park. I found that key structural features (e.g., tall trees and small tree clumps) demonstrated high resistance during drought and wildfire, stressing the importance of reestablishing active-fire conditions to increase dry forest resilience. A key finding emerging from my dissertation is that a frequent and low- to moderate-severity fire regime remains a critical ecological process in dry forest ecosystems in the 21st century which, under moderate fire weather conditions and given strategic multi-scale management, can increase the resilience of these valued forest ecosystems in the face of changing climatic conditions and altered disturbance regimes.

TABLE OF CONTENTS

LIST OF FIGURES

LIST OF TABLES

ACKNOWLEDGMENTS

I would like to thank several people for their support, guidance, and friendship throughout this PhD journey. None of this would have been possible without all of you.

First, thank you Van Kane for your continued, enthusiastic, and genuine support of me and my work over the past five years. I knew we were in for a strong working relationship when our first email exchanges were at 7pm on a Friday night. What I did not know was what an integral piece of my professional career and development you would become. You have always demonstrated a dedication to my professional development – quick to respond, quick to provide feedback, and willing to discuss, at length, the nuances of all things lidar, fire, and forest structure. You have also pushed me step outside of my comfort zone and to take on big ideas and big objectives which have helped me to discover myself both as a researcher and as a person. I look forward to our continued collaborations.

I also thank the rest of my committee members. Malcolm North, you have been key to my success as a researcher and ecologist over the past five years. Your depth of knowledge and experience on forest ecology in the Sierra Nevada is astounding and has helped give practical insight to my research. I sincerely appreciate the many hours you set aside to attend my meetings, thoroughly review my papers and slides, and meet one on one when needed. Monika Moskal, thank you for your leadership and support throughout my time in graduate school. Your perspectives on the bigger picture of research, academia, and career goals have been critical to guiding my ambitions as a scientist. I also thank you for leading me into the world of remote sensing, sparking my own passion for the topic and exemplifying the career of a successful and interesting remote sensing scientist. Brian Harvey, I thank you for your mentorship and guidance over the years. You have helped to shape my thinking as an ecologist and have provided key perspectives on ecological theory, resilience, and landscape ecology that have undoubtedly strengthened my own thinking and research. I am also thankful for the many classes you taught throughout my PhD, especially during the dark days of the pandemic! David Shean, thank you for your commitment to ensuring that this process has been fair and equitable.

I would like to thank several other people who I consider "honorary committee members". First, thank you Alina Cansler for your insights and contributions on all of my projects. You are an exceptional ecologist with a knack for asking intriguing questions while remaining task-oriented. I am lucky that our paths crossed and have learned so much from you over the past five years. Susan Prichard, I am deeply grateful for your mentorship and friendship throughout the years. You offer insightful career advice like no other, and you have always inspired me to conduct rigorous science while focusing on big picture implications. Our journey on the Braiding Sweetgrass project was one of the more eye-opening experiences of my graduate program, and I thank you for inviting me on that journey. Marc Meyer, you have been integral to each chapter of my dissertation, providing critical perspectives on the management applications of my work. I am continuously impressed with your commitment to our collaborations which demonstrates not only your passion for the work but your thoughtfulness as a person.

I would also like to thank Garrett Meigs, Derek Churchill, and Michael Case for your mentorship and friendship throughout grad school. While you were not specifically involved in my dissertation chapters, you were integral to the two "side projects" I completed at UW – Ellsworth Creek and Schneider Springs. Michael, it was great working with you during year one. I learned a great deal from you about westside forests and restoration which guided the subsequent crafting of my dissertation chapters. Garrett Meigs, you have become a key mentor over the past several years. Your passion for applied forest ecology is inspiring and you have taught me the importance of

slowing down and taking time to truly think through the details. Derek Churchill, I also thank you for your guidance over the years. Your perspectives on dry forest ecology have inspired all of my research and I appreciate the levity you bring to site visits.

I would also like to thank Andrew Sanchez Meador, Andi Thode, and the many folks at Northern Arizona University and the Ecological Restoration Institute. Andrew and Andi, you were both foundational to my development as a scientist. Without your encouragement to pursue undergraduate research projects, I would not be where I am today. And a special thank you to Andrew for spending so many hours teaching me how to code.

I would like to thank many members of the Forest Resilience Lab and the Remote Sensing and Geospatial Analysis Lab for your friendship and support. Foremost, thank you Liz van Wagtendonk for being there, as a friend and a mentor, from the beginning. We have navigated parts of grad school together, yes, but your depth of life and research experience has also allowed you to serve as a mentor for me over the years. Thank you for bridging the gap between mentor and friend. I also thank my many other lab mates for walking this journey with me and providing critical moments of humor and debriefing – Bryce Bartl-Geller, Gina Cova, Pratima KC, Astrid Sana, Anthony Stewart, Ray Deininger, Hannah Redford, Deborah Nemens, Iris Mire, Jonathan Kane, Noah Krakoff, Keenan Ganz, and Jonathan Batchelor. I also thank several friends from outside academia who have helped to keep me grounded, and on the rocks, during grad school – Parker Brown, Kyle Thompson, Wes Ward, Megan Hire, Sean Hendrix, Cal Schurman, and Joe Olbrich.

I thank my family for their support and love over the past 32 years. Ten years ago, nobody could've guessed that Caden would be getting a PhD at the University of Washington. But people change, and I thank you all for sticking by my side along the way. Thank you to my mom, Mary Chamberlain, and my dad, Russell Chamberlain, for always being one phone call away during the more stressful hours. You're a reminder of who I am at my core. Thank you to my brother, Connor Chamberlain, Hannah Tosi, and Liz Chamberlain for all of your love and support. And thank you to my grandparents, Nana and Papa, who have been thoroughly enthusiastic about my studies since day one. I am also grateful for the support from the many other Chamberlains and Youngs and the long list of in-laws who have been true believers and supporters along the way.

Finally, and most importantly of all, I thank my wife, partner, and best friend, Kelly O'Neill. I really mean it when I say that none of this would have been possible without you. My strategy of asking you to marry me prior to starting my PhD was a success, obligating you to stick around through the thick of it. I'm also grateful that your training as a counselor coincided with my time as a PhD student – not only are you my wife, but you have been an essential emotional support. You have always believed in me and cared deeply about my endeavors, quick to diminish the imposter syndrome and get me back on track to finishing. You have also been my best friend and climbing partner on our many journeys in the PNW, offering critical contrast to the long days at the desk. I'm proud of our growth together, as people and professionals, and I look forward to our lives ahead.

Last of all, I would like to dedicate this dissertation to our sweet dog, June, who could not make it to defense day. June was literally by my side more than anyone during grad school and her companionship during the first four years was truly integral to my success. We miss you, June.

I would also like to acknowledge several funding sources. I thank the NASA FINESST (#80NSSC21K1588) program for funding three years of my PhD. I thank SEFS and the Nature Conservancy in Washington (#WA-G-200108-011) for funding my first year. I thank the Washington Department of Natural Resources (#93-630 103898), The Nature Conservancy in Oregon (WA-631 G-220211-013), and the Braiding Sweetgrass project for funding portions of my summer RAs. And finally, I thank the Joint Fire Science Program for funding my final two quarters (23-1-01-11).

PUBLISHED MATERIALS

Chapter 1 was published open-access in Elsevier's Forest Ecology and Management and Chapter 2 was published open-access in Springer's Fire Ecology. Data produced as a supplement to Chapter 1 was published with the Forest Service Research Data Archive and through Elsevier's Data in Brief. Data publications are listed here for completeness but are not included as chapters.

Chamberlain CP, Cova GR, Cansler CA, North MP, Meyer MD, Jeronimo SMA, Kane VR. 2023a. Consistently heterogeneous structures observed at multiple spatial scales across fire-intact reference sites. Forest Ecology and Management. 550:121478. doi:10.1016/j.foreco.2023.121478.

Chamberlain CP, Cova GR, Kane VR, Cansler CA, Kane JT, Bartl-Geller BN, van Wagtendonk L, Jeronimo SMA, Stine P, North MP. 2023b. Sierra Nevada contemporary reference site boundaries and corresponding remote sensing-derived canopy structure rasters. Fort Collins, CO: Forest Service Research Data Archive. https://doi.org/10.2737/RDS-2023-0027

Chamberlain CP, Cova GR, Kane VR, Cansler CA, Kane JT, Bartl-Geller BN, van Wagtendonk L, Jeronimo SMA, Stine P, North MP. 2023c. Sierra Nevada reference conditions: a dataset of contemporary reference sites and corresponding remote sensing-derived forest structure metrics for yellow pine and mixed-conifer forests. Data in Brief. 51:109807. doi:10.1016/j.dib.2023.109807.

Chamberlain CP, Bartl-Geller BN, Cansler CA, North MP, Meyer MD, van Wagtendonk L, Redford HE, Kane VR. 2024. When do contemporary wildfires restore forest structures in the Sierra Nevada? Fire Ecology. 20(1):91. doi:10.1186/s42408-024-00324-5.

INTRODUCTION

Forest ecosystems are critical components of the terrestrial biome (Pan et al. 2013; Strassburg et al. 2020). They contribute globally to floral and faunal biodiversity, nutrient cycling, and carbon sequestration (Swingland et al. 2002; Lutz et al. 2018; Watson et al. 2018). In western North America, montane forests regulate snowpack and water levels, provide habitat for many threatened and endangered wildlife species, and represent essential economic and cultural resources in most regions (Franklin et al. 2000; Barnett et al. 2005; Tague and Dugger 2010; Weiskopf et al. 2020). It is within our collective interest as a society to conserve forest ecosystems and the many values they provide (Watson et al. 2018).

Temperatures in the 21st century are increasing at unprecedented rates due to anthropogenic climate change (IPCC 2023). Indirect effects of climate change on biotic and abiotic disturbances pose significant threats to forest ecosystems (Allen et al. 2015; Abatzoglou et al. 2019). For example, the frequency and intensity of wildfires has increased in recent decades due to warmer and drier conditions, lengthened fire seasons, and more extreme fire weather events (Abatzoglou and Williams 2016; Westerling 2016; Parks et al. 2018). A warming climate has also led to more frequent and intense droughts which can weaken tree defenses and catalyze epidemic bark beetle outbreaks (Bentz et al. 2010; Weed et al. 2013; Kolb et al. 2016). While disturbances are critical ecological processes in most forest ecosystems, rapid changes in disturbance frequency and intensity can overwhelm forest adaptions and lead to temporary or permanent forest loss (Fettig et al. 2013; Millar and Stephenson 2015; Johnstone et al. 2016; Coop et al. 2020).

Climate change has impacted most forested regions across western North America in recent decades (Fettig et al. 2013; Weed et al. 2013; Abatzoglou and Williams 2016). However, due to a history of fire-exclusion and logging, these impacts have been particularly severe in dry forest types (Hagmann et al. 2021). Prior to Euro-American colonization in the 1800s and early 1900s, dry

forests were characterized by a frequent (< ~35 year mean fire return interval) and low-severity fire regime, driven by natural ignitions and extensive Indigenous burning (Falk et al. 2011; Taylor et al. 2016; Hagmann et al. 2021). This fire regime served to regulate surface and canopy fuel loads and, through a negative feedback, ensured that subsequent fires and other disturbances had mostly low-severity effects on vegetation (Larson and Churchill 2012; Prichard et al. 2017; Hessburg et al. 2019). These conditions contributed to dry forest's ecological resilience, in which forests historically had the capacity to either resist or recover from subsequent disturbances while maintaining their intrinsic structures, compositions, and functions (Walker et al. 2004; Hessburg et al. 2019; Falk et al. 2022).

Euro-American colonization resulted in an abrupt cessation of the frequent low-severity fire regime that historically characterized dry forest ecosystems and, through subsequent and widespread logging, a concomitant loss of many of the largest and most fire-tolerant trees (Hagmann et al. 2021). Over time, dry forests were characterized by increased surface and canopy fuel loads, lower densities of fire-tolerant trees, and a lack of the critical process of frequent and low-severity fire (Covington and Moore 1994; Knapp et al. 2013; Hagmann et al. 2021). In the modern era, these fire-excluded dry forest landscapes lack resilience to subsequent fires and other disturbances, especially under intensifying climatic conditions (Stevens-Rumann et al. 2018; Coop et al. 2020; Parks and Abatzoglou 2020).

Most dry forest landscapes in western North America are managed by federal agencies. In the face of rapid environmental change, a guiding principle across federal agencies is to improve the ecological resilience and adaptive capacity of dry forest ecosystems (Millar et al. 2007; Bone et al. 2016; Hessburg et al. 2021; North et al. 2022). Restoration thinning and prescribed burning treatments represent reliable techniques for improving dry forest resilience, while also meeting other important objectives related to biodiversity and wildlife habitat (Kalies and Yocom Kent 2016; Stephens et al. 2021; Stephens et al. 2023; Davis et al. 2024). These treatments are used to reduce

canopy and surface fuel loads, restore important structural patterns, reintroduce fire as a key ecological process, and increase landscape-level heterogeneity (Agee and Skinner 2005; Hessburg et al. 2015; Stephens et al. 2021).

Restoration thinning and prescribed burning treatments are essential to modern dry forest management, but implementing these treatments at a pace scale that matches the extent of degraded forests in western North America has proven challenging (Vaillant and Reinhardt 2017; North et al. 2021). With the inevitable occurrence of wildfires in the modern era, other research has begun to explore the effectiveness of wildfires at meeting common restoration objectives (Kane et al. 2019; Huffman et al. 2020; North et al. 2021; Churchill et al. 2022). However, uncertainties remain regarding how contemporary wildfires are affecting dry forest ecosystems and their ecological resilience.

Forests within California's Sierra Nevada provide model ecosystems for studying how climate change and shifting disturbance regimes are impacting forest conditions and resilience. Spanning approximately 5 degrees of latitude and ranging in elevation from 200 to 4400 m, the Sierra Nevada encompasses a diversity of forest types, many of which are emblematic of other forested regions in western North America (North et al. 2016). Forests in the Sierra Nevada regulate snowpack and water runoff for the state of California and support one of top agricultural economies in the world (ACWA 2015). Sierra Nevada forests also provide key habitat for endangered wildlife species and offer extensive economic, recreational, and cultural values for local communities (North et al. 2016). Given the value of this region, it comes as no surprise that the extensiveness of recent wildfire, drought, and bark beetle disturbances have flagged considerable social and ecological concern (Fettig et al. 2019; Safford et al. 2022).

A recent study reported a 6-fold increase in annual area burned by wildfire in California over the past several decades (Williams et al. 2019), marked by distinct increases in the amount and

continuity of high severity effects relative to historical conditions (Stevens et al. 2017; Cova et al. 2023). The 2012-2016 drought, and corresponding beetle outbreaks, also had widespread impacts on forest ecosystems across the region (Fettig et al. 2019; Goulden and Bales 2019). Given these novel conditions, and projected increases in the intensity and frequency of wildfires and droughts in the Sierra Nevada for upcoming decades (Williams et al. 2019), it is essential to understand both the negative and beneficial effects of contemporary disturbances on these valued forest ecosystems.

A particularly unique feature that characterizes the Sierra Nevada is the temporal depth and spatial extent of airborne lidar acquisitions that span the region. Airborne lidar has emerged as a leading tool for characterizing and studying forest ecosystems (Beland et al. 2019; Coops et al. 2021). Most recent acquisitions in the Sierra Nevada offer pulse densities and flight-line overlaps that enable robust three-dimensional mapping of forest structural conditions, providing particularly valuable information on the spatial arrangements and height distributions of mid- and upper-canopy trees (Jeronimo et al. 2018). By enabling tree-level mapping at wall-to-wall spatial extents, airborne lidar offers a synoptic perspective of forest ecosystems that is largely unmatched by spectral remote sensing products and field datasets (Jeronimo et al. 2018; Wiggins et al. 2019). Airborne lidar-based studies provide an important perspective on forest ecosystems that corroborate and build on the decades of field-based ecological studies in the region (Kane et al. 2014; Kane et al. 2015a; Jeronimo et al. 2019; Kane et al. 2019; Steel et al. 2021a). With multiple lidar acquisitions across space and time (i.e., lidar in the Sierra Nevada,) it becomes possible to scale this high-resolution data to characterize forest conditions at high resolutions across broad extents and time periods (Jeronimo et al. 2019).

DISSERTATION OVERVIEW

For my dissertation, I leveraged the capacities of airborne lidar datasets in California's Sierra Nevada, coupled with a variety of other remote sensing and geospatial datasets, to explore interactions between contemporary forest ecosystems and wildfires. While much of the recent ecological research in the region has emphasized the negative impacts of climate change and recent fires (Safford et al. 2022; Steel et al. 2023), I attempted to evaluate and highlight the more beneficial role of fire in dry forest ecosystems. In each of my three dissertation chapters, my intention was to test hypotheses and address objectives that would both expand our ecological understanding of contemporary dry forest processes while also informing ecologically-focused forest and fire management in the Sierra Nevada. While research that develops and improves methods for characterizing forest conditions using airborne lidar is essential to the ongoing utilization of these datasets, my dissertation focused on using *existing* airborne lidar-derived metrics to answer applied ecological questions at unprecedented spatial and temporal scales in the Sierra Nevada. Three overarching questions guided my dissertation research:

- What are the key multi-scale structural characteristics that characterize contemporary fire-intact landscapes and what do these structural patterns suggest about the ecological resilience of these sites in the modern era? (Chapter 1)
- To what extent have recent first-entry wildfires (those burning for the first time since ~1900s) restored structural patterns in the Sierra Nevada and what are the key environmental factors driving restorative fire effects? (Chapter 2)
- How resistant are forest structures to contemporary wildfires, droughts, and bark beetle outbreaks in partially-restored active-fire landscapes? (Chapter 3)

CHAPTER 1: CONSISTENTLY HETEROGENEOUS STRUCTURES OBSERVED AT MULTPLE SPATIAL SCALES ACROSS FIRE-INTACT REFERENCE SITES

For my first chapter, I began by developing a geospatial dataset of contemporary reference sites in California's Sierra Nevada, representing sites where a frequent and low-severity fire regime, similar to the historical fire regime for dry forests, has begun to establish in the modern era (Chamberlain et al. 2023b; 2023c). I then used airborne lidar data to quantify multi-scale structural patterns within and among these contemporary reference sites. Past research has primarily focused on stand-level structural characterizations of contemporary reference sites in the Sierra Nevada (Collins et al. 2011a; Lydersen et al. 2013; Jeronimo et al. 2019; Ng et al. 2020), but has generally lacked detailed characterization of coarser scale structural patterns at the site- and among-site levels, despite the importance of understanding these patterns from an ecological and management perspective (Hessburg et al. 2015; Stephens et al. 2016b; Falk et al. 2019). For this chapter, I leveraged both the fine resolution and broad spatial coverage of airborne lidar to compare multi-scale structural patterns between contemporary reference site and fire-excluded landscapes, revealing fundamental structural patterns produced by a contemporary frequent and low-severity fire regime (Chamberlain et al. 2023a).

CHAPTER 2: WHEN DO CONTEMPORARY WILDFIRES RESTORE FOREST STRUCTURES IN THE SIERRA NEVADA?

While sites in the Sierra Nevada with a recent history of frequent low-severity fire effects are relatively rare (Jeronimo et al. 2019), a recent study from Yosemite National Park showed that *first-entry* wildfires (those burning for the first time since ~1900s) can sometimes have restorative effects on structural conditions (i.e. shifting structural patterns toward those associated with reference conditions) (Kane et al. 2019). For my second chapter, I expanded on this past work by evaluating first-entry fire effects within 35 wildfires that spanned 121,000 ha of dry forests in the Sierra

Nevada. I quantified the extent to which these first-entry wildfires produced structural patterns that aligned with contemporary reference sites, and then identified key environmental conditions that drove restorative fire effects. Structural metrics derived from airborne lidar, and the contemporary reference dataset developed in Chapter 1, enabled a robust analysis of first-entry fire effects across a diversity of biophysical conditions (Chamberlain et al. 2024). This chapter offered key ecological insights about how contemporary first-entry fires are affecting forest structural patterns, while also providing management-relevant information describing the conditions under which recent wildfires were most likely to meet management objectives.

CHAPTER 3: ACTIVE-FIRE LANDSCAPES DEMONSTRATE STRUCTURAL RESISTANCE TO SUBSEQUENT FIRE AND DROUGHT

My first and second chapters hinged on a key assumption – that the structural patterns produced by a partially-restored, frequent, and low-severity fire regime in the modern era would increase the resilience of these sites to subsequent disturbances and climate change. While evidence supporting this assumption has accumulated over recent decades (Ritter et al. 2020; Atchley et al. 2021; Murphy et al. 2021; Steel et al. 2021a; Furniss et al. 2022), we still lack extensive empirical evidence that contemporary active-fire landscapes demonstrate increased resilience under changing climatic conditions and novel disturbance regimes. As such, for my third chapter, I assessed the *resistance* (one component of resilience) of structural patterns within partially-restored active-fire landscapes in Yosemite National Park during a period of high-intensity drought and moderate-intensity wildfire. I used a bi-temporal airborne lidar dataset to track changes in tree densities, spatial patterns, and height distributions through time, and then assessed how structural changes varied across environmental gradients. Analyses from my third chapter provide critical information regarding the resistance of active-fire landscapes in the modern era, which supports ongoing efforts in the Sierra Nevada aimed at reestablishing active-fire conditions to improve dry forest resilience.

CHAPTER 1. CONSISTENTLY HETEROGENEOUS STRUCTURES OBSERVED AT MULTIPLE SPATIAL SCALES ACROSS FIRE-INTACT REFERENCE SITES

Caden P. Chamberlain, Gina R. Cova, C. Alina Cansler, Malcolm North, Marc D. Meyer, Sean M.A. Jeronimo, Van R. Kane

1.1. ABSTRACT

Yellow pine and mixed-conifer (YPMC) forests of California's Sierra Nevada have experienced widespread fire suppression for over a century, resulting in ingrowth and densification of trees, heavy fuel accumulation, and shifts in species composition. Under warmer and drier climates, these forests are primed for stand-replacing fires and severe drought mortality, requiring management interventions to improve their resilience and mitigate future impacts. Observations from functioning frequent-fire systems (e.g., contemporary reference sites) can provide key insights about pattern-process relationships in fire-intact systems, which can be used to inform regional management efforts. In this study, we used airborne lidar data to quantify and compare forest structure at multiple spatial scales between contemporary reference sites (i.e., forests with a restored frequent, low-severity fire regime) and control sites (i.e., typical fire-suppressed forests). We evaluated structures at the neighborhood- (~1 ha), site- (~100-1000 ha), and among-site- (~1000-10000 ha) levels. In reference sites, high proportions of individual trees, small clumps of 2-4 trees, and open space formed mostly open canopy structures at the neighborhood-level, and patches of these neighborhood-level structures were arranged in heterogeneous spatial patterns within sites. We observed low variability in site-level structures *among* reference sites, indicating a stabilizing effect of frequent, low- and moderate-severity fire across broad, ecosystem scales. In fire-suppressed control

sites, edaphic factors and other non-fire disturbances occasionally produced heterogeneity at the neighborhood- and site-level, but the degree of heterogeneity was not consistent across sites. Structural patterns in contemporary reference sites suggest improved resilience to future disturbances and climate change, and increased provisioning of ecosystem services relative to control sites. We suggest applying these metrics to help inform multi-scale and multi-resource management in Sierra Nevada forests.

1.2. INTRODUCTION

For centuries, fire has played a key role in shaping the structure and composition of the yellow pine and mixed-conifer (YPMC) forests of California's Sierra Nevada (North et al. 2016; Safford and Stevens 2017). Prior to Euro-American colonization, lightning ignitions and Indigenous burning practices maintained a frequent (< 20-year fire return interval), low-severity fire regime, supporting mostly low-density forest structures and dominance of large fire-tolerant trees (Stephens et al. 2015; Taylor et al. 2016; Safford and Stevens 2017; North et al. 2022). Historical YPMC forests represented an archetypical example of ecosystem resilience by maintaining a stable range of structure and composition through centuries of repeat fires, climatic variability, and other disturbances (Walker et al. 2004; Hessburg et al. 2019; Ziegler et al. 2021).

Beginning in the late 1700s, Euro-American colonization led to disruption of Indigenous burning, extensive logging and livestock grazing, and widespread fire suppression, over time resulting in increasingly dense and fuel-loaded forests (Knapp et al. 2013; Taylor et al. 2016; Safford and Stevens 2017; Hagmann et al. 2021). With warmer and drier climatic conditions in the 21st century, these contemporary forests are susceptible to uncharacteristically severe wildfires and droughts (Steel et al. 2015; Restaino et al. 2019; Williams et al. 2019), often with enormous

environmental and social consequences (Coop et al. 2020; Safford et al. 2022; Schulze et al. 2020; Meigs et al. 2022).

Management efforts across much of the Sierra Nevada are focused on improving resilience to fire, drought, and climate change, while also protecting or enhancing key ecosystem services like wildlife habitat and biodiversity (North et al. 2009, Stephens et al. 2016a; Safford and Stevens 2017; Stephens et al. 2021a; Forest Management Task Force 2021). Observations of structural patterns from functioning frequent-fire forests are critical to informing management efforts in pursuit of these broad objectives (Keane et al. 2009; Hessburg et al. 2015; Collins et al. 2016; Jeronimo et al. 2019; Wiggins et al. 2019). Such observations offer important insights about pattern-process relationships in fire-intact ecosystems which are essential to the successful design and implementation of resilience-focused and multi-resource management (North et al. 2009; Larson and Churchill 2012; Churchill et al. 2013; Hessburg et al. 2015; Jeronimo et al. 2019).

Historical datasets and reconstruction studies have provided many detailed descriptions of structural conditions in frequent-fire forests prior to Euro-American colonization (e.g., Collins et al. 2011a; Larson and Churchill 2012; Lydersen et al. 2013; Safford and Stevens 2017). While these datasets offer extensive information about finer-scale structures (i.e., neighborhood- to stand-level) they typically lack thorough and quantitative descriptions about coarser-scale structures and spatial patterns (i.e., site- to watershed-level) (Figure 1.1). However, characterizing structural patterns at these coarser-scales is essential, since pattern-process relationships often unfold across multiple, interacting scales and because multi-resource management (i.e., fire resistance at the tree-scale and wildlife habitat across landscapes) is inherently multi-scaled (Stephens et al. 2016b; Falk et al. 2019; Koontz et al. 2020; Falk et al. 2022; Loudermilk et al. 2022).

In recent decades, several sites across the Sierra Nevada have experienced multiple overlapping fires with low- to moderate-severity effects (< 75% tree mortality). These sites – often

termed contemporary reference sites – represent forests where a frequent, low-severity fire regime has begun to reestablish after decades of fire suppression (Collins et al. 2009; Collins et al. 2016; Jeronimo et al. 2019; Pawlikowski et al. 2019; Wiggins et al. 2019; Ng et al. 2020). Contemporary reference sites provide important opportunities to measure and analyze multi-scale structural patterns in 21st century fire-intact systems. These characterizations are especially enhanced where high-fidelity and spatially extensive remote sensing datasets, like airborne lidar, are available (Jeronimo et al. 2019; Wiggins et al. 2019). Contemporary reference sites also have the advantage of representing forests that have developed, at least partially, under modern climate conditions; thus, structural observations from these sites can be used to inform forward-looking, climate-smart management strategies (Lydersen and North 2012; Churchill et al. 2013; Collins et al. 2016; Jeronimo et al. 2019; Wiggins et al. 2019).

Ecological resilience can be defined as the capacity of ecosystems to withstand or recover from common disturbances and climatic variability while maintaining a relatively stable range of structure and composition across relevant time scales (Walker et al. 2004). Some researchers (Westman 1978; Carpenter et al. 2001; DeRose and Long 2014) have suggested that definitions of resilience must specify resilience of what and to what, at appropriate spatial and temporal scales. Therefore, in this study, we define resilience as the ability of YPMC forests to retain their structure, composition, and functional integrity in response to stresses common to this forest type (e.g., fire, drought, and bark beetles) at the ecosystem scale and over the age span of the dominant trees (i.e., 300-400 years).

Indicators of resilience describe the mechanisms that enable forests to either withstand or recover from disturbances (Falk et al. 2022). At the neighborhood-level (Figure 1.1), arrangements of individual trees, small clumps of trees, and open space (an ICO pattern) can indicate increased resilience, as these patterns can reduce fire-induced mortality of dominant trees while also reducing

competition and increasing drought tolerance (Larson and Churchill 2012; Ziegler et al. 2017; Ritter et al. 2020; Ziegler et al. 2021; Atchley et al. 2021). At the within-site-level (Figure 1.1), heterogeneity in forest patch densities can also indicate improved resilience, as variability in forest densities can reduce the likelihood of large high severity burned areas which have the potential to inhibit post-fire seed dispersal and recovery (Hessburg et al. 2019; Coop et al. 2020; Francis et al. 2023). Researchers have also theorized that low-severity and frequent fire regimes historically represented a strong bottom-up control on forest structure across broad spatial scales (e.g., Larson and Churchill 2012; Knapp et al. 2017). Thus, resilience among-sites (Figure 1.1) may best be characterized as a *consistency* in finer-scale heterogeneity, due to the pervasive bottom-up influence of a frequent and low-severity fire regime.

We currently lack a comprehensive analysis of structural patterns across multiple, hierarchical scales in contemporary reference sites of the Sierra Nevada. Past studies have proposed a conceptual model of a nested hierarchical structure in frequent-fire forests prior to Euro-American colonization – where neighborhood-level tree clump and opening patterns scaled up to produce heterogeneous patch arrangements within stands and sites, together supporting resilience across ecosystems (Bonnicksen and Stone, 1980; Larson and Churchill 2012; Reynolds et al. 2013; Collins et al. 2015; Hessburg et al. 2019). Now, with recent and extensive collections of high-fidelity airborne lidar covering large extents of the Sierra Nevada, including many contemporary reference sites, this hierarchical ecosystem structure can be empirically quantified and analyzed. Such structural characterizations will provide essential diagnostics that can be used when managing for resilience and other ecosystem services across the region (North et al. 2009; Churchill et al. 2013; Hessburg et al. 2015; Greiner et al. 2020).

In this study, we analyzed forest structural patterns across contemporary reference sites (hereafter, reference sites) at multiple spatial scales in the Sierra Nevada YPMC zone and compared

these structures against control sites representing fire-suppressed forests. Our comparisons of structures between fire-intact reference sites and fire-suppressed control sites allowed us to identify the effects of frequent-fire while controlling for topographic, climatic, and productivity influences. We used airborne lidar data (hereafter 'ALS') to quantify a scalable set of horizontal forest structure metrics at three spatial scales including (1) neighborhood-level tree clump and opening patterns, (2) within-site patch arrangements, and (3) among-site variability (Figure 1.1). We sought to address two primary objectives in our analyses:

1) Identify and classify the diversity of horizontal forest structures across reference and control sites at the neighborhood-level (~1 ha) and aggregate these measures to quantify site-level (~100-1000 ha) and among-site-level structural patterns (~10,000-100,000 ha).
2) Compare structures between reference and control sites at each spatial scale to discern key structural patterns produced by a contemporary, frequent, and low-severity fire regime.

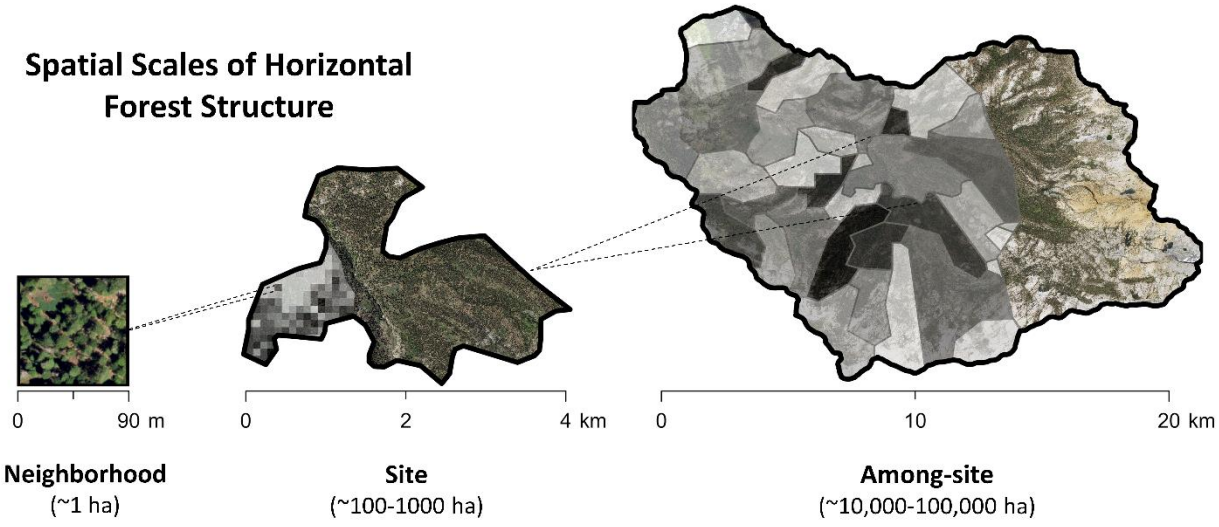

Figure 1.1. Conceptual diagram showing the three nested spatial scales explored in this study including neighborhood-level (~1 ha pixel), site-level (~100-1,000 ha), and among-site-level (~10,000-100,000 ha). True color National Agriculture Imagery Program (NAIP) imagery shown in background for each spatial scale.

1.3. METHODS

1.3.1. STUDY AREA

California's Sierra Nevada is characterized by a Mediterranean climate in which approximately 85% of precipitation falls between November and May and summer months are consistently dry. Interannual fluctuations in climate are largely driven by El Niño-Southern Oscillation (ENSO) patterns causing general shifts from wetter to drier periods every 3-5 years (North et al. 2016). Broad-scale topographic factors result in higher precipitation, cooler temperatures, and more persistent snowpack at higher elevations and latitudes, while fine-scale topography influences variability in plant water availability and solar radiation (North et al. 2016; van Wagtendonk et al. 2018). Soils in the western Sierra Nevada are generally young, acidic, and have relatively deep organic horizons (North et al. 2016; van Wagtendonk et al. 2018).

Yellow pine and mixed-conifer (YPMC) forests cover nearly 3 million ha of the Sierra Nevada ecoregion (EPA 2023), and represent an area of high ecological, social, and economic importance (Safford and Stevens 2017). Major tree species in the YPMC zone include ponderosa pine (*Pinus ponderosa*), Jeffrey pine (*Pinus jeffreyi*), sugar pine (*Pinus lambertiana*), Douglas-fir (*Pseduotsuga menziesii*), white fir (*Abies concolor*), red fir (*Abies magnifica*), incense cedar (*Calocedrus decurrens*), and black oak (*Quercus kelloggii*). We used the FVEG dataset to define the specific boundaries of the YPMC zone. The FVEG dataset provides 'best available' landcover type maps for California for years approximately 1990-2014 (FVEG 2015). We focused our analyses on the FVEG Wildlife Habitat Relationship (WHR) classes including Montane Hardwood-Conifer, Ponderosa Pine, Jeffrey Pine, Douglas Fir, and Sierran Mixed Conifer, which generally align with YPMC forest types described in Safford and Stevens (2017).

Prior to Euro-American colonization beginning in the 1700s, YPMC forests were characterized by a frequent, low-severity fire regime driven by natural lightning ignitions and

Indigenous burning (Anderson and Moratto 1996; Safford and Stevens 2017). The historical mean fire return interval was 11-16 years with most fire resulting in low- and moderate-severity effects and only about 8-15% high-severity effects (Safford and Stevens 2017). Across broad temporal scales (i.e., millennia), droughts historically occurred every 80 to 260 years with most droughts lasting 20 to 100 years (Safford and Stevens 2017). Major droughts led to increased moisture stress on trees which subsequently led to periodic and isolated bark beetle outbreaks and tree mortality (North et al. 2016; Safford and Stevens 2017).

Sierra Nevada forests are managed by a variety of private landowners and local, state, and federal agencies. Most forests fall under the jurisdiction of the United States Forest Service (FS) where, outside of wilderness areas, they are managed for multiple resources including timber, wildlife, water protection, and recreation (North et al. 2009). A considerable proportion of the Sierra Nevada is also managed by the National Park Service (NPS) where management is centered on preservation and recreation (Allen et al. 2019; Wood and Jones 2019). Current NPS and FS wilderness policies and federal fire management policy guidance permit lightning-ignited fires to be managed for resource objectives as specified in land or resource management plans, yet most ignitions are still typically suppressed (van Wagtendonk 2007; Massip 2020; Young et al. 2020).

1.3.2. REFERENCE AND CONTROL SITES

Across the Sierra Nevada YPMC zone, we sought to compare forest structural patterns at multiple scales between reference sites (i.e., sites with repeat low/moderate-severity fire effects) and control sites (i.e., fire-suppressed forests with no recent fire activity). We followed an approach initially developed by Jeronimo et al. (2019) to identify a set of reference sites for our study. Here we provide a summary of this approach, with additional detail provided in a supplemental Data in Brief publication (Chamberlain et al. 2023c). The general approach for identifying reference and control

sites involved (1) scoring rasters across our study area based on the degree to which each 30 m pixel represented either a restored fire regime (for reference sites) or fire-suppressed forests (for control sites), and (2) defining site polygons around clusters of high scoring pixels using the national catchment dataset (EPA 2021) along with fire perimeters, burn severity layers, and ESRI imagery.

DATASETS

We used fire history datasets to identify areas with a restored frequent, low-severity fire regime (reference sites) or areas with no recent fire history (control sites). We used CALFIRE's Fire Resource and Protection Program (FRAP) fire history dataset to map all fires occurring in the YPMC zone from 1957 to 2020 (FRAP 2021; Cova et al. 2023). Records for all fires > 4 ha including prescribed burns were included. We used the Parks et al. (2019) Google Earth Engine script to quantify and map predicted Composite Burn Index (CBI) burn severity for all fires intersecting our study area (see detailed methods in Cova et al. 2023). Thresholds recommended by Miller and Thode (2007) were used to classify continuous CBI rasters into categories of unburned-, low-, moderate-, and high-severity. Prior to 1985, Landsat data was not available for modeling burn severity. Thus, for all pre-1985 fires in our dataset that intersected potential reference sites, we visually examined imagery and a lidar-derived canopy height layer (more detail below) for evidence of past stand-replacing fire and excluded all expected high-severity burn areas from our analyses.

We mapped management history to ensure that neither reference nor control sites had been impacted by treatments or harvest in recent decades. We used (1) a dataset developed by Knight et al. (2022) for years 1985-2020 and (2) the Forest Service FACTS database for years prior to 1985 (USDA 2021). The Knight et al. (2022) dataset provides a compiled and organized record of treatment history across private, state, and federal lands for years 1985-2020. Tables provided in the Knight et al. (2022) supplemental materials (Tables S4-S8) were used to classify and discard records representing administrative, monitoring, and prescribed burning tasks. For years prior to 1985, we

relied solely on the USDA Forest Service FACTS dataset to track treatment history on federal lands and used the same tables from Knight et al. (2022) supplemental materials to classify and discard administrative-, monitoring-, and fire-related treatments.

We used the FVEG forest type dataset to ensure both reference and control sites represented primarily YPMC forests. The Landscape Change Monitoring (LCMS) dataset was used to identify and exclude areas impacted by non-fire disturbances in our control sites (Housman et al. 2022). Lastly, the national catchment dataset (EPA 2021) and ESRI imagery (ESRI 2021) were used to delineate individual site boundaries (more detail provided below).

IDENTIFYING REFERENCE AND CONTROL SITES

We followed methods initially presented in Jeronimo et al. (2019) to identify reference sites for our analyses. We implemented a raster scoring approach in which each 30 m pixel in a representative raster across our study area was scored based on the degree to which it represented a restored, low-severity, and frequent fire regime in the YPMC zone. Specifically, each pixel was given a point for (1) at least 2 fires in the last 60 years, (2) at least one fire in the last 30 years, (3) at least one fire with moderate-severity effects, (4) no high-severity effects, (5) no record of late 20th or early 21st century timber management, and (6) representing one of the desired FVEG YPMC forest types (defined in Section 1.1.). Specific site boundaries were then defined using the national catchment dataset (EPA 2021). We selected all catchments that were dominated by 'score 6' cells and were > 100 ha in size. We then made minor manual adjustments to selected catchment boundaries using fire perimeters, burn severity rasters, and ESRI imagery to ensure that our sites represented primarily forested areas and excluded roads, infrastructure, and major rock outcrops. Detailed methods are provided in the supplemental Data in Brief manuscript (Chamberlain et al. 2023c). We identified 119 reference sites and described and quantified their characteristics in the aforementioned paper.

For this study, we reduced and focused the reference site datasets to sites where ALS data was collected at least 5 years following the most recent fire (see details on ALS data in Section 2.1.). This selection criterion was applied to improve quantification of *live* forest structure metrics (as recent drought and extensive wildfires have driven widespread tree mortality across the region (Steel et al. 2023)) and ensure more reliable comparisons of structural patterns between reference and control sites. Five years was selected based on rates of post-fire mortality identified by van Mantgem et al. (2011) and Jeronimo et al. (2020). We acknowledge that this criterion did not guarantee removal of all snags prior to quantifying forest structure metrics; instead, it minimized the impact of snags while maintaining a large sample of sites upon which we could draw ecological inferences. Nevertheless, we acknowledge that trees that died and/or snags that remained standing > 5 years post-fire had some influence on ALS metrics.

To identify a set of control sites representing typical fire-suppressed forests, we applied a raster scoring approach similar to that used to identify reference sites. Specifically, each 30 m pixel across our study area was given a point for each of the following true statements: (1) no fire history, (2) no record of late 20th or early 21st century timber management, and (3) no "Fast Change" detected by the LCMS dataset (Housman et al. 2022). The LCMS criterion was applied to ensure that control sites had not been heavily affected by other sudden non-fire disturbances in recent decades (Housman et al. 2022). Then, using the same method for defining reference sites, we selected all catchment polygons (EPA 2021) with majority 'score 3' pixels that were > 100 ha, then used fire perimeters, burn severity layers, and ESRI imagery to make minor adjustments to polygons to ensure control sites represented forested areas and excluded roads, infrastructure, and major rock outcrops.

The reference and control site datasets were further filtered to ensure that observed differences in forest structure between the site types were indeed the result of fire and fire-

suppression, respectively, rather than differences in climate, topography, or forest age. Specifically, we compared distributions of climatic water deficit (CWD) (Flint et al. 2021), topographic position index (TPI), and ALS-derived canopy height (a proxy for stand age, more detail provided below) between the site types. We first observed the distributions of CWD, TPI, and canopy height between the reference and control sites and removed sites from our analyses that clearly represented outlier climate, topographic, or stand age conditions (e.g., mean canopy height < 20 m). Then, we used Wilcoxon Rank Sum (WRS) and Kolmogorov-Smirnov (KS) tests to confirm no significant differences ($\alpha > 0.05$) in the median or distribution, respectively, of mean site-level CWD, TPI, or canopy height between the reference and control sites (Figure 1.2) (Gotelli and Ellison 2018). Scatter plots showing the distributions of reference and control sites across CWD, TPI, and canopy height are also provided in Appendix Figure 1.A.1. After applying these filters, we had a final set of 42 reference sites and 42 control sites. Final reference and control site metrics are provided in Table 1.1. The lack of reference and control sites in the southern Sierra is primarily due to the lack of ALS datasets that met the 5-year post-fire criterion. To facilitate replicability of our analyses, reference sites are publicly available on the Forest Service Research Data Archive (Chamberlain et al. 2023b), and control site boundaries are available on the Zenodo Digital Repository (https://doi.org/10.5281/zenodo.8401035).

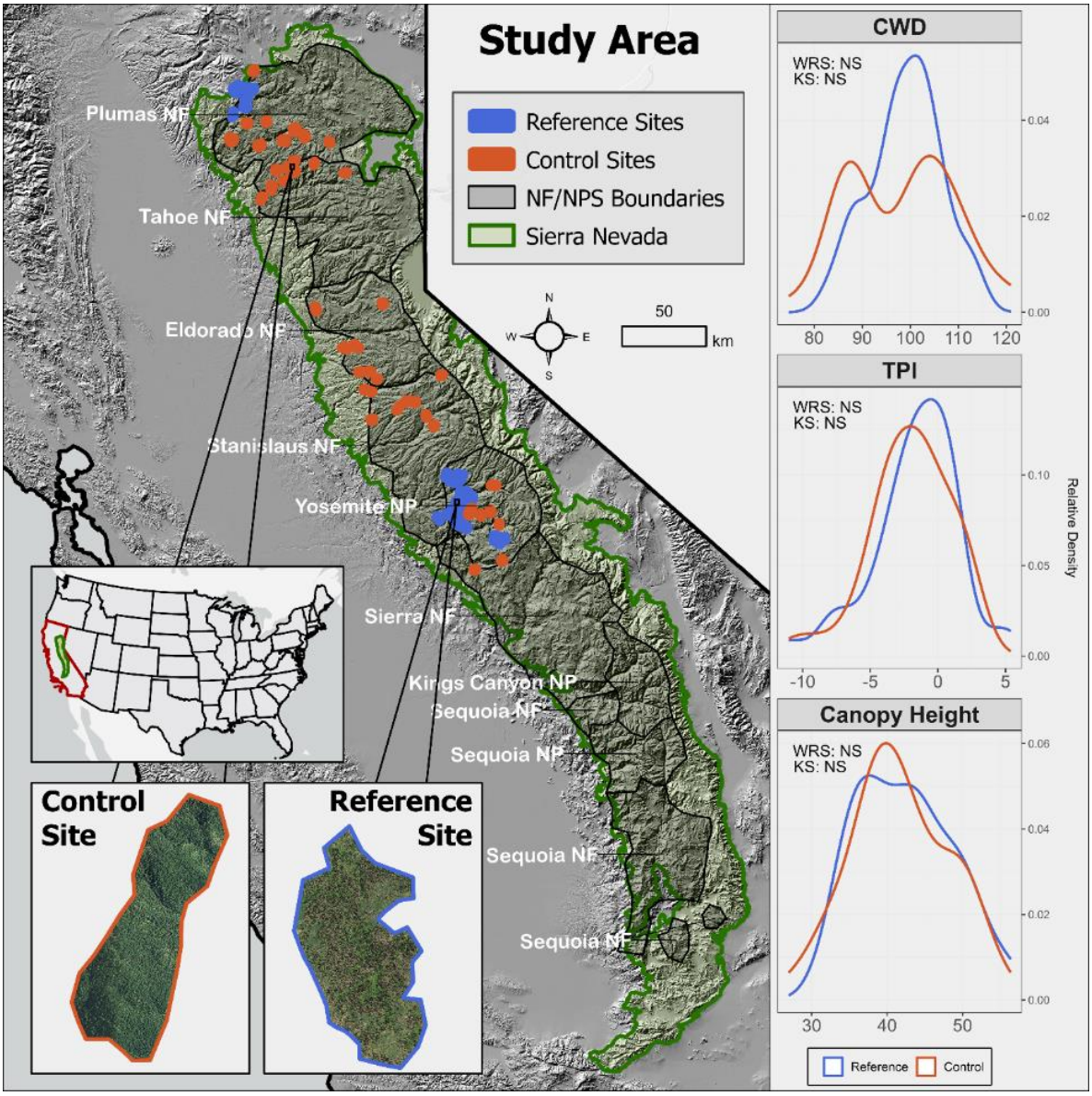

Figure 1.2. California's Sierra Nevada ecoregion defined by the Environmental Protection Agency's Level IV Ecoregions dataset (EPA 2023) with all intersecting National Forest (NF) and National Park Service (NPS) administrative boundaries (smoothed for visualization). Geographic distribution of reference (blue) and control (orange) sites used in analyses with example of each site type (left). Density curves for climatic water deficit (CWD), canopy height, and 2000 m topographic position index (TPI) compared between reference and control sites (right). No significant differences ($\alpha > 0.05$) found in median (Wilcoxon Rank Sum, WRS) or distribution (Kolmogorov-Smirnov, KS) between climate, canopy height, or topographic indices between reference and control sites.

Table 1.1. Total area, count, and mean, maximum, and minimum size for reference and control sites.

Site Type	Total Area (ha)	# Sites	Mean Size (ha)	Max Size (ha)	Min Size (ha)
Reference	11,850	42	282	841	102
Control	10,031	42	238	692	114

1.3.3. TREE CLUMP AND OPENING METRICS WITH ALS

We used high fidelity airborne laser scanning (ALS) data to quantify and compare a multi-scale set of forest structure metrics between reference and control sites. ALS data is currently available for large portions of the Sierra Nevada YPMC forests. For this study, we used six primary acquisitions that were collected between 2018 and 2020 including North and South Plumas National Forest, Eldorado National Forest, Tuolumne County, Yosemite National Park, and the Southern Sierra All Resource Restoration (SSARR) project area. These ALS acquisitions were each collected via aircraft during leaf-on months and provide high fidelity, georeferenced point cloud and ground model datasets. The ALS data met minimum pulse density and flight line overlap standards recommended for performing forest structure-based analyses (Gatziolis and Andersen 2008). Details for each acquisition are provided in Table 1.2.

We used the USDA Forest Service's FUSION software to process all six ALS acquisitions. Primary steps included (1) normalizing return heights, (2) producing canopy height models, (3) segmenting trees, and (4) deriving structure metrics from segmented trees (McGaughey 2020). Using FUSION's Lidar Toolkit, we first used vendor-provided ground models to normalize each ALS acquisition so that Z coordinates represented vegetation height above ground. The resultant normalized point clouds were then used to produce 0.75 m resolution canopy height models (CHMs). CHMs were smoothed using a 3x3 cell mean filter to reduce the effects of noise on the tree segmentation algorithm (Jeronimo et al. 2018). CHMs were further filtered to remove all cells < 2 m

so that derived structure metrics were representative of overstory tree structures rather than shrubs or other understory vegetation.

Individual trees were segmented in FUSION using the watershed algorithm (Vincent and Soille 1991), a computationally efficient algorithm that is widely used in other ALS-based forest structure research (Jeronimo et al. 2018). After applying the algorithm, FUSION produced an X and Y coordinate for each tree, a maximum tree height value, and a polygon representing the approximate crown dimensions of each tree. Past work has demonstrated that ALS-segmented trees are not fully representative of on-the-ground trees since many of the subcanopy trees are not identified in the segmentation process (Richardson and Moskal 2011; Jeronimo et al. 2018; Wiggins et al. 2019). Thus, we hereafter refer to all ALS-segmented trees as Tree Approximate Objects (TAOs) to explicitly recognize the limitations of segmentation algorithms while facilitating the production of ecologically meaningful metrics (Jeronimo et al. 2018; 2019).

We produced a set of ICO (individual tree, clump, and opening) and canopy height metrics from the ALS-derived TAOs that are known to be important metrics related to resilience in historically frequent-fire forests (Larson and Churchill 2012; Churchill et al. 2013; Lydersen et al. 2013). We followed methods from past work to produce ALS-derived ICO metrics (Jeronimo et al. 2019; Kane et al. 2019; Wiggins et al. 2019). All metrics were computed at 90 m resolution (~1 ha) as this is the approximate scale at which fine-scale tree spatial patterns are known to emerge in frequent-fire forests (Larson and Churchill 2012). TAOs were considered part of the same clump if their estimated crown polygons overlapped. Within each 90 m pixel, we computed the percent total canopy area occupied by individual TAOs and clumps of 2-4, 5-9, and 10+ TAOs. We also computed a percent area gap metric as the percentage of area within the pixel not occupied by TAO crowns. Lastly, we computed the 95th percentile of TAO heights (i.e., 'canopy height') within each pixel.

We applied the above workflow to each of the six ALS acquisitions to derive a final set of 90 m resolution ICO and height metrics spanning the reference and control sites. Lastly, we mosaicked rasters across acquisitions into a final set of rasters with uniform spatial resolutions (90 m) and projections (EPSG: 3310) to enable cross-acquisition comparisons of structure.

Table 1.2. Information for six airborne lidar (ALS) acquisitions including acquisition name, year(s) flown, total area, mean pulse density/m^2, and average flight line overlap. SSARR refers to Southern Sierra All Resource Restoration project area.

Acquisition Name	**Years Flown**	**Total Area (ha)**	**Mean Pulse Density (pulse/m^2)**	**Average Flight Line Overlap**
North Plumas NF	2018	466,774	13.3	> 50%
South Plumas NF	2018	560,370	12.6	> 50%
Eldorado NF	2019	577,109	28.0	> 50%
Tuolumne County	2018/2019	694,330	15.3	> 50%
Yosemite NP	2019	369,824	23.5	> 50%
SSARR	2020	569,810	22.0	> 50%

1.3.4. NEIGHBORHOOD-LEVEL STRUCTURE

Analysis of individual ICO metrics can be challenging to interpret and difficult to translate into straightforward, operational management objectives and evaluation metrics (North et al. 2022). Thus, we used hierarchical clustering to produce a set of horizontal structure classes from the ICO structure metrics to (1) produce outputs that could be more easily interpreted for management applications and (2) could be aggregated to characterize broader site-level structures. We defined a set of structure classes for all pixels intersecting the reference and control sites described above (Section 1.2.). Hierarchical clustering algorithms can quickly overwhelm computer memory when building distance matrices, so we first performed clustering on a random stratified sample of 27,000 pixels, then produced a Random Forest model to predict the resultant structure classes for all pixels across the reference and control sites.

We stratified pixels using the percent area gap and the 95th percentile of TAO height metrics (described above) to ensure that our sample captured a range of forest conditions. We then applied

an unsupervised agglomerative hierarchical clustering algorithm using a Euclidean distance measure on all ICO metrics (i.e., % area gap, % single TAOs, and % 2-4, 5-9, and 10+ TAO clumps) to define a set of horizontal structure classes (Gotelli and Ellison 2018). To determine the most ecologically meaningful and statistically distinct number of structure classes (i.e., where to "prune" the resultant dendrogram), we evaluated a dendrogram (Figure 1.1) and scree plot (Figure 1.A.2) from the hierarchical clustering analysis and analyzed the distribution of input metrics in different class combinations. After deciding on the number of structure classes, we produced a Random Forest classification model using the ICO metrics as explanatory variables and the structure classes as a response and applied this model to predict the structure class of all pixels across the reference and control sites (Cutler et al. 2007). All analyses were performed in R using the *terra* (Hijmans et al. 2023) and *randomForest* (Liaw and Wiener 2002) packages and other base R functions. We used default parameters for the Random Forest model.

1.3.5. WITHIN- AND AMONG-SITE-LEVEL STRUCTURE

Fine-scale forest structure patterns (i.e., neighborhood-level structure classes) describe a key spatial scale of forest structures in frequent-fire forests (Larson and Churchill 2012); however, it is also useful to quantify and analyze coarser scale structural patterns (i.e., within- and among-sites) to better inform management and understand repeat fire effects at these broader spatial scales (Turner and Romme 1994; Larson and Churchill 2012; Hessburg et al. 2019; Francis et al. 2023). For example, site-level heterogeneity indices including patch size or spatial aggregation metrics can provide key information about the proportions and spatial configurations of finer-scale structures across a site (McGarigal and Marks 1995; He et al. 2000; Hessburg et al. 2000). Furthermore, measuring among-site variability in heterogeneity metrics can provide information about the consistency of patterns across broader spatial scales (i.e., multiple sites). Thus, to analyze these coarser spatial scales, we quantified and compared (1) within-site heterogeneity indices of the finer-

scale structure classes (described in section 1.4.) and (2) among-site variability of these site-level indices.

We first derived the proportions of each structure class by site type (reference vs. control) and compared these distributions to identify dominant patterns of fine-scale structures. Next, we characterized site-level heterogeneity and spatial configurations of forest structure using a parsimonious set of heterogeneity indices (Cushman et al. 2008) including aggregation index (AI), interspersion-juxtaposition index (IJI), area-weighted mean patch size (AWMPS), and Shannon's evenness index (SHEI) (McGarigal and Marks 1995; He et al. 2000). Aggregation index describes the likelihood that pixels are adjacent to pixels of the same class and provides a measure of "clumpiness" across a site (He et al. 2000). Interspersion-juxtaposition index is referred to as the "salt and pepper" index and ranges from 0 to 100. A value of 0 suggests that classes, on average, are only adjacent to patches of a single other class type, while a value of 100 suggests that classes, on average, are equally adjacent to patches of all other class types. Area-weighted mean patch size describes the average patch size that a randomly selected pixel belongs to, and thus indicates whether a site is composed primarily of small or large patches of finer-scale structures. Lastly, Shannon's evenness index describes how similar the proportions of different classes are across a site (Table 1.3) (McGarigal and Marks 1995). We computed all heterogeneity indices using the *terra* (Hijmans et al. 2023) and *landscapemetrics* (Hesselbarth et al. 2019) packages in R. We used an 8-neighbor rule for defining patches of classes and computed site-level indices (i.e., across patches of all structure class types).

Table 1.3. Name, abbreviation, description, interpretation, and range for four heterogeneity indices including aggregation index, interspersion-juxtaposition index, area-weighted mean patch size, and Shannon's evenness index. Table adapted from Cova et al. (2023) and Singleton et al. (2019).

Metric	Abbreviation	Description	Interpretation of Low Values	Interpretation of High Values	Range (units)
Aggregation Index	AI	Likelihood that pixels from one class are adjacent to pixels of the same class	Low clumping of pixels of the same class	High clumping of pixels of the same class	0 – 100 (unitless index)
Interspersion-juxtaposition Index	IJI	Describes the degree to which the edge of patches are likely to be adjacent to all other patch types (high value) or only one other patch type (low value)	Low intermixing of patch types	High intermixing of patch types	0 – 100 (unitless index)
Area-weighted mean patch size	AWMPS	Mean area of patches weighted by relative patch size within each site	Pixel chosen at random will belong to small patch	Pixel chosen at random will belong to large patch	0.81-427 (ha)
Shannon's Evenness Index	SHEI	Degree of similarity in proportions of classes	Distributions are not even, and a few classes dominate	Distributions are even, and no single class dominates	0 – 1 (unitless index)

To assess differences in heterogeneity indices between reference and control sites, we first compared the distributions of each index (aggregation index, interspersion-juxtaposition index, area-weighted mean patch size, and Shannon's evenness index) using boxplots and violin plots. Next, we tested for multivariate differences (i.e., across all heterogeneity indices) between the reference and control sites. We used PERMANOVA to test for significant differences in the centroids of heterogeneity indices and used PERMDISP to test for significant differences in dispersion, using an α of 0.05 for both statistical tests. We first scaled each heterogeneity index by its range, then

produced a Euclidean distance matrix from the scaled heterogeneity indices. We used the *adonis2* function from the *vegan* package in R (Oksanen et al. 2022) to run PERMANOVA and used the *betadisper* function from the *vegan* package and the base *aov* function to run PERMDISP. Lastly, we visualized differences in centroid and dispersion between reference and control sites using the first two axes of a Principal Coordinates Analysis derived from the input heterogeneity indices.

1.4. RESULTS

1.4.1. NEIGHBORHOOD-LEVEL STRUCTURES

Our hierarchical clustering analysis produced a distinct set of four structure classes representing neighborhood-level (~1 ha) ICO patterns characteristic of the reference and control sites. Cutting the dendrogram at four classes was most appropriate for our dataset, as further splitting or grouping would have produced less distinct classes (Figure 1.3). We provide distributions of ALS-derived tree clump and opening metrics across all pixels within reference and control sites in Figure 1.A.3; however, we focus our results and discussion on the derived neighborhood-level structure classes since structure classes (1) are easier to interpret from a management perspective and (2) represent the metrics that were scaled up to quantify site- and among-site structural patterns.

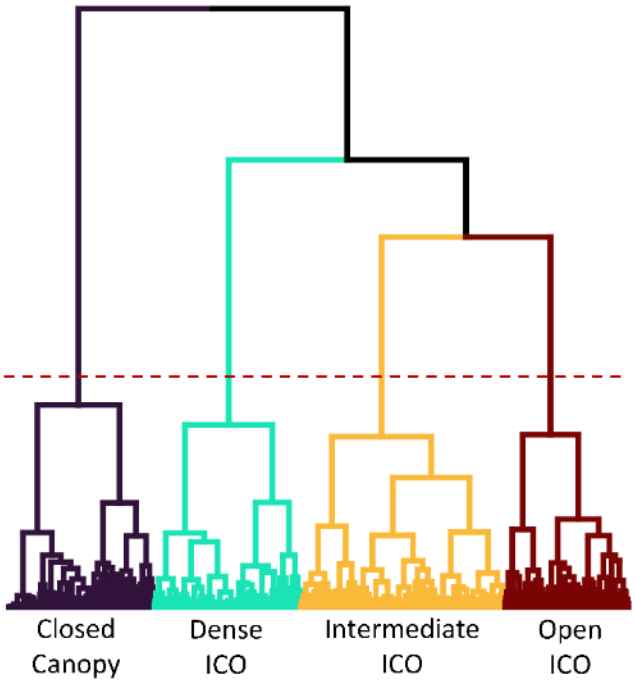

Figure 1.3. Dendrogram illustrating the hierarchical clustering analysis applied to the five ICO metrics, with the horizontal line depicting the cut in the dendrogram defining four distinct structure classes (see Figure 1.4). ICO refers to fine-scale spatial patterns of individual tree approximate objects (TAOs), clumps of TAOs, and open space.

Distributions of ICO metrics comprising each structure class and visualizations of a representative sample from each class are shown in Figure 1.4. We assigned names to each structure class based on interpretations of the resultant metric distributions. The "closed canopy" class was characterized by mean 64.0% canopy area of large clumps and < 15.0% mean canopy area of single TAOs and 2-4 and 5-9 TAO clumps. On the other hand, the dense, intermediate, and open ICO structure classes were all composed of > 35% mean canopy/pixel area of at least one key ICO structure metric (i.e., single TAOs, 2-4 TAO clumps, or 5-9 TAO clumps). These ICO-dominated structure classes were distinguished, however, based on the relative proportion of constituent ICO metrics. The "dense ICO" class was dominated by 5-9 TAO clumps (mean 37.5% canopy area); "intermediate ICO" was dominated by 2-4 TAO clumps (mean 63.5% canopy area); and "open

ICO" was dominated by open space (mean 63.3% pixel area) and single TAOs (mean 81.9% canopy area). The first and second row in Figure 1.4 provide top-down visualization of the horizontal spatial structures in each class, showing the decreasing canopy cover and more distinguished ICO structures moving from closed canopy (left) to open ICO structures (right). In Figure 1.5 we provide photographs taken within representative patches (> 4 contiguous 90 m pixels) of each structure class within Yosemite National Park during summer of 2022.

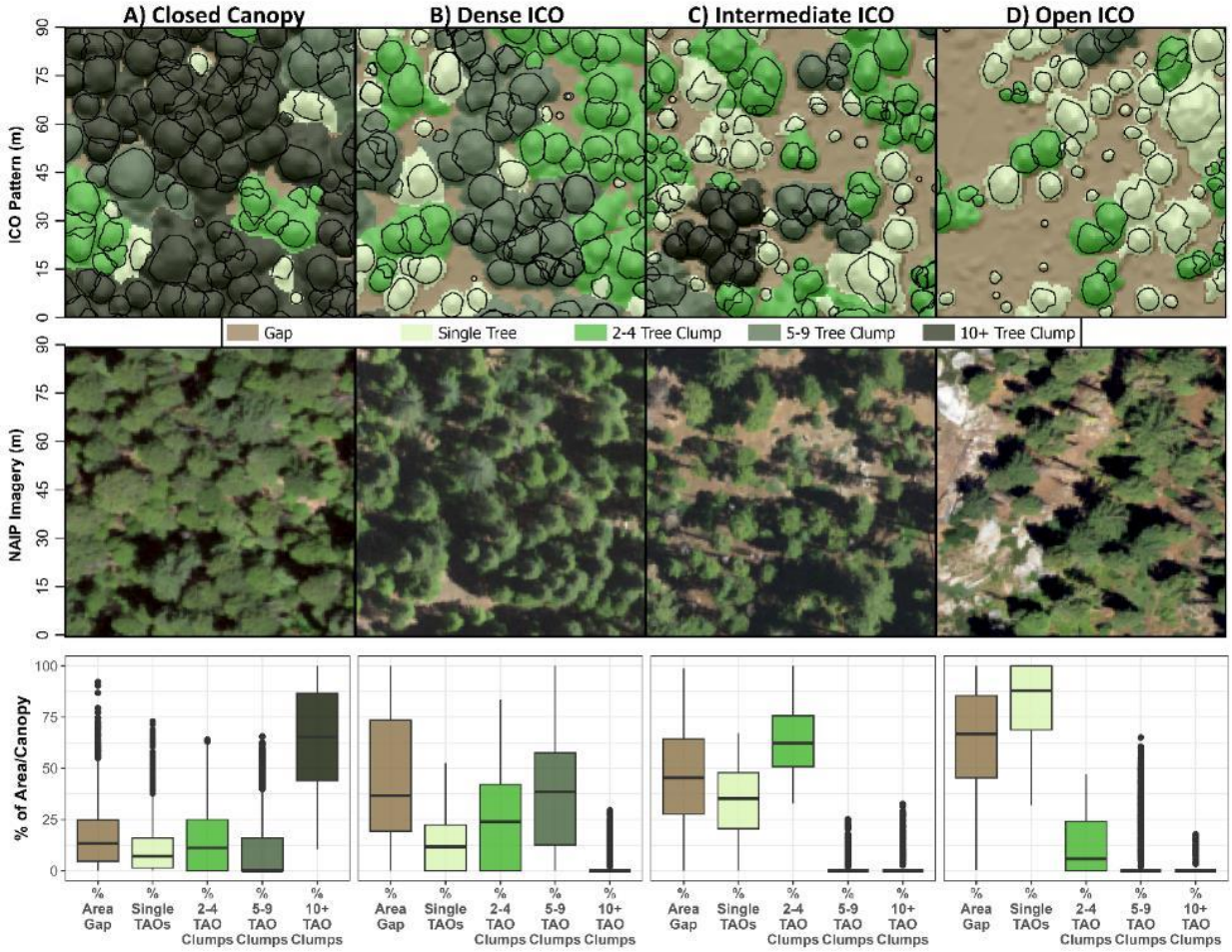

Figure 1.4. Visualizations and metrics for representative samples of the four structure classes. Top row shows top-down visualization of TAO clump and opening patterns within 90x90 m (~1 ha) pixels; middle row shows top-down visualization of 0.6 m resolution National Agricultural Imagery Program (NAIP) true color images; and bottom row shows distributions of input structure metrics that define each structure class (% area for area gap metric and % canopy for all other metrics). ICO refers to fine-scale spatial patterns of individual tree approximate objects (TAOs), clumps of TAOs, and open space.

Figure 1.5. Photos taken within representative patches (> 4 continugous 90 m pixels) of each forest structure class during summer of 2022 site visits in Yosemite National Park. ICO refers to fine-scale spatial patterns of individual tree approximate objects (TAOs), clumps of TAOs, and open space. Photo credit Caden Chamberlain.

Comparing the mean and variance of the proportions of neighborhood-level structure classes indicated key differences between reference and control sites (Figure 1.6). Reference sites on average were characterized by 29.6% open ICO structures, 39.5% intermediate ICO structures, and only 9.9% closed canopy structures. In contrast, control sites on average were composed of 48.2% closed canopy structures, 20.1% intermediate ICO structures, and only 9.8% open ICO structures. Both site types had approximately 21% dense ICO structures (Figure 1.6).

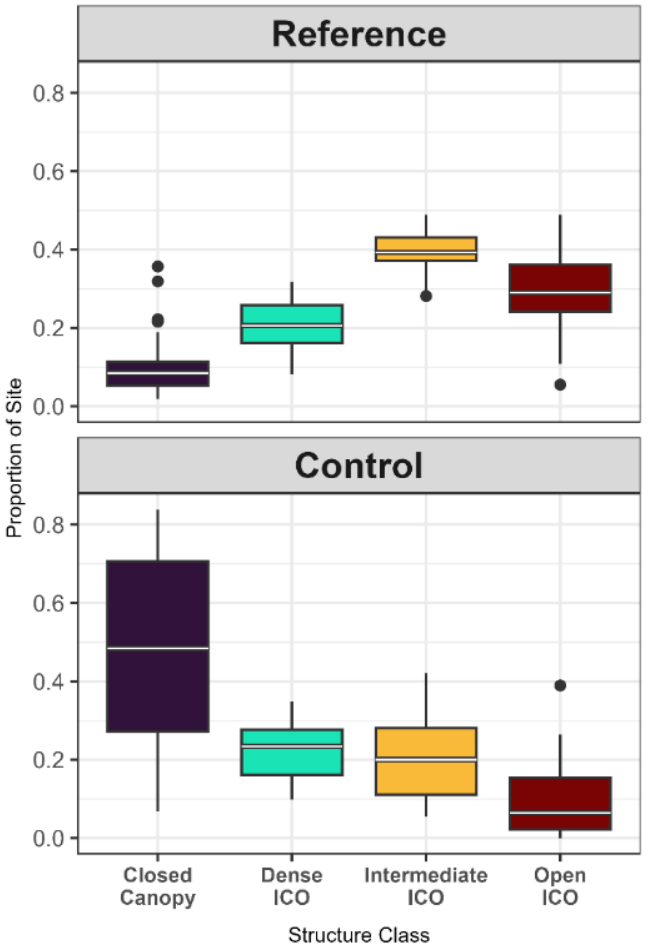

Figure 1.6. Distributions of structure class proportions between reference (top) and control (bottom) sites. Each data point represents the proportion of a given structure class for a single site. Reference sites are dominated by open and intermediate ICO classes with lower proportions of dense ICO and closed canopy classes. Control sites dominated by closed canopy and to a lesser extent dense ICO structure classes, and lower portions of intermediate and open ICO classes. ICO refers to fine-scale spatial patterns of individual tree approximate objects (TAOs), clumps of TAOs, and open space.

1.4.2. SITE-LEVEL SPATIAL PATTERNS

Comparisons of site-level heterogeneity indices indicated a more heterogeneous spatial arrangement of finer-scale structure classes in reference sites compared to controls (Figure 1.7). References sites exhibited lower aggregation index, higher interspersion-juxtaposition index, smaller area-weighted mean patch size, and higher Shannon's evenness index (median AI = 33.5; median IJI = 87.1; median AWMPS = 22.3; median SHEI = 0.91) relative to controls (median AI = 41.5; median IJI = 85.2; median AWMPS = 37.2; median SHEI = 0.86). (Figure 1.7A). Our multivariate comparisons (i.e., using PERMANOVA to compare all input heterogeneity indices between reference and control sites) indicated a significant difference in the centroid of heterogeneity indices between site types ($\alpha < 0.05$), suggesting that reference sites exhibited greater site-level heterogeneity (Figure 1.7A/B).

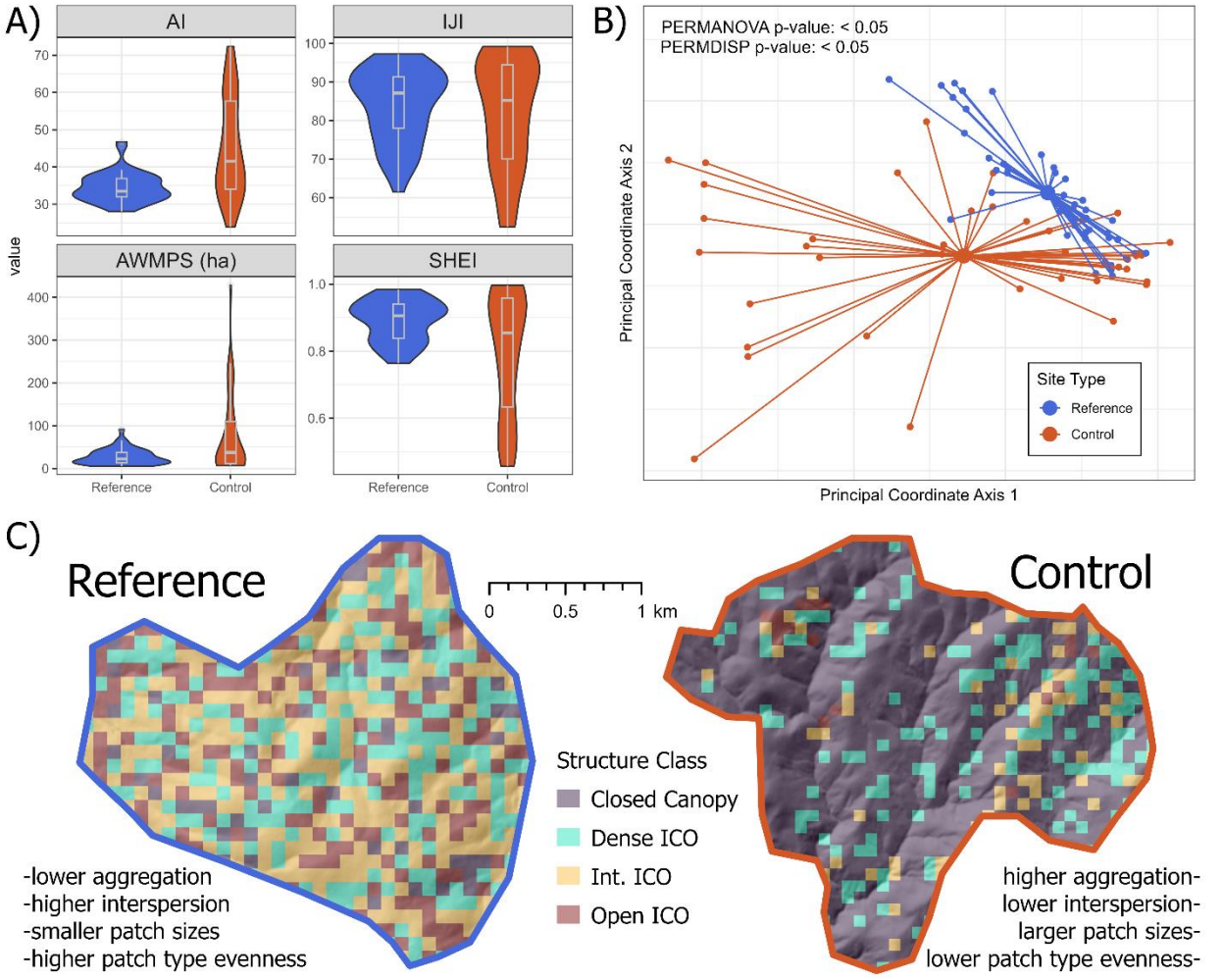

Figure 1.7. Comparisons of the distributions of heterogeneity indices between the reference (blue) and control (orange) sites (panel A). Heterogeneity indices were calculated using all four structure classes. Indices include aggregation index (AI), interspersion-juxtaposition index (IJI), area-weighted mean patch size (AWMPS), and Shannon's evenness index (SHEI). Principal Coordinates Analysis (PCoA) ordination derived from the input site-level heterogeneity indices comparing the multivariate centroid and dispersion between reference and control sites (panel B). PCoA Axis 1 was most strongly correlated with SHEI and AI. PCoA Axis 2 was most strongly correlated with AWMPS and IJI. Difference in centroids between sites tested using PERMANOVA and differences in dispersion between sites tested using PERMDISP (α = 0.05). Visualization of representative reference (left) and control (right) sites with mapped forest structure classes showing differences in aggregation, interspersion, patch sizes, and evenness between the sites (panel C).

1.4.3. AMONG-SITE VARIABILITY

Comparisons of among-site variability and dispersion between reference and control sites indicated that, across the Sierra Nevada YPMC zone, sites with ongoing fire-suppression (i.e., control sites) were more variable in terms of their site-level heterogeneity indices. In contrast, reference sites were more consistently heterogeneous (i.e., lower variability in heterogeneity indices) across the Sierra Nevada YPMC zone. Standard deviations of each heterogeneity index were higher in control sites (standard deviation AI = 13.2; standard deviation IJI = 14.1; standard deviation AWMPS = 92.7; standard deviation SHEI = 0.18) compared to reference sites (standard deviation AI = 3.97; standard deviation IJI = 9.42; standard deviation AWMPS = 18.6; standard deviation SHEI = 0.06) (Figure 1.7A). Additionally, we observed significantly higher multivariate dispersion of heterogeneity indices in control sites compared to reference sites (Figure 1.7B).

1.5. DISCUSSION

Our analyses provide key insights about the effects of a contemporary, frequent, and low-severity fire regime on multi-scale forest structural patterns, and how these structures compare against typical fire-suppressed forests in the Sierra Nevada YPMC zone. Frequent and low-severity fires produced distinct horizontal spatial patterns at the neighborhood-level in reference sites, with structures characterized primarily by individual TAOs, small clumps of TAOs, and high proportions of open space (Figures 1.5 and 1.6). In contrast, fire-suppressed control sites were dominated primarily by closed canopy structures at the neighborhood-level, with only moderate proportions of dense and intermediate ICO structures. We observed more heterogeneous spatial arrangements of neighborhood-level structure classes within reference sites compared to controls, based on low aggregation of pixels, high interspersion of patch types, small patch sizes, and high evenness of patch types (Figure 1.7). Furthermore, we found that site-level heterogeneity indices consistently fell

within a relatively small range of variation *among* reference sites, while controls exhibited higher among-site variance (Figure 1.7). This consistency in site-level heterogeneity among reference sites suggests a coarse-scale stabilizing effect of contemporary frequent-fire regimes, where fire as an active process ultimately leads to greater consistency of spatial patterns across broad, ecosystem scales. The multi-scale structural patterns observed in reference sites indicate improved resilience to future disturbances and climate change and will likely support other key ecosystem services; therefore, these structures can be used to help inform management efforts across the Sierra Nevada.

1.5.1. NEIGHBORHOOD-LEVEL STRUCTURES (~1 ha)

Across our reference and control sites, we observed four ecologically and statistically distinct structure classes – closed canopy, dense ICO, intermediate ICO, and open ICO. The closed canopy structure class was characteristic of fire-suppressed forests, in which key components of the ICO pattern, including individual TAOs, small clumps of TAOs, and open space, were absent. This condition is common in fire-suppressed forests due to infilling of more shade-tolerant species which increases continuity of surface, ladder, and canopy fuels (Collins et al. 2011a; Lydersen et al. 2013). The three ICO structure classes (dense ICO, intermediate ICO, and open ICO), however, were characterized by higher proportions of open space, individual TAOs, and small clumps of TAOs, which represent the key horizontal structural components that define frequent-fire forests (Larson and Churchill 2012; Lydersen et al. 2013).

Our results provide evidence that the reintroduction of a frequent, low-severity fire regime in previously fire-suppressed forests has begun to reestablish neighborhood-level ICO patterns that are similar to pre-Euro-American colonization (Larson and Churchill 2012; Churchill et al. 2013; Lydersen et al. 2013; Safford and Stevens 2017). Lower severity fires can produce open space, single TAOs, and small clumps of TAOs by iteratively disaggregating larger contiguous clumps of TAOs, like those found in our fire-suppressed control sites (Kane et al. 2013; Kane et al. 2019; Ritter et al.

2020). Ultimately, this "breaking up" of larger clumps likely led to the formation and dominance of intermediate and open ICO structure classes in our reference sites. Importantly, our findings of mostly individual TAOs and small clumps of TAOs in fire-intact forests are consistent with past studies that analyzed TAO spatial patterns in contemporary reference sites (Jeronimo et al. 2019; Wiggins et al. 2019). Despite the dominance of intermediate and open ICO structure classes, we note that reference sites on average were composed of 9.9% of the closed canopy structure class which was characterized by large TAO clumps and < 10% area gap. These patches of denser canopy structures in reference sites, likely concentrated in valleys and areas with higher productivity (Collins et al. 2016; Jeronimo et al. 2019; Ng et al. 2020), contribute to other important ecosystem services like wildlife habitat and biodiversity (Meyer et al. 2007a; Stephens et al. 2016b; Kramer et al. 2021; Stephens et al. 2021b; Steel et al. 2022).

Our results suggest that the fine-scale ICO structures produced from first-entry low- and moderate-severity fires can remain relatively stable through the occurrence of subsequent fires. Kane et al. (2019) found that first-entry low- and moderate-severity fires exhibited structures dominated by individual TAOs and 2-4 TAO clumps. Across our reference sites, which experienced *multiple* low- and moderate severity fires, we found high proportions of individual TAOs and 2-4 TAO clumps, suggesting that the fine-scale ICO patterns produced during first-entry burns (Kane et al. 2019) persisted through multiple fire events. Hankin and Anderson (2022) found stability in tree density and ladder fuel density through multiple low- and moderate-severity fires in the Sierra Nevada; our results provide additional insight about the stability of TAO spatial patterns, which represent a critical structural component in frequent-fire systems (Larson and Churchill 2012; Lydersen et al. 2013). However, it should be noted that without pre- and post-fire data for each fire, we are unable to know for certain if the neighborhood-level structures were either present prior to fire or were produced by first or subsequent burns.

While we found that fire-suppressed control sites were indeed dominated by closed-canopy structures, we also observed that nearly half of the area of control sites was characterized by dense and intermediate ICO structures (24% and 19%, respectively). This highlights that the signal of edaphic-driven structures has persisted, to some extent, through fire suppression – where edaphic conditions can produce persistent canopy gaps that do not support tree regeneration or formation of large tree clumps (North et al. 2004; Meyer et al. 2007b; Fry et al. 2014). It is also likely that other non-fire disturbances contributed to the formation of dense and intermediate ICO structures in controls. While we used LCMS data to partially account for the effects of other disturbances, it is likely that this dataset did not capture all isolated drought, insect, and pathogen induced mortality (Housman et al. 2022), which could theoretically produce dense or intermediate ICO structures (Steel et al. 2023). Importantly, these lower density ICO structures observed in control sites could potentially provide anchors for future resilience-focused treatments in the Sierra Nevada (Larson et al. 2013).

1.5.2. SITE-LEVEL STRUCTURES (~100-1000 ha)

Within reference sites (~100-1000 ha), our results suggest that frequent low- and moderate-severity fires produced a disaggregated and interspersed arrangement of mostly small (< 50 ha) patches, primarily representing intermediate and open ICO structure classes. We assert that greater interspersion of neighborhood-level structures, smaller patch sizes, and higher evenness of patch types (compared to controls) is indicative of increased *heterogeneity* at the within-site level in reference sites (see Figure 1.7C). This site-level heterogeneity demonstrates the capacity of a restored, low-severity, and frequent fire regime to create variable structures within previously fire-suppressed forests, like those found in our control sites.

The spatial variability and stochasticity of recent fire intensity and resultant severity was likely a driving force of the site-level heterogeneity observed in our reference sites. Stochasticity and

variability in fire behavior is driven by variability in fire weather, fuels, topography, and moisture gradients at fine- to moderate-spatial scales (Parsons et al. 2017; Sullivan 2017; Jeronimo et al. 2020). As fires burn across a site they interact with the biophysical environment and the legacies of recent disturbances (Kane et al. 2015b; Harvey et al. 2016; Hessburg et al. 2019). For example, higher productivity sites may have higher fuel moisture, which could reduce fire intensity and result in reduced overstory mortality and therefore patches of denser ICO structures (Lydersen et al. 2013; Jeronimo et al. 2019; Ng et al. 2020). In contrast, exposed topographic positions may burn at higher intensities and result in more intermediate and open ICO structures (Lydersen et al. 2013; Jeronimo et al. 2019; Ng et al. 2020). Subsequent fires then interact with this variability in structure and fuels to further increase heterogeneity across the landscape (Kane et al. 2015b; Koontz et al. 2020), as evidenced by the highly interspersed, disaggregated, and small patch sizes of forest structure classes observed within reference sites in our study.

1.5.2. AMONG-SITE-LEVEL STRUCTURES (~10,000-100,000 ha)

We observed lower *among*-site (~10,000-100,000 ha) variance and dispersion in heterogeneity indices (i.e., aggregation index, interspersion-juxtaposition index, area-weighted mean patch size, and Shannon's evenness index) for reference sites compared to control sites. This suggests a possible coarse-scale stabilizing effect of a frequent, low-severity fire regime. For example, area-weighted mean patch size ranged from 6-91 ha across reference sites but ranged from 7-427 ha across controls. Importantly, reference sites exhibited this relatively high site-level heterogeneity regardless of variability in other fire regime and biophysical drivers, such as variability in the intensity and resultant severity of past fires, past fire frequencies (2 versus 4 recent fires), topographic conditions, or productivity gradients. Therefore, we contend that a frequent and low-severity fire regime represents a strong driver of site-level heterogeneity, producing consistent patterns across broad, ecosystem scales. This inference is strengthened by comparison to reconstructed historical frequent-

fire forests in the Pacific Northwest where Churchill et al. (2013), Churchill et al. (2017), and LeFevre et al. (2020) all found similar ranges of variation in forest structure and spatial patterns across relatively disparate ecosystems (eastern Washington Cascades, southern Blue Mountains, and northeastern Washington Rockies, respectively).

We found relatively higher variance in aggregation, interspersion, patch size, and patch type evenness indices in the control sites compared to the reference sites. While other minor disturbance agents and edaphic drivers may sometimes result in moderate or high levels of heterogeneity in the absence of fire, our results suggest that these drivers do not consistently produce heterogeneous structures across the region, especially not to the same extent as a restored, frequent, and low-severity fire regime. Nonetheless, it is important to note that nearly half of control sites *were* characterized by heterogeneity indices similar to reference sites, indicating a potential boon for restoration efforts in the Sierra Nevada. Fire suppressed forests with edaphic or other disturbance-driven heterogeneity may exhibit improved resilience to future disturbances and climate change due to their structural variability (Hessburg et al. 2019). In these sites, perhaps only minimal restoration treatments or the use of unplanned ignitions to support resource objectives (i.e., wildland fire use) will be required to improve resilience (Weatherspoon and Skinner 1995; North et al. 2021; Ziegler et al. 2021).

1.5.3. MANAGEMENT IMPLICATIONS

RESILIENCE AND ECOSYSTEM SERVICES

We posit that the neighborhood-level ICO structure classes dominating the reference sites, as well as the increased site-level heterogeneity of these ICO structures, will confer greater resilience in the face of future fires, droughts, and climate change (Moritz et al. 2010; Hessburg et al. 2015; Hessburg et al. 2019; Newman et al. 2019; Francis et al. 2023). We define resilience as the capacity of YPMC forests to maintain a stable range of structure, composition, and functional integrity through

periodic disturbances like fire, drought, and bark beetle outbreaks (Walker et al. 2004; North et al. 2022). Heterogeneity at the site-level in reference sites also suggests improvements to other important ecosystem services like wildlife habitat, biodiversity, and ecosystem capacity for climate adaptation (Dudney et al. 2018; Kramer et al. 2021; Stephens et al. 2021b). As such, the multi-scale structural patterns observed in reference sites can be used by managers as diagnostics when designing and implementing restoration treatments or when evaluating the effects of recent disturbances on resilience and other ecosystem services.

At the neighborhood-level, high proportions of open space in the intermediate and open ICO structure classes suggests reduced and discontinuous surface fuels, which will likely minimize crown fire initiation and subsequent high severity fire (Agee and Skinner 2005; Ziegler et al. 2021). Additionally, during future fires, convective cooling around single TAOs and 2-4 TAO clumps may increase overstory tree survival and thus reduce burn severity (Pimont et al. 2009; Ziegler et al. 2017; Ritter et al. 2020). Higher proportions of sun-exposed gaps and bare mineral soil will also increase the probability of post-fire regeneration and recovery, especially for more fire-resistant and shade-intolerant species like ponderosa pine and Jeffrey pine (Zald et al. 2008; Bigelow et al. 2011). Additionally, lower tree densities will lead to reduced competition for water and light which may increase individual tree health and allow trees to better resist second-order post-fire mortality (Jeronimo et al. 2020). More vigorous trees may also exhibit improved defense mechanisms against future drought and bark beetle disturbances and increased survival under projected warmer and drier climates (Hood et al. 2015; Koontz et al. 2021; Furniss et al. 2022).

The site-level heterogeneity observed in our reference sites also suggests improved resilience to future disturbances and climate change. First, more heterogeneous patch structures will promote variability in future fire behavior across these sites (Hessburg et al. 2019). This variability in fire behavior could theoretically reduce the likelihood of large contiguous high-severity patches (Koontz

et al. 2020; Francis et al. 2023) which are known to negatively impact non-serotinous conifer re-establishment and thus post-fire recovery (Coop et al. 2020; Jeronimo et al. 2020; Steel et al. 2021a). Site-level heterogeneity also indicates a mosaic of microclimates with varying temperature and moisture gradients, which may provide distinct microsites of cooler and wetter conditions that promote regeneration success of key conifer species under a warmer and drier climate (De Frenne et al. 2013; Davis et al. 2019). Some research also indicates that more heterogeneous structures across sites and landscapes can impede the spread of bark beetles or other pathogens, which may ensure that these disturbances remain at endemic levels under increasingly unfavorable climatic conditions (Fettig et al. 2007; North 2012; Pile et al. 2019).

Heterogeneous structures at the neighborhood- and site-level in reference sites also suggest improvements to other important ecosystem services like wildlife habitat, biodiversity, and climate adaptive capacity. Variability in structures across sites, ranging from closed canopy to open ICO structure classes, provide a range of habitat components that support nesting and foraging for species like the California spotted owl (White et al. 2013; Stephens et al. 2016b; Kramer et al. 2021; Steel et al. 2023). Increased heterogeneity at multiple scales will also increase floral and faunal biodiversity (Tingley et al. 2016; Kelly et al. 2017; Stephens et al. 2021b). For example, patches of dense ICO structures likely have higher proportions of shade-tolerant species like white and red fir while patches of intermediate and open ICO structures are likely dominated by shade-intolerant species like Jeffrey pine and sugar pine (Zald et al. 2008; Bigelow et al. 2011; Stephens et al. 2021b). This variability in vegetation structures in reference sites may also promote increased adaptive capacity under climate change (Gunderson 2000; Dudney et al. 2018). Heterogeneity across different spatial scales promotes redundancy of resilience mechanisms, which supports a wider range of vegetation responses to shifting climates and disturbance regimes across space and time (Peterson et al. 1998; Dobrowski 2011; Hannah et al. 2014).

HIERARCHICAL STRUCTURES TO GUIDE ECOSYSTEM MANAGEMENT

We quantified a nested, hierarchical set of forest structure metrics in restored frequent-fire reference sites of the Sierra Nevada YPMC zone, which provides a scalable set of observations that managers can use to guide management efforts in the region. Past work has described hierarchical arrangements of structural patterns in both historical and contemporary frequent-fire forests (e.g., Larson and Churchill 2012; Reynolds et al. 2013; Churchill et al. 2017; Hessburg et al. 2019). However, our study is unique in using lidar data to explicitly quantify and describe structures at these nested hierarchical scales.

We suggest conceptualizing ecosystem structures of frequent-fire forests as a hierarchy of structural components – beginning with trees and open space and scaling these components up to the neighborhood-, site-, and among-site-level (Figure 1.8). At the finest scale, individual trees, small clumps of mostly 2-4 trees, and open space represent the primary structural components, with only moderate representation of larger tree clumps. At the neighborhood-level (~1 ha), individual trees and small clumps of trees are arranged within a matrix of open space. At the site-level (~100-1000 ha), these neighborhood structures can be grouped into small patches (mostly < 50 ha in size) of similar structures and arranged in heterogeneous and intermixed patterns across the site. Arrangements of structure class patches can be guided by topographic position and productivity gradients (i.e., dense ICO and small patches of closed canopy structures in more productive sites and open and intermediate ICO structures in less productive sites) (Collins et al. 2016; Jeronimo et al. 2019; Ng et al. 2020). Lastly, at the among-site-level, for example across a watershed or Forest Service district, all sites should fall within a narrow range of site-level heterogeneity indices (i.e., patch sizes ranging from ~5-90 ha, or aggregation indices ranging from ~28-46) and should be representative of a diversity of neighborhood-level structures (Figure 1.8).

An important outcome of our work is that our within-site analysis fills a critical information gap between fine- and broad-scale spatial patterns in a way that is applicable to operational forest landscape restoration. Frameworks have been proposed and applied for both landscape-scale prioritization and planning (Manley et al. 2020; Larson et al. 2022) and within-stand treatment guidelines (North et al. 2009; Churchill et al. 2013; Knapp et al. 2017) but linking these two scales has been a challenge in practice. Our analyses suggest that a relatively simple set of fine-scale structural components – proportions of individual trees, clumps of trees, and open space – can be scaled up to characterize reference site structures at the neighborhood-, within-site, and among-site-levels. These structural patterns thus provide guidelines for landscape restoration that (1) capture the hierarchical and cross-scale structure of ecosystems and (2) can be operationalized at each spatial scale by aggregating metrics from finer-scales (Hessburg et al. 2015).

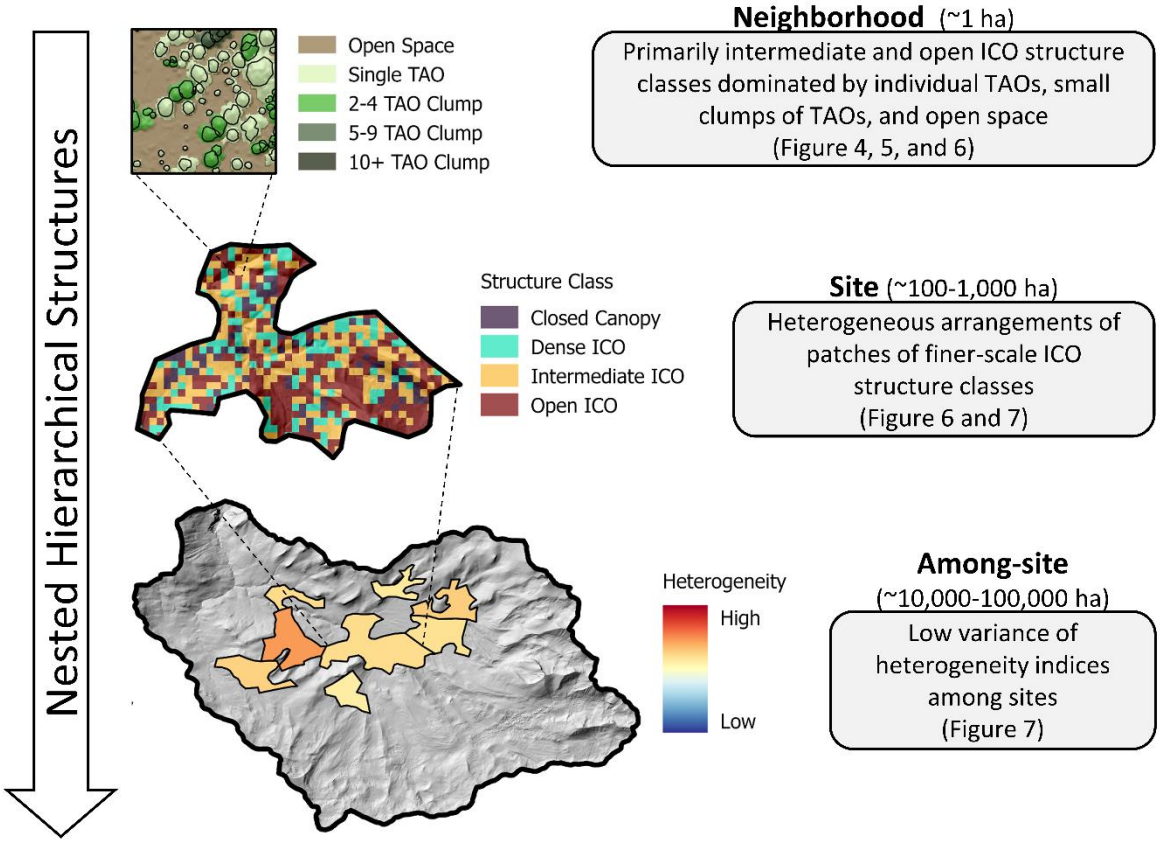

Figure 1.8. A nested hierarchical set of structural patterns observed in reference sites characterized by a frequent, low-severity fire regime. At the neighborhood-level (~1 ha), structures are dominated by intermediate and open ICO structures consisting primarily of individual TAOs, small clumps of TAOs, and high proportions of open space. At the site-level (~100-1000 ha), patches of ICO structure classes are arranged heterogeneously, with small patch sizes and high interspersion of patch types. Among-sites (~10,000-100,000 ha) there is low variance of heterogeneity indices; all sites consistently exhibit high interspersion of patches, small patch sizes, and high evenness of patch types. ICO refers to fine-scale spatial patterns of individual tree approximate objects (TAOs), clumps of TAOs, and open space.

1.5.4. STUDY LIMITATIONS

We acknowledge several limitations to the present study that should be considered by managers and ecologists when interpreting our results. These limitations present opportunities for future research in active-fire landscapes of the Sierra Nevada.

Structural conditions observed in the reference sites only represent a snapshot in space and time and may continue to change as additional fires burn through these sites and structures are

influenced by both direct and indirect effects of climate change. While recent research suggests that continued occurrence of low- to moderate-severity fires in these sites is unlikely to substantially alter structural patterns beyond their current conditions (Hankin and Anderson 2022), other work suggests that long-term shifts in climate and its influence on future fire intensities may indeed lead to considerable shifts in structures in these sites (Crompton et al. 2022). As such, we recommend that managers use the reference conditions defined in our analyses as a baseline for designing and evaluating treatments in the 21st century in combination with adaptive management frameworks that update management strategies to account for uncertainty and changing conditions (Gunderson 2000; Stephens et al. 2010; Millar et al. 2007). Additionally, managers could consider designing treatments based on reference conditions from future, rather than current, climate conditions, as described in Churchill et al. (2013). Further research that explicitly tests the resilience of these reference sites based on the capacity of structures to persist and recover under future disturbances and climate change is also needed (e.g., Lydersen et al. 2014; Hankin and Anderson 2022).

We focused our analyses on horizontal forest structures since these structures are known to be important mechanisms of resilience in historically frequent-fire forests and since they can more easily be aggregated to characterize coarser resolution structures (Larson and Churchill 2012). Yet, we recognize that vertical canopy arrangements are important structural features in frequent-fire systems as well (North et al. 2009; Ziegler et al. 2017). For example, reduced fuel laddering can reduce the likelihood of crown fire initiation (Agee and Skinner 2005), while within clump variability in tree heights can be a proxy for uneven aged distributions which may engender greater resilience to bark beetle outbreaks (Restaino et al. 2019). While not explicitly evaluated in our analyses, past research suggests that the ICO patterns observed in contemporary reference sites in the Sierra Nevada are indeed characterized by reduced lower strata canopy cover and higher variability in tree heights both within and among tree clumps (Kane et al. 2014; Kane et al. 2015b; North et al. 2017;

Kane et al. 2019). Therefore, we expect similar patterns in the reference sites analyzed in the present study. Additional summaries of vertical structure metrics across reference sites are also provided in the supplemental Data in Brief paper (Chamberlain et al. 2023c).

While ALS data enables high fidelity and extensive characterization of overstory canopy structures across reference sites, these ALS datasets also have several limitations. For example, a single tree segmented from ALS data may realistically represent multiple on-the-ground trees if the segmentation algorithm fails to separate interlocked canopies and subordinate trees, hence our use of the term 'tree approximate objects' (TAOs) (Jeronimo et al. 2018). Because of this, our metrics related to tree clumping patterns should be interpreted as broad trends. Since one TAO may represent several on-the-ground trees (especially those falling under the canopy of larger trees), we expect that our clumping metrics tend to report smaller clump sizes than would be expected from *in situ* field measurements that include lower-canopy trees (Jeronimo et al. 2018; Wiggins et al. 2019). This assertion is justified by comparing our clumping metrics against tree spatial patterns recorded in historical datasets which generally reported larger clump sizes (Lydersen et al. 2013).

We also acknowledge the inability of ALS data to characterize and quantify species composition and surface fuel conditions, which are certainly important factors that influences forest resilience (Lydersen et al. 2013; Prichard et al. 2017; Bernal et al. 2022). Based on the occurrence of multiple low- to moderate-severity fires in the contemporary reference sites, we contend that these sites are likely dominated by more fire-resistant species like ponderosa pine, Jeffrey pine, and Douglas-fir (Safford and Stevens 2017), and that surface fuel loading is reduced compared to control sites. Still, we encourage future research that explicitly maps and quantifies species and surface fuels in contemporary reference sites, especially as climate change continues to influence post-fire tree recruitment and overstory tree survivorship (Liang et al. 2017; Davis et al. 2023).

1.6. CONCLUSION

In yellow pine and mixed-conifer (YPMC) forests of California's Sierra Nevada, more than a century of fire suppression and long-term shifts in land management practices have led to considerable changes in forest processes and structures (Collins et al. 2011a; Knapp et al. 2013). In recent years, these altered conditions, coupled with climate change, have brought a new fire regime to the Sierra Nevada, characterized by larger and often more severe fires than historical conditions (Stevens et al. 2017; Williams et al. 2019; Williams et al. 2023). However, this changing fire landscape has also enabled the formation of several contemporary reference sites across the Sierra Nevada where repeated low/moderate-severity fires have occurred in recent decades, and thus a frequent, low-severity fire regime has begun to reestablish in the modern era (Jeronimo et al. 2019; Cova et al. 2023). In this study, we analyzed forest structural patterns at multiple scales in contemporary reference sites and compared structures against typical fire-suppressed control sites to identify key structures produced by a contemporary frequent low-severity fire regime.

We observed a nested and hierarchical set of structural patterns across reference sites that indicate a stabilizing effect of a frequent, low-severity fire regime across broad, ecosystem scales. High proportions of individual TAOs, small clumps of TAOs, and open space formed intermediate and open ICO structures at the neighborhood-level, and these structures were consistently arranged in heterogenous spatial patterns across all reference sites. In fire suppressed control sites, edaphic factors and other non-fire disturbances produced variability in structures at different spatial scales, but this structural variability was not as consistent compared to reference sites. Importantly, control sites with higher proportions of closed canopy structures and low site-level heterogeneity indices could be prioritized in regional restoration planning efforts to ensure treatment of higher-risk areas. We encourage forest and fire managers in the Sierra Nevada to use the multi-scale and hierarchical structural patterns identified in reference sites to inform and guide management across the region.

1.7. APPENDIX A

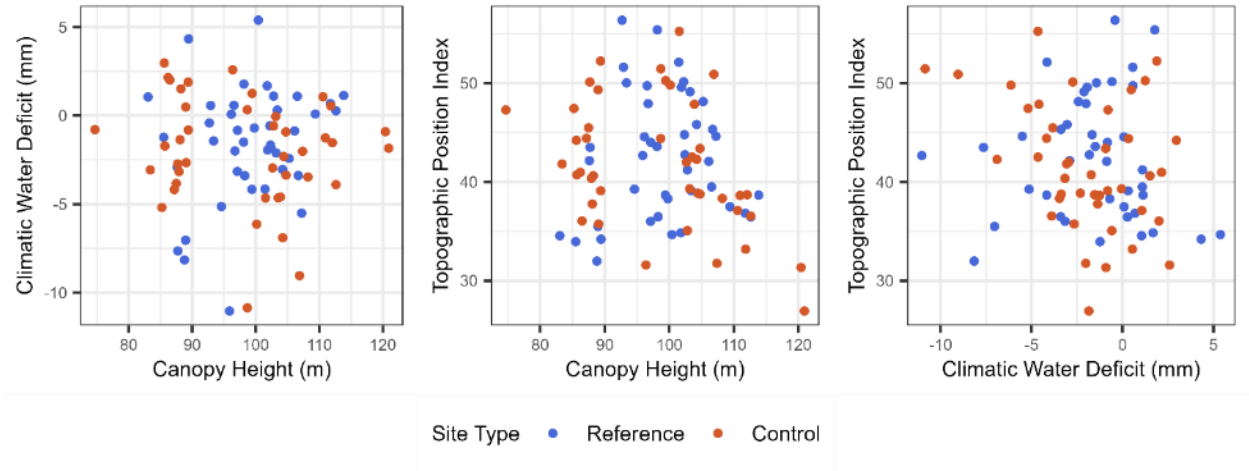

Figure 1.A.1. Scatterplots showing mean canopy height (m) vs. climatic water deficit (mm) vs. topographic position index for reference and control sites. Canopy height represents lidar-derived 95th percentile of tree approximate object (TAO) heights.

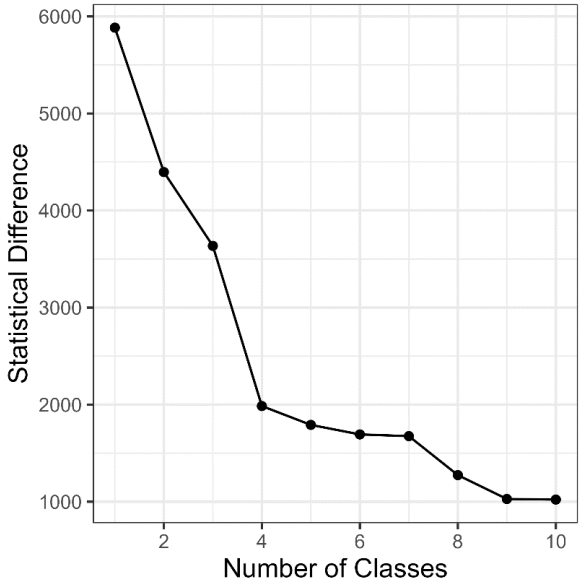

Figure 1.A.2. Scree plot derived from the hierarchical clustering applied to the five ICO structure metrics. Four classes represent an appropriate place to cut the dendrogram as further splitting or grouping does not lead to substantial increases in statistical difference.

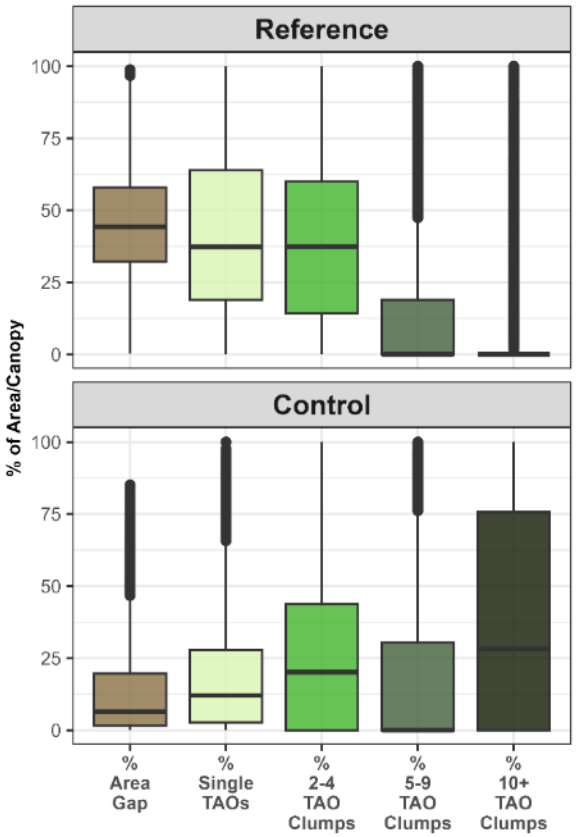

Figure 1.A.3. Distributions of neighborhood-level (i.e., 90m pixel) structure metrics across reference (top) and control (bottom) sites (% area for area gap metric and % canopy for all other metrics). ICO refers to fine-scale spatial patterns of individual tree approximate objects (TAOs), clumps of TAOs, and open space.

CHAPTER 2. WHEN DO CONTEMPORARY WILDFIRES RESTORE FOREST STRUCTURES IN THE SIERRA NEVADA?

Caden P. Chamberlain, Bryce Bartl-Geller, C. Alina Cansler, Malcolm P. North, Marc D. Meyer, Liz van Wagtendonk, Hannah E. Redford, Van R. Kane

2.1. ABSTRACT

Background: Following a century of fire suppression in western North America, managers use forest restoration treatments to reduce fuel loads and reintroduce key processes like fire. However, annual area burned by wildfire frequently outpaces the application of restoration treatments. As this trend continues under climate change, it is essential that we understand the effects of contemporary wildfires on forest ecosystems, and the extent to which post-fire structures are meeting common forest restoration objectives. In this study, we used airborne lidar to evaluate fire effects across yellow pine and mixed conifer (YPMC) forests of California's Sierra Nevada. We quantified the degree to which forest structures in first-entry burned areas (previously unburned since ~1900s) and unburned controls aligned with restoration targets derived from contemporary reference sites. We also identified environmental conditions that contributed to more restorative fire effects. **Results:** Relative to unburned controls, structural patterns in first-entry burned areas aligned more closely with reference sites. Yet, across all burn severities, first-entry wildfires were only moderately successful at meeting targets for canopy cover (48% total area) and ladder fuels (54% total area), and achieving these targets while also producing tree clump and opening patterns aligning with reference sites was less common (16% total area). Moderate severity patches had the highest proportion of restorative fire effects (55-64% total area), while low and high severity patches were either too dense or too open, respectively. Our models (and publicly-available mapped predictions) indicated a higher probability of restorative effects within 1 km of previous fires, within the mid-

upper climate range of the YPMC zone, and under moderate fire intensities (~1-2 m flame lengths). **Conclusions:** First-entry wildfires can sometimes restore structural conditions by reducing canopy cover and ladder fuels and increasing structural heterogeneity, especially within moderate severity patches. However, these initial fires represent just one step toward restoring dry forest ecosystems. Post-fire landscapes will require additional low- to moderate-intensity fires and/or strategic management interventions to fully restore structural conditions. In yet unburned forests, managers could prioritize mechanical treatments at lower elevations, early-season burning at mid- to high-elevations, and resource objective wildfires in landscapes with mosaics of past wildfires.

2.2. INTRODUCTION

Most of the dry, conifer-dominated forests of western North America adapted under a frequent, low-severity fire regime, where fires historically served to regulate vegetation dynamics and support overall ecosystem function (Falk et al. 2011; Hessburg et al. 2019; Hagmann et al. 2021). Following a century of fire suppression, eradication of Indigenous burning, and recent climate change, contemporary wildfires are increasingly distinguished by large patches of high severity effects (> 75% basal area mortality) (Lydersen et al. 2016; Westerling et al. 2016; Parks and Abatzoglou 2020; Cova et al. 2023), which can have widespread ecological impacts (Coop et al. 2020; Hagmann et al. 2021; Parks et al. 2023). However, while increased high severity fire is a critical management concern, recent work suggests that area burned at low and moderate severity (~20-95% basal area mortality) has also increased considerably over recent decades (> 60% total burned area in California fires 1985-2020) (Lydersen et al. 2016; Cova et al. 2023). These low- to moderate-severity effects highlight an alternate scenario in which first-entry wildfires (those burning for the first time since the start of fire exclusion) may indeed be restoring ecosystem structures and functions as they

return to dry forest landscapes (Meyer 2015; Lydersen et al. 2016; Kane et al. 2019; Churchill et al. 2022).

In the fire-suppressed yellow pine and mixed conifer (YPMC) forests of California's Sierra Nevada, land managers rely on forest treatments to reduce fuel loads, restore key processes like fire, and mitigate the negative impacts of future disturbances and climate change (hereafter referred to as "restoration treatments") (Safford et al. 2012; Forest Management Task Force 2021; North et al. 2022; Hankin et al. 2023). However, annual area burned by wildfires continues to drastically outpace the implementation of restoration treatments in the region (Vaillant and Reinhardt 2017; North et al. 2021), with a documented 6-fold increase in annual area burned over the past two decades (Williams et al. 2019). With trends of increasing annual area burned likely to continue under climate change (Abatzoglou et al. 2019; Williams et al. 2019), it is critical to understand how contemporary fires are impacting forest ecosystems, and the extent to which post-fire structures are aligning with common restoration objectives (North et al. 2015; 2021; Meyer et al. 2021).

Reference conditions have long been used by forest managers to design and evaluate restoration treatments (Moore et al. 1999; Safford and Stevens 2017; Bohlman et al. 2021). These conditions can be derived from historical datasets, palaeoecological reconstructions, traditional knowledge systems, simulations, or contemporary reference sites (Fulé et al. 1997; Lydersen et al. 2013; Collins et al. 2016; Lake et al. 2017). In any case, reference conditions describe ecosystems that are maintained by key processes (*e.g.,* a frequent low-severity fire regime in YPMC forests of the Sierra Nevada) where structural and compositional attributes are expected to be more resilient (*i.e.,* able to resist or recover) under subsequent disturbances and climate change (Landres et al. 1999; Moore et al. 1999; Collins et al. 2016; Jeronimo et al. 2019). Contemporary reference sites offer a promising approach for quantifying reference conditions. These sites are at least partially adapted to contemporary and future climates, and they enable detailed inventories of structure and composition

using modern inventory techniques (*e.g.,* remote sensing) (Collins et al. 2016; Jeronimo et al. 2019; Wiggins et al. 2019; Chamberlain et al. 2023a). These sites have limitations as well; for example, contemporary reference sites in the Sierra Nevada may still reflect some of the residual effects of 20th century fire suppression (Lydersen et al. 2014).

Recent airborne lidar-based assessments have characterized structural conditions across contemporary reference sites in the YPMC zone of California's Sierra Nevada (Jeronimo et al. 2019; Kane et al. 2019; Chamberlain et al. 2023a; 2023c). These lidar-based characterizations may not cover all aspects of functioning ecosystems (*e.g.,* species composition, surface fuel loading, etc.) but they do provide useful targets for key structures that contribute to overall ecosystem function (Jeronimo et al. 2019; Kane et al. 2019). Past work shows that Sierra Nevada contemporary reference sites are characterized by low total canopy cover, tree densities, and ladder fuels (Jeronimo et al. 2019; Kane et al. 2019). Fine-scale spatial patterns reflect mosaics of individual trees, small clumps of trees, and relatively high proportions of open space (*i.e.,* an individual, clump, and opening (ICO) pattern) (Jeronimo et al. 2019; Chamberlain et al. 2023a). These neighborhood-level structural patterns can increase resilience to subsequent fires, droughts, beetle outbreaks, and other disturbances (Larson and Churchill 2012; Churchill et al. 2013; Ritter et al. 2020; Atchley et al. 2021; Steel et al. 2021a; Furniss et al. 2022), while also serving as proxies for other key ecosystem services such as biodiversity and wildlife habitat (Larson and Churchill 2012; Kramer et al. 2021; Stephens et al. 2021). At broader spatial scales, tree densities and ICO patterns vary across topographic and climatic gradients (Lydersen and North 2012; Kane et al. 2015b; Jeronimo et al. 2019; Ng et al. 2020). Cooler climate zones, valleys, and north-facing slopes support more closed canopy structures, while drier climate zones, ridges, and south-facing slopes support more open structures (Jeronimo et al. 2019; Wiggins et al. 2019; Ng et al. 2020). Evaluating the extent to which contemporary wildfires

are shifting forests and landscapes toward these reference conditions represents a critical management objective in the Sierra Nevada (Safford and Stevens 2017; Meyer et al. 2021).

In addition to quantifying the extent and patterns of contemporary fire effects, it is important to understand the environmental factors that influence fire effects so that managers can better plan for and manage future fires (Kane et al. 2019; Huffman et al. 2020). Past work shows that fire effects are governed by complex interactions between broad bioclimatic trends, pre-fire forest structure and composition, fire weather, and topographic factors, as well as the broader landscape context within which an area burns (Sullivan 2017; Parks et al. 2018; Jeronimo et al. 2020). While several studies have begun to quantify environment-fire effects relationships using moderate-resolution (30-m) burn severity indices (Kane et al. 2015a; Parks et al. 2018; Povak et al. 2020; Cansler et al. 2022), fine-resolution (~1-m) airborne lidar datasets support more detailed assessment and comparison of how environmental factors influence resultant post-fire structures (McCarley et al. 2017; Kane et al. 2019).

In this study, we evaluated the extent to which first-entry wildfires contributed to restoring structural patterns in Sierra Nevada YPMC forests. We classified fire effects as restorative when structure metrics aligned with a site's natural range of variation (NRV), based on measures derived from contemporary reference sites (Chamberlain et al. 2023b; 2023c). We focused on three structural components that represent important attributes of functioning YPMC forests and can be measured using airborne lidar: total canopy cover, ladder fuel density, and clump complexity (an index of fine-scale ICO patterns). We also used machine learning to evaluate how various environmental factors influenced restorative fire effects, then mapped modeled predictions under mild and moderate fire weather scenarios for previously unburned areas. We sought to address four primary objectives in our study:

1) Quantify the extent to which contemporary first-entry wildfires have restored forest structural patterns.
2) Evaluate patch size distributions of restored structures resulting from first-entry wildfires.
3) Identify the pre-fire and active-fire (*i.e.,* day-of-burn fire weather) conditions under which first-entry wildfires were most likely to have restorative effects.
4) Map the probability of restorative fire effects across unburned areas in the Sierra Nevada for the year 2020.

2.3. METHODS

We used airborne lidar data to evaluate and compare structural patterns across 55 contemporary reference sites, 35 wildfires, and a set of unburned control sites in the Sierra Nevada YPMC zone (Figure 2.1). We subdivided the reference sites to define topographically and climatically adjusted NRVs for each of our three structure metrics (canopy cover, ladder fuel density, and clump complexity) (Figure 2.2; Table 2.2; Figure 2.3; Table 2.A.2). Post-fire structures and control sites were then assessed as below, within, or above their respective topo-climatic NRV (Objective 1). We also produced three restoration indices to define scenarios in which multiple structure metrics fell within NRV – cover restoration (canopy cover within NRV), partial restoration (canopy cover and ladder fuel density within NRV), and full restoration (all three structure metrics within NRV). We quantified proportions (Objective 1) and patch size distributions (Objective 2) of each of these restoration indices. Next, to identify the environmental conditions that influenced restorative fire effects (Objective 3), we fit and evaluated Random Forest (RF) classification models with full restoration as the response (binary index) and a large set of bioclimatic, fire weather, topographic, pre-fire forest structure, and other metrics as predictors (Table 2.3). Finally, to demonstrate the application of our modeling results, we mapped the probability of the full

restoration index, under two weather scenarios, across all previously unburned areas within the Sierra Nevada YPMC zone in the year 2020 (Objective 4). We performed all primary analyses in R (R Core Team 2023).

2.3.2. STUDY AREA

The Sierra Nevada region is characterized by a mediterranean climate with relatively wet, cold winters and hot, dry summers. YPMC forests span the low to mid montane region of the Sierra Nevada, ranging in elevation from approximately 500 m in the north to 2,500 m in the south. Dominant species include Jeffrey pine (*Pinus jeffreyi* Balf.*)*, ponderosa pine (*Pinus ponderosa* Lawson & C. Lawson*)*, Douglas-fir (*Pseudotsuga menziesii* (Mirb.) Franco var. *menziesii*), sugar pine (*Pinus lambertiana* Douglas), incense-cedar (*Calocedrus decurrens* (Torr.) Florin), and white fir (*Abies concolor* (Gord. & Glend.) Lindl. Ex Hildebr.) with California black oak (*Quercus kelloggii* Newberry) intermixing at lower elevations and red fir (*Abies magnifica* A. Murray bis) and lodgepole pine (*Pinus contorta* Douglas ex Loudon var. *murrayana* (Balf.) Engelm.) intermixing at higher elevations (North et al. 2016; Safford and Stevens 2017). Prior to Euro-American colonization, YPMC forests were characterized by a frequent, low-severity fire regime, driven by natural- and human-ignited fires, with a mean fire return interval of 11-16 years (Taylor et al. 2016; Safford and Stevens 2017; Klimaszewski-Patterson et al. 2024).

To identify the Sierra Nevada YPMC zone, we limited our study area to the intersection of two layers: (1) the Environmental Protection Agency's Level IV Ecoregions dataset (EPA 2023) and (2) the FVEG Wildlife Habitat Relationship classes (FVEG 2015). We buffered the Sierra Nevada ecoregion by 5-km to ensure inclusion of a few contemporary reference sites that fell just north of the official boundary. We then selected five FVEG Wildlife Habitat Relationship codes – Montane Hardwood-Conifer, Ponderosa Pine, Jeffrey Pine, Douglas Fir, and Sierran Mixed Conifer – to represent the YPMC zone (Figure 2.1). We also restricted our analyses to three of the Sierra Nevada

climate zones defined by Jeronimo et al. (2019): Warm Dry Low Montane, Warm Mesic Low Montane, and Cool Dry Mid Montane. Jeronimo et al. (2019) defined these climate classes based on measures of 1981-2010 climatic water deficit, actual evapotranspiration, and January minimum temperature. In our analyses, we used these classes to define climatically adjusted NRVs (see details in section 2.6). The three climate classes used in our study spanned 54% of the total YPMC zone. Other climate classes were excluded from our analyses due to insufficient sample sizes of contemporary reference site pixels (< 500). We also excluded the Foothill Low Montane Transition zone since exploratory analyses revealed that contemporary reference site structures from this zone were questionable compared to other climate zones (Jeronimo et al. 2019; Chamberlain et al. 2023c).

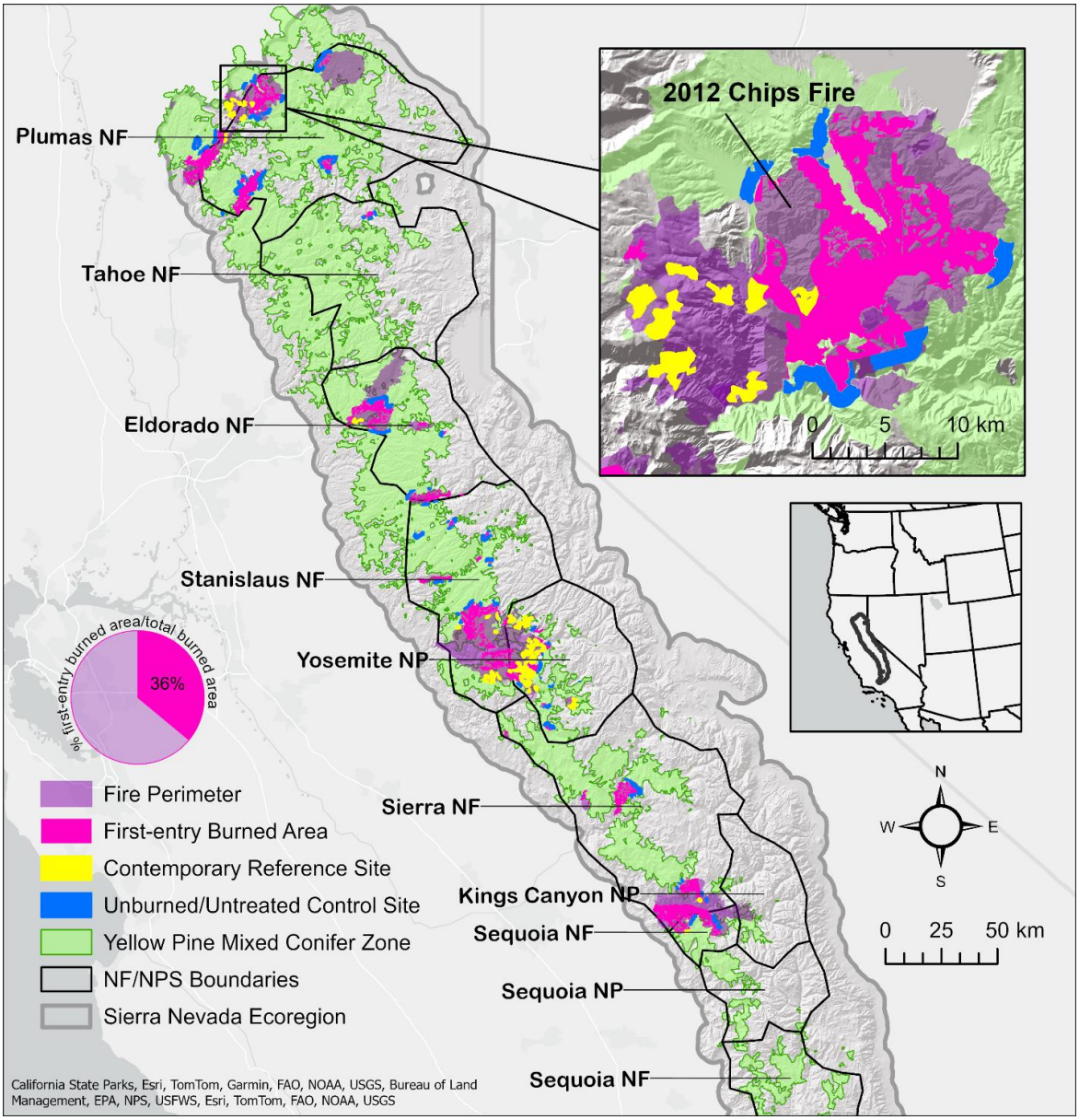

Figure 2.1. Study area showing wildfire perimeters, first-entry burned area within fire perimeters, contemporary reference sites, and unburned and untreated controls (for the year 2015) within the yellow pine and mixed conifer (YPMC) zone in the Sierra Nevada ecoregion, California, USA. Inset shows a close up of the 2012 Chips Fire which contains first-entry burned area and several contemporary reference sites. National Forest and National Park Service boundaries are shown for context, with polygon boundaries smoothed for visualization. The pie chart shows the percentage of first-entry burned area out of total fire area. NF: National Forest; NP: National Park.

2.3.2. DATASETS

CONTEMPORARY REFERENCE SITES

We used a dataset of contemporary reference sites to define NRVs for the three structure metrics. The reference site dataset was described in detail in Chamberlain et al. (2023a) and (2023b), and Jeronimo et al. (2019). These sites primarily cover the YPMC zone and represent areas where a frequent, low-severity fire regime has begun to reestablish after decades of fire suppression (Jeronimo et al. 2019; Chamberlain et al. 2023a). To be identified as a reference area, sites must have experienced at least 2 fires with low- or moderate-severity effects in the last 30 years, with one fire having mostly moderate-severity effects. Sites ranged in size from ~100-1,000 ha and could not have been previously harvested or treated and could only contain small (< 10-ha) patches of high severity (Chamberlain et al. 2023c). The full reference site dataset contains 119 sites. For this study we used a subset of 55 sites (Figure 2.1) that (1) were covered by airborne lidar (section 2.5), (2) burned 5-15 years prior to the lidar acquisition, and (3) were within one of the three Jeronimo et al. (2019) climate classes (described in Section 2.1).

FIRST-ENTRY WILDFIRES

We identified 35 first-entry wildfire polygons (121,730 ha) for our study (Figure 2.1; Table 2.A.1). To do so, we first selected all fire perimeters from CALFIRE's Fire and Resource Assessment Program (FRAP) fire history dataset (FRAP 2021) that intersected our study area excluding prescribed burns. We then subset these fire perimeters to ensure that airborne lidar (described in Section 2.5) had been collected 5-15 years post-fire. A five-year post-fire interval was used to account for lags in post-fire mortality, while a 15-year maximum was selected so that observed forest canopy structures were less likely to be driven by post-fire regeneration (van Mantgem et al. 2011; Jeronimo et al. 2020).

From these fire perimeters, we produced a set of polygons that met two further criteria: (1) were first-entry wildfires and (2) had not previously experienced harvest, thinning, or fuel treatments. First, we masked out all areas within fire perimeters that had previously burned, and where subsequent fires had occurred between the fire date and the lidar acquisition date (FRAP 2021). Next, we masked out previously treated areas from this subset of fire perimeters, and any areas where treatments occurred between the fire date and the lidar acquisition date. Treatment history data was derived from a dataset produced by Knight et al. (2022) for the years 1985-2020 and the Forest Service FACTS database for pre-1985 (see full methods for producing this dataset in Chamberlain et al. 2023c). After applying these masks to all fire perimeters, we discarded any polygons <100 ha so that fire sizes were similar to contemporary reference sites.

UNBURNED CONTROL STIES

We identified a set of unburned and untreated control sites in the year 2015 to serve as a proxy for pre-fire conditions (Figure 2.1). We produced these control sites by creating a buffered region 100-1,000 m outside the perimeters of our analysis fires. As with our fire perimeters, we masked out any areas that had burned or been treated prior to their corresponding lidar acquisition, and we discarded any final polygons <100 ha. Based on these criteria, not all analysis fires had a corresponding control, so the resulting dataset represents unburned conditions for the full study area.

2.3.3. MEASURING FOREST STRUCTURE WITH AIRBORNE LIDAR

We used point cloud data from six airborne lidar acquisitions (Table 2.1) to measure forest structures within our reference sites, analysis fires, and control sites (Figure 2.2). Mean pulse density ranged from 12.6 m^{-2} (Tuolumne County) to 28.0 m^{-2} (Eldorado National Forest), representing data suitable for vegetation-related research using airborne lidar (*i.e.,* meeting the United States

Geological Survey's Quality Level 1 (Mitchell et al. 2018)) (Table 2.1). We used the Forest Service's FUSION software (McGaughey 2020) to process all six airborne lidar acquisitions and produce metrics of (1) canopy cover for all vegetation ≥2 m (hereafter, canopy cover), (2) relative canopy cover in the 2-8 m height stratum (hereafter, ladder fuel density), and (3) canopy fractal dimension index (hereafter, clump complexity) (Table 2.2; Figure 2.2). We produced all metrics at 90-m resolution since past research suggests that fine-scale tree clump and opening patterns generally emerge at approximately this scale in fire-adapted forests (Larson and Churchill 2012; Knapp et al. 2017). We first normalized point clouds so that Z coordinates represented vegetation height above ground. We also produced 0.75-m canopy height models (CHMs) from the normalized point clouds, which were smoothed using a 3x3-cell mean filter.

Table 2.1. Statistics for six airborne lidar acquisitions ordered from north to south, covering portions of the Sierra Nevada ecoregion, California, USA. NF: National Forest; NP: National Park.

Acquisition name	Years flown	Total area (ha)	Mean pulse density (pulse m^{-2})
North Plumas NF	2018	466,774	13.3
South Plumas NF	2018	560,370	12.6
Eldorado NF	2019	577,109	28.0
Tuolumne County	2018-2019	694,330	15.3
Yosemite NP	2019	369,824	23.5
SSARR (Sierra NF)	2020	569,810	22.0

We used established methods for quantifying canopy cover (Kane et al. 2014; Kane et al. 2023) and ladder fuel density (Kramer et al. 2014; Hankin and Anderson 2022). For clump complexity, we developed a modified version of the FRAGSTATS fractal dimension index (McGarigal and Marks, 1995). The original index describes, on average, the degree of fragmentation of patches within an area of interest. Our modified version is more computationally efficient and describes the degree of fragmentation of the entire canopy area within a 90-m pixel. Exploratory analyses (see Figure 2.A.1) revealed that this clump complexity index was closely related to the fine-

scale tree clump and opening patterns previously identified in the contemporary reference sites (Chamberlain et al. 2023a). As shown in Figure 2.A.1, low clump complexity values (~ < 1.3) suggest structures dominated by large contiguous tree clumps, moderate values (~1.3-1.6) suggest fine-scale patterns of individual trees and small clumps of trees with high proportions of open space (an ICO pattern), and high values (~ > 1.6) indicate very low canopy cover composed primarily of standing snags within high-severity burn patches (Figure 2.A.1).

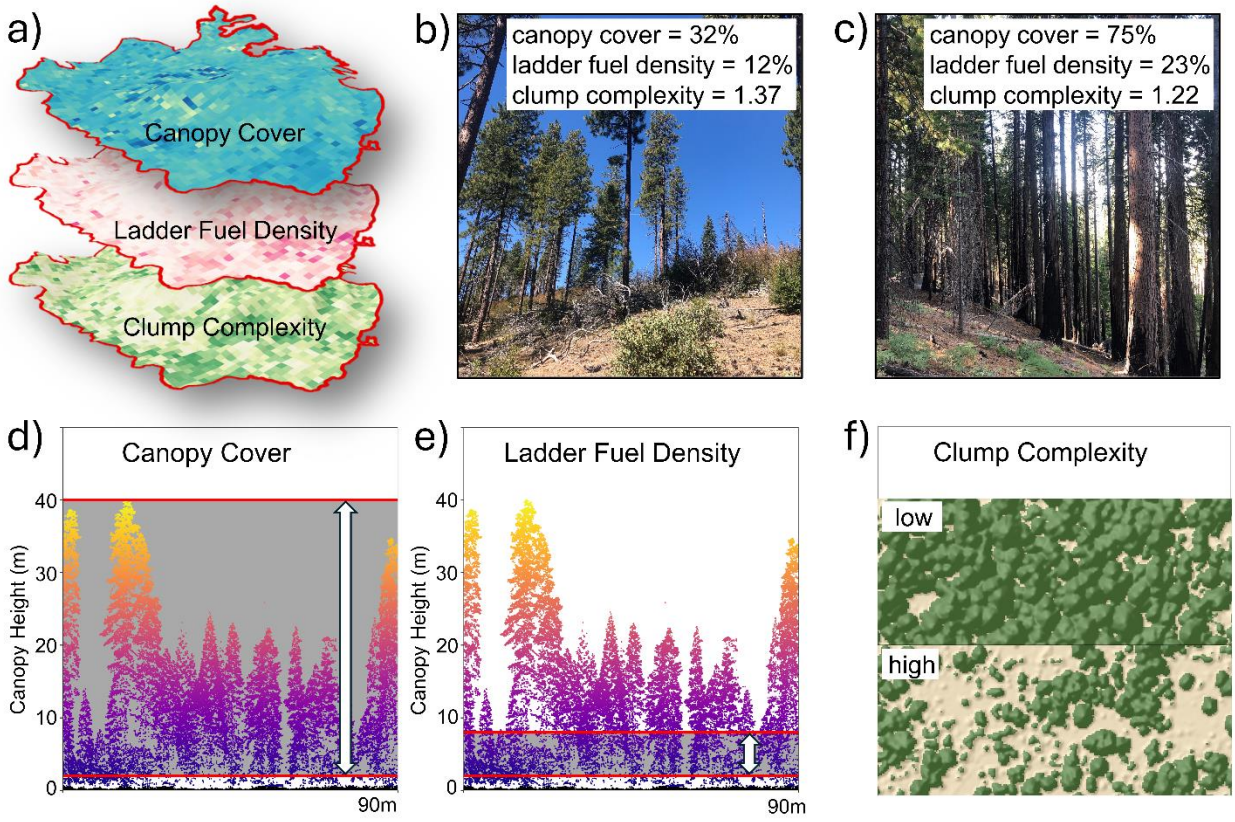

Figure 2.2. Visualizations and photos of the three airborne lidar-derived structure metrics that represent key forest structures in yellow pine and mixed conifer forests of the Sierra Nevada, California, USA. (a) Example 90-m resolution rasters of each metric within the 2,036-ha 2004 Meadow Fire. (b) Photo of site that met the full restoration index (canopy cover, ladder fuel density, and clump complexity all within the natural range of variation (NRV)) in the Plumas National Forest in summer 2023. (c) Photo of site that fell outside NRV for each metric on the Stanislaus National Forest in summer 2023. Cross-section of lidar point cloud shows how (d) canopy cover and (e) ladder fuel density metrics were computed from airborne lidar point clouds. (f) Illustration of low and high clump complexity values for a top-down view of a canopy height model. Photo credits: Caden Chamberlain.

Table 2.2 Equations and ecological importance for the three airborne lidar-derived structure metrics that represent key structural conditions in Sierra Nevada YPMC forests, California, USA.

Metric name	Computation	Ecological importance	Range	Units
Canopy Cover	$\frac{\sum_{i=1}^{n} z_i \geq 2}{n}$ Where n is the number of points in the 90-m cell and z_i is the height above ground of the i^{th} point; units in meters	Higher canopy cover leads to higher crown fire spread rates and increased water stress and competition which relate to fire and drought resistance; lower canopy cover relates to increased area gap which increases likelihood of successful post-fire regeneration	0-100	Percent
Ladder Fuel Density	$\frac{\sum_{i=1}^{n} 2 \leq z_i < 8}{\sum_{i=1}^{n} z_i < 8}$ Symbols defined as above	Higher ladder fuel density suggests higher density of short, sub-canopy trees, which results in higher likelihood of crown fire initiation	0-100	Percent
Clump Complexity	$\frac{2 \ln(0.25 \sum_{i=1}^{n} P_i)}{ln(\sum_{i=1}^{n} A_i)}$ Where n is the number of canopy patches in the 90-m cell, P_i is the perimeter of the i^{th} patch, and A_i is the area of the i^{th} patch; modified version of FRAGSTATS FRAC metric which improves computational efficiency	Clump complexity provides a single-metric proxy for describing fine-scale patterns of individual trees, clumps of trees, and openings which are essential to frequent-fire forest structures; moderately high complexity (~1.3-1.6) leads to reduced crown fire initiation and spread rates, and increased post-fire regeneration; moderate clump complexity also suggests improved wildlife habitat and biodiversity	Approx. 1-2	Unitless; high values = increased complexity

2.3.4. QUANTIFYING THE EXTENT OF RESTORATIVE FIRE EFFECTS

We defined NRVs from the lidar-derived structure layers spanning the 55 reference sites (Figure 2.3; Table 2.A.2). We subdivided the reference sites by climate and topographic classes to account for variability in forest structure across these gradients. For climate classes, we used the three Jeronimo et al. (2019) classes described in Section 2.1. We then subdivided each climate class into four topographic classes using the land management units (LMUs) defined by Underwood et al. (2010) which include ridges, valleys, southwest-facing slopes, and northwest-facing slopes. Each NRV was then defined as the inner 68% (1 standard deviation around the mean) of the distribution of reference values for a given structure metric, within each topo-climatic class. This process resulted in 12 topo-climatic NRVs for each structure metric (Figure 2.3; Table 2.A.2). Defining NRVs as +/- 1 SD from the distribution mean is recommended when adequate sample sizes are

possible and is similar to the "range of means" approach that has previously been used to define the historical range of variation for dry forest ecosystems (Safford and Stevens 2017; Bohlman et al. 2021).

We evaluated and compared the extent to which first-entry wildfire and control sites aligned with topographically and climatically matched NRVs for each structure metric. Specifically, we matched all first-entry wildfire and control pixels with NRVs from the same topo-climatic classes, then evaluated whether pixels fell below, within, or above NRV for each structure metric. Prior to comparing first-entry wildfire and control sites, we balanced the number of samples between first-entry and control sites in each topo-climatic class (randomly sampling from first-entry wildfire and control samples to reach the minimum sample size for a given class) to ensure similar representation of biophysical conditions.

We defined two sets of summary statistics: (1) for individual structure metrics and (2) for each of the restoration indices described in section 2.1 (cover, partial, and full restoration). For individual structure metrics, we measured the proportion of total burned area or control area that fell below, within, or above NRV. For the restoration indices, we measured the proportion of total burned area or control area that either met the criteria or did not (*i.e.,* binary indices). We selected the three restoration indices as they represent a gradient of increasingly restored conditions, each of which may be an acceptable measure of restoration under certain circumstances. We also plotted raw distributions of structure metrics across each topo-climatic class and split by first-entry wildfire, reference site, and control sites in Figure 2.A.2 for more detailed interpretations.

Finally, we assessed how summaries of individual structure metrics and restoration indices varied across commonly used spectral measures of burn severity classes. We produced rasters of the Composite Burn Index (CBI) for each of our analysis fires using Google Earth Engine scripts

developed by Parks et al. (2019). We used the bias-corrected CBI outputs from their script, then classified rasters as low (0.1-1.24), moderate (1.25-2.24), and high (2.25-3.0) severity.

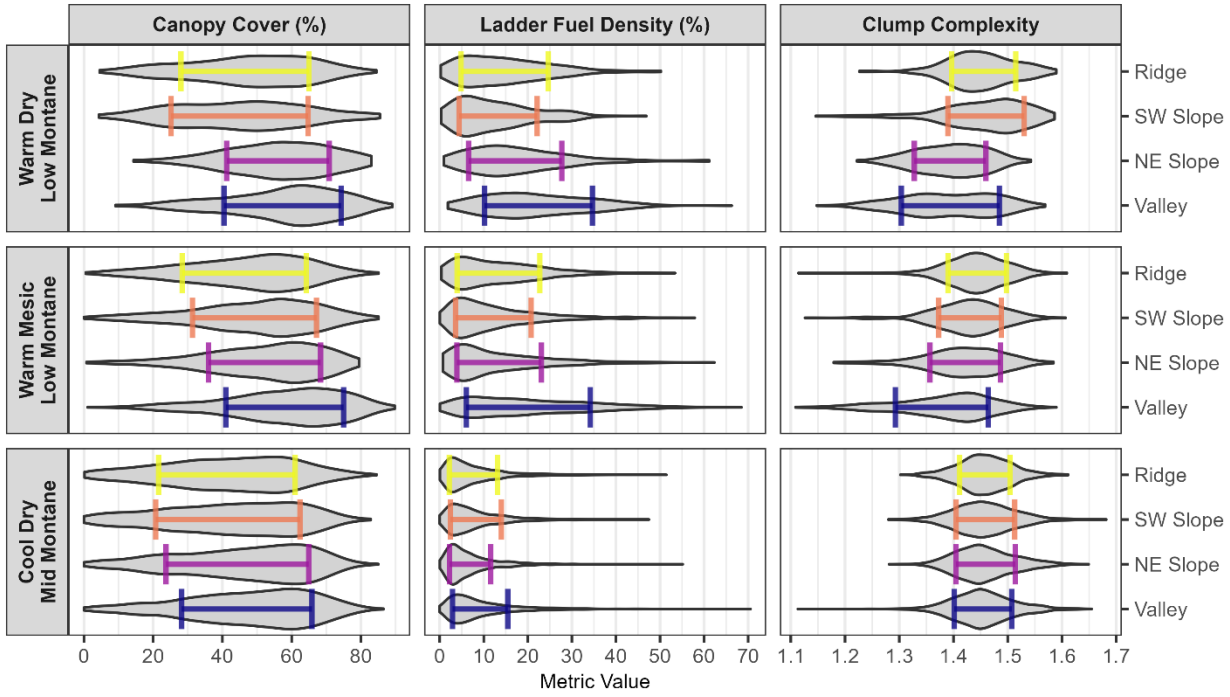

Figure 2.3. Natural Ranges of Variation (NRV) as defined from contemporary reference sites for three airborne lidar-derived structure metrics across three climate classes and four topographic classes in the Sierra Nevada ecoregion, California, USA. We defined NRVs (colored bars) as the inner 68% of the full distribution of each metric for each unique topo-climatic class, with full distributions shown in grey violin plots. SW, southwest; NE, northeast

2.3.5. SPATIAL PATTERNS OF RESTORATIVE FIRE EFFECTS

To understand the landscape spatial patterns of restorative fire effects, we evaluated the spatial distribution and arrangement of contiguous patches of the three restoration indices. We defined patches of each restoration index using an 8-neighbor rule based on adjacency of like-cells. Then for each restoration index, we reported total counts of different patch sizes, as well as cumulative distribution curves of total patch area across the full extent of our analysis fires.

2.3.6. DRIVERS OF RESTORATIVE FIRE EFFECTS

To evaluate the drivers of restorative fire effects, we fit RF classification models predicting the full restoration index (as a binary response) using a set of predictor variables describing pre- and active-fire burning conditions. In other words, we evaluated how pre- and active-fire burning conditions influenced the probability that post-fire structures simultaneously met canopy cover, ladder fuel density, and clump complexity targets. We conducted all modeling using the *tidymodels* package (Kuhn and Wickham 2020).

We first compiled a large set of predictor variables spanning all areas within our analysis fire perimeters. These predictors captured a range of conditions that were likely to influence fire behavior and effects, including bioclimatic, fire weather, topographic, and pre-fire forest structure, as well as four landscape context variables (*e.g.,* distance to past fires). Full descriptions of all 34 predictor variables are provided in Supplemental Methods 1 and Table S3, while the 13 predictors included in the final model (post-variable reduction) are described in Table 2.3. We describe our full variable reduction procedure in Supplemental Methods 2.

Table 2.3. Continuous predictor variables used in final random forest (RF) model predicting the full restoration index for first-entry burned sites in the Sierra Nevada ecoregion, California, USA. Variables represent the subset of all predictors post-variable reduction, listed in order of importance, first by category then by variable. Full variable list provided in Table S1. PRECIP: average annual precipitation; CWD: climatic water deficit; TPI: topographic position index; DEM: digital elevation model.

Data category	Variable name	Variable description	Resolution (m)	Units	References
Landscape Context	Distance to Past Fire	Distance to nearest previous fire	90	m	FRAP 2021; Hijmans et al. 2023
	Distance to Water	Distance to nearest river, stream, or lake	90	m	Hijmans et al. 2023
	Distance to Treatment	Distance to nearest prior treatment	90	m	Knight et al. 2022; Hijmans et al. 2023

	Distance to Roads	Distance to nearest national, state, or Forest Service road	90	m	Hijmans et al. 2023
Climate	Elevation	Elevation	10	m	USGS 2022
	PRECIP 1981-2010	Mean annual total precipitation across years 1981-2010	270	mm	Flint et al. 2021
	Fire Resistance Score	Community fire resistance score	250	continuous numeric	Stevens et al. 2020
	CWD 1981-2010	Mean climatic water deficit across years 1981-2010	270	mm	Flint et al. 2021
Topographic	Topographic Position Index (TPI) 510-m	Topographic position index derived from USGS 10-m DEM using a 510-m window; lower values represent moderate-scale valleys and higher values represent moderate-scale ridges	30	unitless	USGS 2022; Evans and Murphy 2021
	Topographic Ruggedness	Topographic ruggedness index derived from USGS 10-m DEM using a 130-m window; 0-80 = level terrain; 81-116 = nearly level surface; 117-161 = slightly rugged surface; 162-239 = intermediately rugged surface; 240-497 = moderately rugged surface; 498+ = highly-extremely rugged surface	30	unitless	USGS 2022; Evans and Murphy 2021
	Solar Radiation Index	Solar radiation index derived from USGS 10-m DEM; 0 is land oriented in north-northeast direction, 1 is land oriented in south-southwest direction	30	unitless	USGS 2022; Evans and Murphy 2021
Fire Weather	Burning Index	Index of fire intensity; "combines the spread component and energy release component to relate to the contribution of fire behavior to the effort of containing a fire"	30	unitless	Abatzoglou 2013
Forest Structure	Diameter Diversity Index	"measure of the structural diversity of a forest stand, based on tree densities in different DBH classes"	30	continuous index	GNN 2023

We produced a grid of sample points across our analysis fires using the centroid of each cell in the full restoration layer. We then subsampled this grid so that sample points were spaced ≥270 m

apart to reduce effects of spatial autocorrelation in our modeling (Kane et al. 2015a; Povak et al. 2020; Cansler et al. 2022). We also discarded all sample points that fell within a 30-m buffer of any roads or powerlines. We extracted the 13 continuous predictor variables (Table 2.3) to our sample points to create a final modeling dataset and balanced that dataset on the binary full restoration response. Our final modeling dataset had 1,844 observations. We used the full model dataframe to tune hyperparameters using 5-fold cross validation. We tuned all possible hyperparameters for RF models that were available from the *ranger* engine (Wright and Ziegler 2017), using the *tune_race_anova* function from the finetune package (Kuhn 2023). We computed overall model accuracy as the mean accuracy across all five cross-validation folds for the optimized models. Lastly, we fit a final RF model using the full modeling dataframe, and computed permutation importance for each predictor variable. We also produced partial dependence plots (PDPs) for each predictor using the *DALEXtra* package (Maksymiuk et al. 2020). We provide PDPs for the top 6 predictor variables. We provide the full set of 13 PDPs for all predictors in Figure 2.A.3, and two-variable PDPs to show the interaction between burning index and other top predictors in Figure 2.A.4.

2.3.7. MAPPING THE PROBABILITY OF RESTORATIVE FIRE EFFECTS

We used the final RF model to predict and map the probability of restorative fire effects (full restoration) across all previously unburned areas in the Sierra Nevada YPMC zone for the year 2020. We began by producing a polygon representing potential first-entry wildfire area for year 2020 using the CALFIRE FRAP fire history dataset (FRAP 2021). This was accomplished by masking out all areas that had burned prior to or during 2020 (but did not account for areas that burned after 2020). Next, we compiled all predictor variable rasters covering this potential first-entry wildfire area. We then predicted the probability of restorative fire effects (full restoration) across this region and classified it as a binary outcome using a 0.5 threshold. We made predictions under two fire weather scenarios, mild and moderate, by setting burning index at its 25th and 75th percentile, which

represented burn indices of 53 and 71, respectively. Finally, to improve visualizations of mapped outputs across the full Sierra Nevada, we aggregated 90-m pixel predictions to the national NHDPlusV2 catchments dataset (EPA 2021) using the majority class prediction within each catchment. We provide mapped predictions of the cover only and partial restoration indices in Figure 2.A.5 and 2.A.6, respectively. We have also made raster layers of the mapped predictions publicly available in a Zenodo Digital Repository (https://doi.org/10.5281/zenodo.12802224).

2.4. RESULTS

2.4.1. EXTENT OF RESTORATIVE FIRE EFFECTS

Across all topo-climatic classes within the contemporary reference sites, canopy cover NRVs ranged from 21.56% to 74.99%, ladder fuel density ranged from 2.18% to 34.66%, and clump complexity ranged from 1.29 to 1.53 (Figure 2.3; Table 2.A.2). Generally, ridges and southwest-facing slopes had lower targets for canopy cover and ladder fuel density and higher targets for clump complexity. In contrast, valleys and northwest-facing slopes were characterized by higher canopy cover and ladder fuel densities and lower clump complexities. Additionally, canopy cover and ladder fuel density NRVs were lower and clump complexity NRVs were higher within the Cool Dry Mid Montane zone, relative to the Warm Dry Low Montane and Warm Mesic Low Montane zones (Figure 2.3; Table 2.A.2)).

For all three structure metrics, first-entry wildfires produced higher proportions of area within NRV relative to the unburned control sites (a proxy for pre-fire conditions) (Figure 2.4a). First-entry wildfires were most successful at achieving NRV targets for ladder fuel density (54% total area; 32% more area within NRV than controls), followed by canopy cover (48% total area; 13% more area within NRV than controls), and then by canopy complexity (41% total area; 11% more area within NRV than controls). Patches of moderate severity contained considerably higher proportions of area

within NRV for all three individual structure metrics (55-64%), compared to patches of low or high severity. Although 48% of low severity patches had ladder fuel densities within NRV, canopy cover fell above NRV across 50% of sites and clump complexity fell below NRV across 58% of sites. Conversely, in high-severity patches, although ladder fuel densities were often within NRV (57% total area), canopy cover was below NRV across 68% of sites and clump complexity was above NRV across 68% of sites (*i.e.,* loss of fine-scale heterogeneity) (Figure 2.4a).

Across all three restoration indices (representing a gradient of restored structures), first-entry burned areas consistently had higher proportions within NRV relative to unburned controls – 13%, 18%, and 11% higher proportion within NRV for cover, partial, and full restoration, respectively (Figure 2.4b). However, it remained relatively uncommon for first-entry wildfires to simultaneously produce two, and especially three, structural characteristics within NRV. For example, only 27% of first-entry burned area met the partial restoration target (*i.e.,* restoring both canopy cover and ladder fuels) and only 16% met the full restoration target (*i.e.,* restoring all three structure metrics) (Figure 2.4b). Patches of moderate severity had the highest proportion of total area within NRV across all three levels of restoration, with 37% and 24% of total area meeting the partial and full restoration targets, respectively (Figure 2.4b).

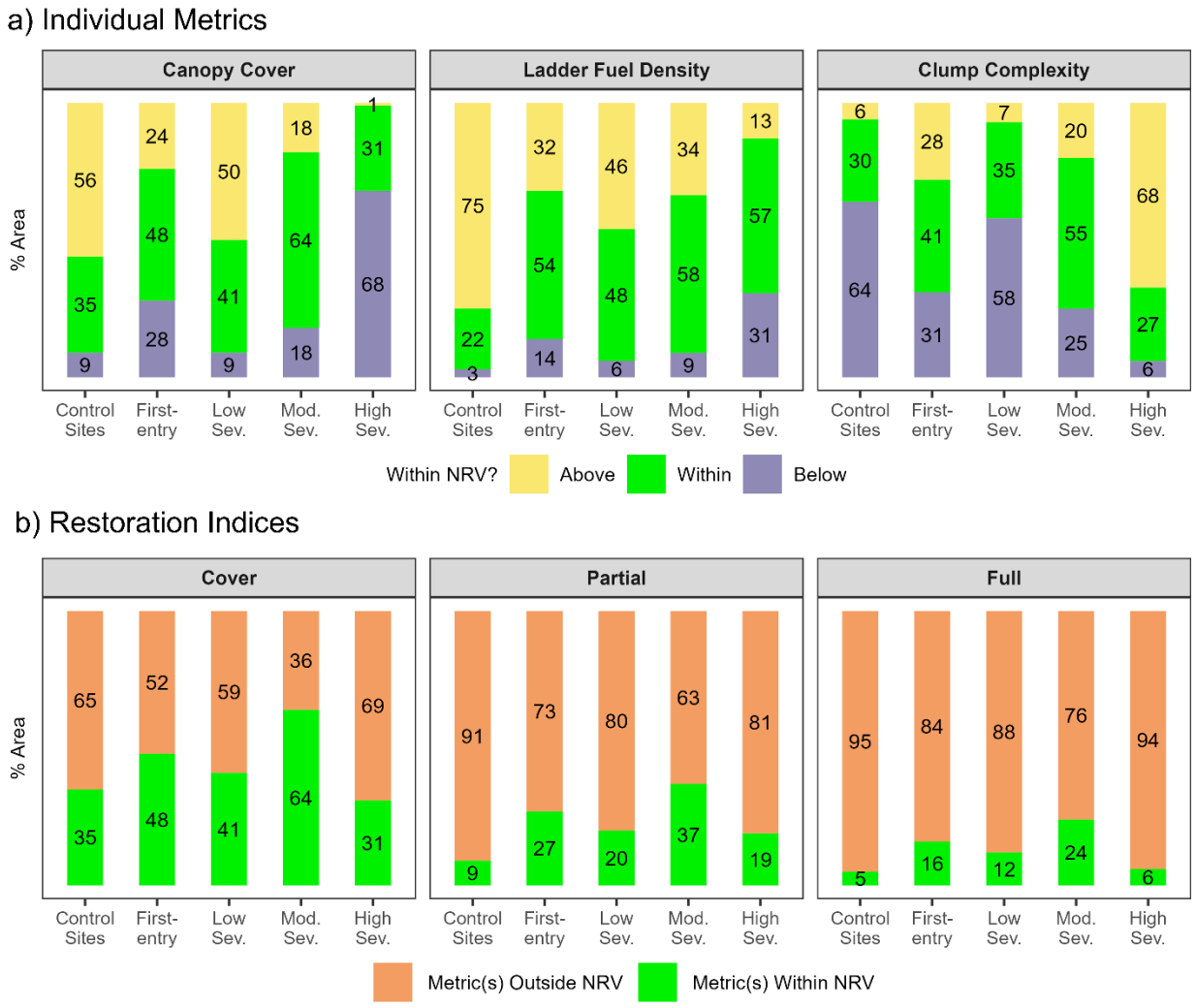

Figure 2.4. (a) Percent of total area above, within, or below the topographically and climatically adjusted natural range of variation (NRV) for individual metrics and (b) percent of total area meeting each of the restoration indices for sites in the Sierra Nevada ecoregion, California, USA. Cover index signifies only cover within NRV, partial index signifies canopy cover and ladder fuel density within NRV, and full index signifies canopy cover, ladder fuel density, and clump complexity within NRV. X-axes show proportions by control area (a proxy for pre-fire conditions), all first-entry burned area, and patches of low- (0.1-1.24), moderate- (1.25-2.24), and high- (2.25-3) severity effects as defined using Composite Burn Index (CBI). Burn severity patches were defined using an 8-neighbor rule; proportions are only representative of first-entry area completely within burn severity patches. Mod: moderate; NRV: natural range of variation.

2.4.2. SPATIAL PATTERNS OF RESTORATIVE FIRE EFFECTS

Across all analysis fires in our study, first-entry wildfires produced relatively small patches of restored structures, which were interspersed within larger patches where post-fire structural conditions were either above or below NRV targets (Figure 2.5). For all three restoration indices, patches of restorative effects were dominated by small (< 10-ha) patches, with low total counts of 10-500-ha patches. Patches of the cover restoration index were larger compared to patches of the partial and full restoration indices (Figure 2.5a). For the cover only index, patches > 100 ha contributed to 55.8% of total patch area, suggesting a high proportion of large contiguously restored area. Conversely for the partial and full restoration indices, patches > 100 ha contributed to only 25.2% and 5.2% total patch area (Figure 2.5b), respectively, indicating that first-entry wildfires were dominated by small, interspersed patches of partially and fully restored sites, as shown in Figure 2.5c.

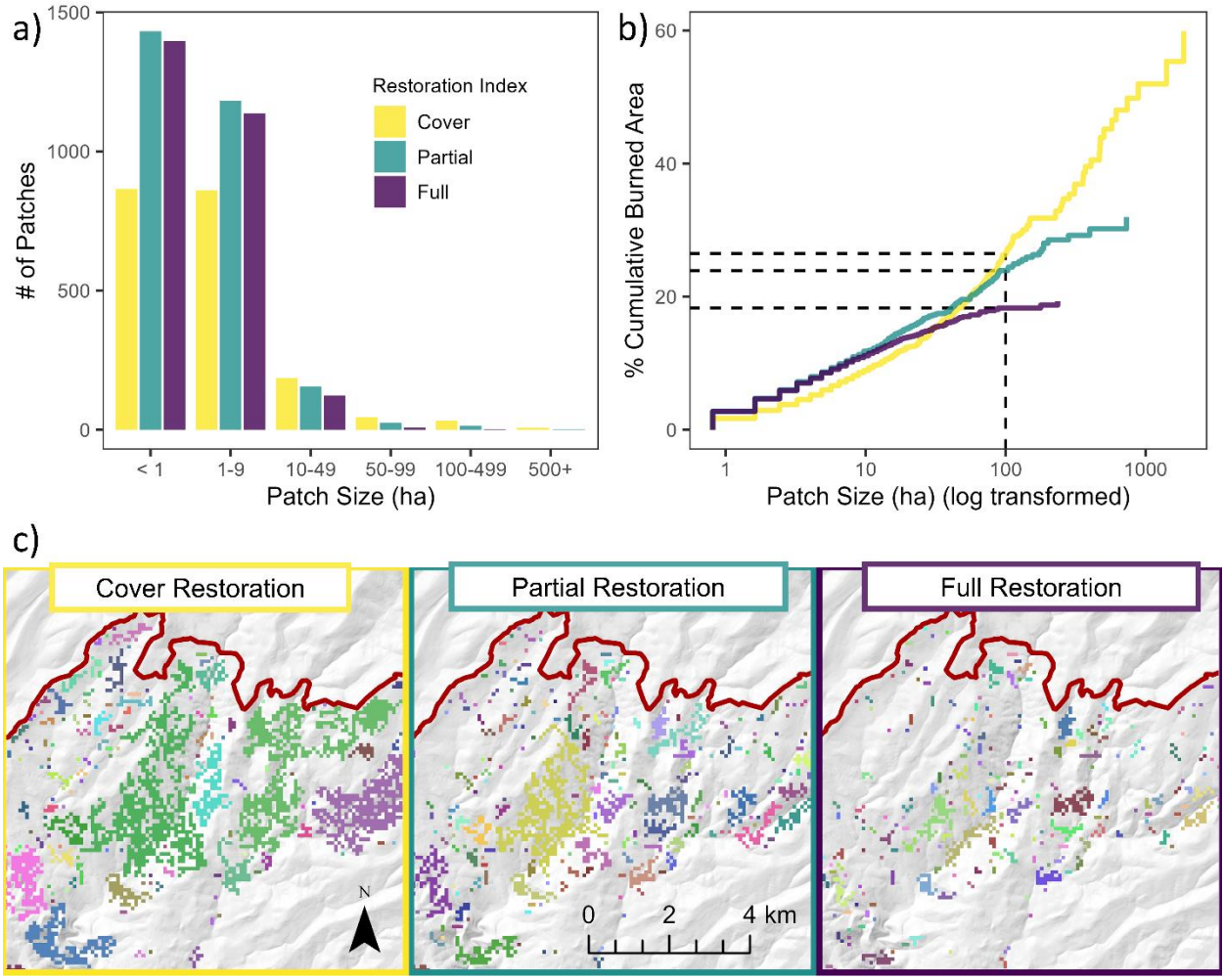

Figure 2.5. (a) Patch size distributions and (b) cumulative patch area distributions for patches of restorative fire effects under three restoration indices – cover restoration (canopy cover only), partial restoration (canopy cover plus ladder fuel density), and full restoration (canopy cover plus ladder fuel density plus clump complexity), for sites in the Sierra Nevada ecoregion, California, USA. (c) Visualizations of patch sizes and spatial distributions under each restoration index within the northern portion of the 2013 Rim Fire, where each color represents a distinct patch. We transformed patch sizes on the y-axis in plot b for visualization. We defined contiguous patches using the 8-neighbor rule for adjacent pixels of like-classes. Dashed lines mark the cumulative proportion of total burned area for each restoration index at a patch size of 100 ha to assist in interpretation.

2.4.3. DRIVERS OF RESTORATIVE FIRE EFFECTS

Our models had an overall prediction accuracy of 62.1%, indicating that pre- and active-fire conditions had a moderate influence on the probability of full restoration. Distance to past fire, a

measure of the landscape context within which an area burned, had the strongest influence on the probability of restorative fire effects. Important bioclimatic and fire weather influences included elevation, long-term (1981-2010) mean annual precipitation, and day-of-burn burning index, representing top-down influences. Important bottom-up drivers included topographic position index and pre-fire diameter diversity index (Figure 2.6a).

We observed a mix of both linear and non-linear relationships between restorative fire effects and the top landscape context, bioclimatic, fire weather, topographic, and forest structure metrics (Figure 2.6b). We found that the probability of restorative fire effects declined as distance to past fire increased (with a distinct threshold at ~1 km) and as fire weather became moderate to extreme (burning index > 60). We also found that higher elevations (~ > 1500 m) and sites within the mid-range of long-term annual precipitation had the highest probability of restorative effects. Finally, we observed that valleys tended to support more restorative fire effects compared to ridges and slopes, as well as sites with higher (> 5) pre-fire diameter diversity index (Figure 2.6b).

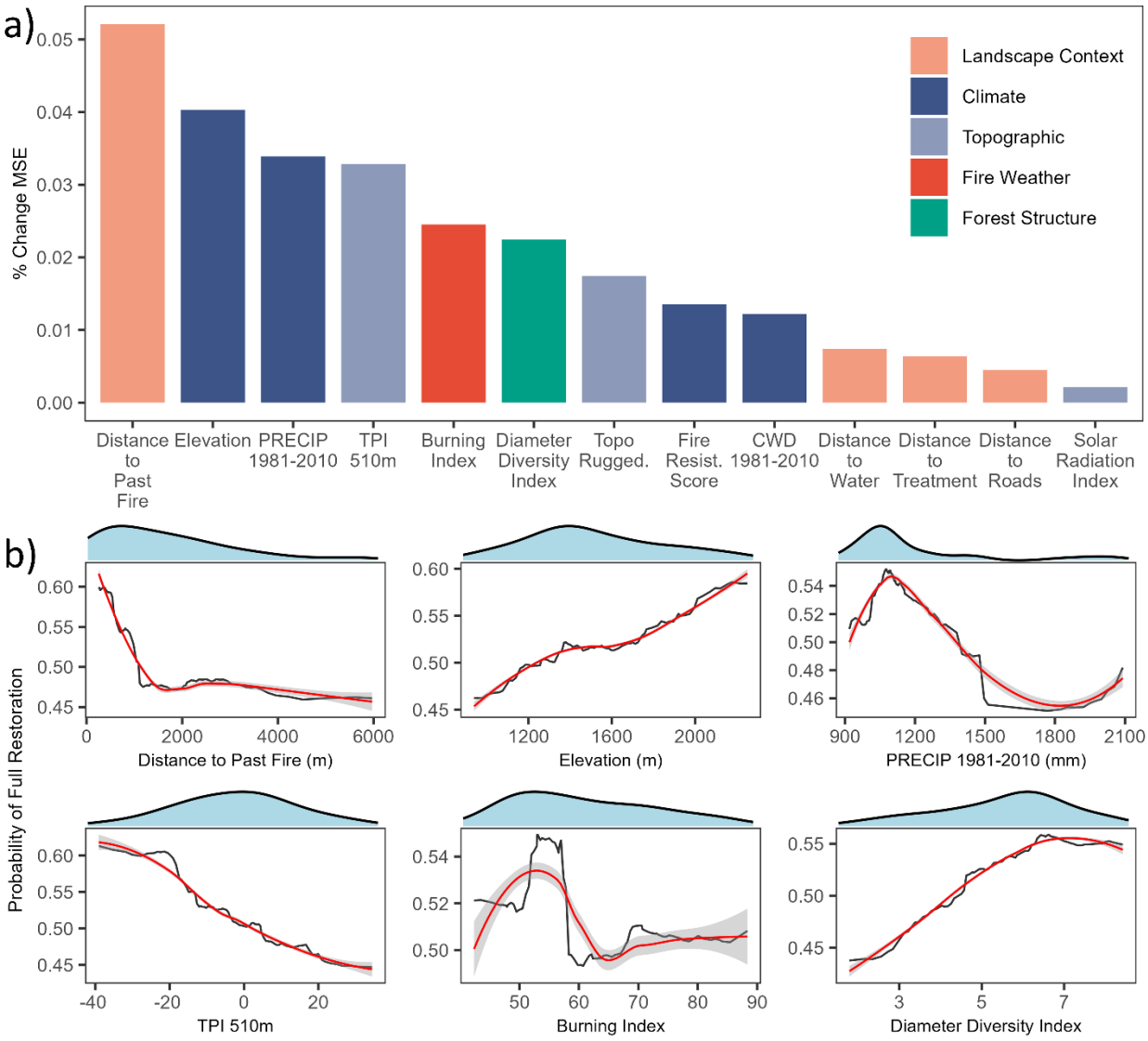

Figure 2.6. (a) Variable importance and (b) partial dependence plots (PDPs) from the final Random Forest model predicting the full restoration index (*i.e.,* canopy cover, ladder fuel density, and clump complexity all within the natural range of variation (NRV)) as a binary response. Models represent conditions in the Sierra Nevada ecoregion, California, USA. Variable importance plots colored by variable categories. We only show PDPs for the top six most important predictors (PDPs for all predictor variables are provided in Figure 2.A.3). Black line shows predictions, while red line shows loess smooth with standard error in grey. Density plots in blue show counts of observations across the range of values for each variable. PRECIP, average annual precipitation; TPI: topographic position index; CWD: average annual climatic water deficit.

2.4.4. MAPPED PROBABILITY OF RESTORATIVE FIRE EFFECTS

We found that 48% of previously unburned areas in the year 2020 would be likely to experience restorative fire effects under moderate fire weather conditions (burning index = 71; flame lengths ~2 m), and 58% under mild fire weather conditions (burning index = 53; flame lengths ~1.5 m). The remaining 42% would be unlikely to experience restorative first-entry wildfire effects, regardless of fire weather conditions. Mapping the probability of restorative fire effects across the Sierra Nevada YPMC zone revealed clear geographic and spatial patterns (Figure 2.7). For example, most of the previously unburned area within Yosemite National Park and Sequoia and Kings Canyon National Parks would be likely to experience restorative fire effects even under moderate fire weather conditions. In Stanislaus, Eldorado, Tahoe, and Plumas National Forests, relatively large portions of the mid- to upper-elevation sites showed high probability of full restoration under a mild fire weather scenario. Across the Sierra Nevada, lower elevation sites, especially in the northern portions of the region, had a low probability of restorative effects, even under mild fire weather conditions (Figure 2.7).

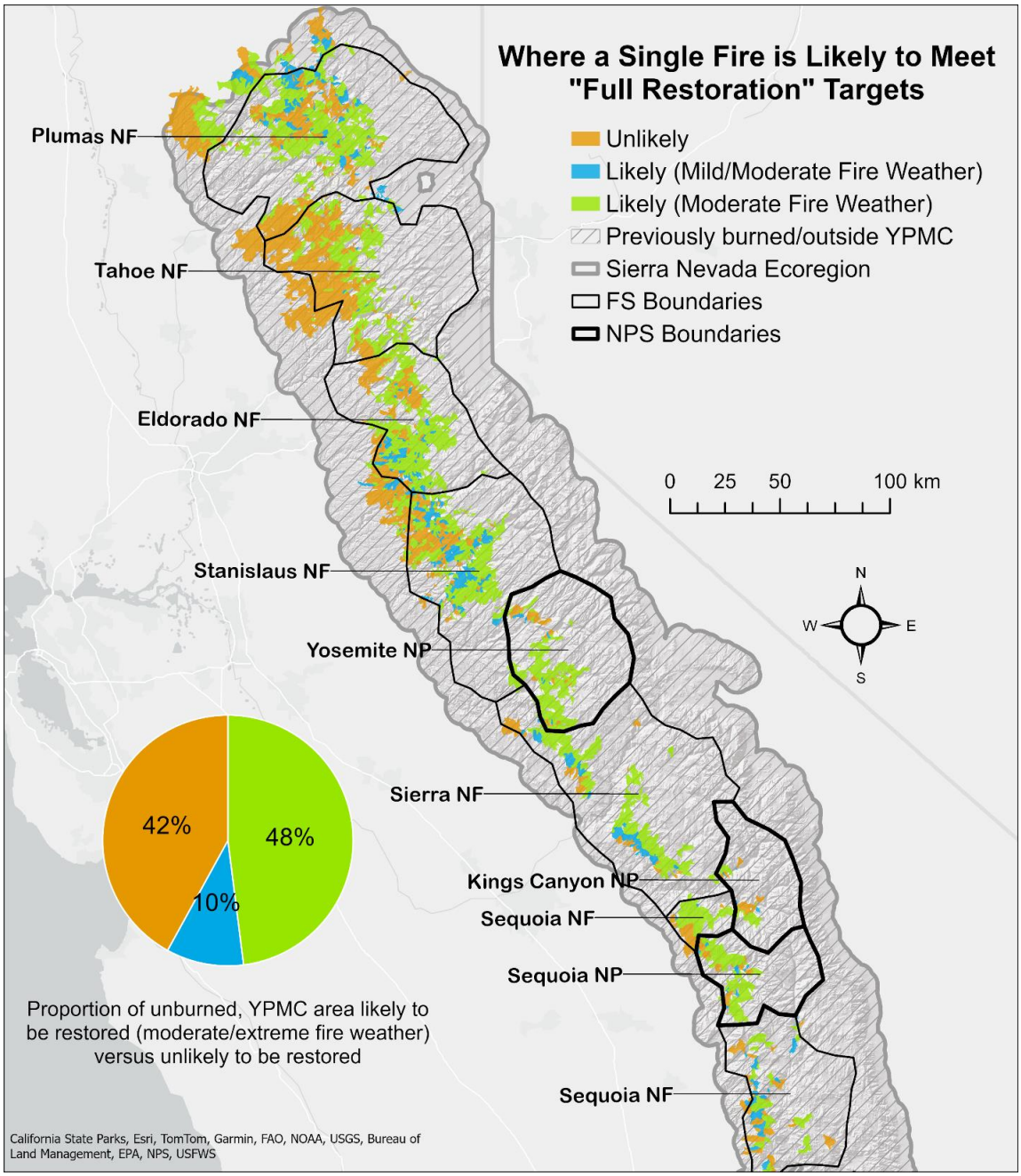

Figure 2.7. Mapped predictions of the full restoration index (*i.e.,* canopy cover, ladder fuel density, and clump complexity all within the natural range of variation (NRV)) for previously unburned area in the year 2020 in the Sierra Nevada yellow pine and mixed conifer (YPMC) zone, California, USA. Blue and green sites represent a probability of full restoration > 0.5 under a mild (burning index = 53) and moderate (burning index = 71) fire weather scenario, respectively. Orange represents a probability of full restoration < 0.5 under both weather scenarios. For visualization, 90-m pixel predictions were aggregated to the catchment level using the majority class prediction within each catchment. NF: National Forest; NP: National Park; YPMC: yellow pine mixed conifer.

2.5. DISCUSSION

As wildfires make their return to fire-suppressed YPMC forests of the Sierra Nevada, it is essential to understand how these contemporary fires are affecting forest structural patterns, the extent to which these patterns align with common restoration objectives, and the factors that contribute to more restorative fire effects (Williams et al. 2019; Kane et al. 2019; Meyer et al. 2021; North et al. 2021). Our results suggest that contemporary, first-entry wildfires were moderately successful at shifting canopy cover and ladder fuel density toward NRVs, but less successful at producing the complex tree clump and opening patterns that characterize contemporary reference sites. Additional wildfires and, in some instances, post-fire management will be required to fully shift structural patterns toward those associated with fire-intact ecosystems. We found that the probability of restorative fire effects was primarily influenced by landscape disturbance history (*i.e.,* sites located within mosaics of past wildfires) along with a suite of bioclimatic, fire weather, topographic, and pre-fire structural conditions. The bounds of these relationships may inform managers regarding when and where future fires could be successfully managed for resource objectives (North et al. 2024). Achieving conditions associated with fire-intact ecosystems, which are likely to exhibit increased resilience under future disturbances and climates, will require land management plans that encourage beneficial low- and moderate-severity wildfires, strategic and proactive post-fire management strategies that leverage restorative fire effects, and continued efforts to increase the pace and scale of restoration treatments in high-risk areas (Hessburg et al. 2021; Meyers et al. 2021; North et al. 2024).

2.5.1. STRUCTURAL TARGETS FROM CONTEMPORARY REFERENCE SITES

Our characterizations of structural patterns from contemporary reference sites generally aligned with previous assessments from contemporary and historical reference datasets in Sierra

Nevada YPMC forests. The frequent low-severity fire regime that historically characterized these forests, and the reestablishment of this regime in the modern era, tends to produce relatively low canopy covers (21-75% in our study), low ladder fuel densities (2-35% in our study), and fine-scale heterogeneity in tree spatial patterns (reflected in this study by moderate values (1.3-1.5) of the clump complexity index) (Knapp et al. 2013; Lydersen et al. 2013; Jeronimo et al. 2019; Hankin and Andersen 2022; Chamberlain et al. 2023a). Similar to work by Ng et al. (2020) and Jeronimo et al. (2019), we found that structural patterns indeed varied by topographic gradients and, to a lesser extent, climatic gradients, such that increased topographic and climatic variability begets site- to landscape-level structural heterogeneity. This among-site variation has also been observed in historical datasets in the Sierra Nevada (Collins et al. 2015; Knapp et al. 2017), underscoring that landscape-level heterogeneity is a key structural component produced by a frequent low-severity fire regime, and that capturing these multi-scaled structural components is critical when evaluating the restorative work of wildfires (Wiggins et al. 2019; Chamberlain et al. 2023a).

2.5.2. FIRST-ENTRY WILDFIRE EFFECTS

Relative to unburned controls (characterized by high canopy cover (> 61-75%), dense ladder fuels (> 12-35%), and low clump complexity (< 1.3-1.4)), we found that first-entry wildfires were indeed effective at restoring structural characteristics, especially in moderate severity patches. In this sense, our results support recent work by Kane et al. (2019) who found that first-entry wildfires in Yosemite National Park tended to realign tree clump and opening patterns with those found in contemporary reference sites. Our results also align with other remote sensing and field-based studies showing that structural patterns in moderate-severity sites were most similar to historical reference conditions (Collins et al. 2011a; Kane et al. 2013; Lydersen et al. 2016). However, while our results suggest that first-entry wildfires improved conditions relative to unburned controls, sites in which NRV was achieved for all three structure targets were relatively rare across our study fires

(16% of total area and 24% of moderate severity patches). This suggests that a large portion of first-entry burned areas, even within moderate severity patches, may still require additional low- to moderate-intensity wildfires or other forms of post-fire management (Coppoletta et al. 2016; Meyer et al. 2021; Steel et al. 2021a). First-entry burn sites where canopy cover and ladder fuel densities remained above NRV may require additional fire entries or post-fire mechanical thinning to further consume and disaggregate overstory structures (Collins et al. 2011b; Meyer et al. 2021; Ziegler et al. 2021), whereas sites with excessive overstory consumption will likely require strategic post-fire planting to promote the recovery of low-density ICO patterns (North et al. 2019; Meyer et al. 2021).

We found that first-entry wildfires were least likely to meet targets related to clump complexity relative to other structure metrics, suggesting that the complex clump patterns characteristic of fire-intact ecosystems may only be achieved after multiple, moderate-intensity fires, rather than just a single fire event. Low- to moderate-intensity surface fires produce fine-scale tree clump and opening patterns as a function of fine-scale patterns of fuel moisture, wind patterns, soil moisture gradients, existing vegetation, and fine-scale variations in past disturbances (Collins et al. 2015; Kane et al. 2015b; Hessburg et al. 2019; Jeronimo et al. 2020). A single fire may produce some degree of fine-scale heterogeneity (Kane et al. 2019), but it is the interplay among these factors across multiple fire events that ultimately leads to the characteristic tree clump and opening patterns observed in fire-intact ecosystems (Larson and Churchill 2012; Kane et al. 2015b; Churchill et al. 2017; Greenler et al. 2023).

First-entry burn areas frequently produced large (> 100-ha) patches of cover only restoration, with smaller, dispersed patches of partial and full restoration embedded within those larger patches. This suggests that first-entry wildfires are beginning to increase stand- and landscape-level heterogeneity (*i.e.,* increased diversity in 90-m structures across a site). Heterogeneity contributes to improved wildlife habitat and increased biodiversity while also increasing resilience to

future disturbances and climate change (Stephens et al. 2016b; Koontz et al. 2020; Kramer et al. 2021; Francis et al. 2023). Heterogeneity begets heterogeneity (Harvey et al. 2023); thus, we expect future, low-intensity fires to further increase stand-level heterogeneity within these large patches of cover only restoration (Kane et al. 2015a; Koontz et al. 2020). After several fires, these sites may begin to resemble the highly heterogeneous patch mosaics that characterize historical and contemporary fire-intact ecosystems (Collins et al. 2015; Jeronimo et al. 2019; Chamberlain et al. 2023a).

Species composition and surface fuel loading represent critical components of fire-intact ecosystems. Yet, methods for measuring these components using airborne lidar are not fully developed, especially at regional scales (Akay et al. 2009; Beland et al. 2019). Recent field-based studies have found that repeated fire entries (and mechanical thinning) in Sierra Nevada forests have failed to shift species composition toward historical densities of fire-resistant pines (May et al. 2022; Zald et al. 2024). Additionally, other field-based studies have found that surface fuels are unlikely to be reduced following first-entry wildfires (Cansler et al. 2019; Lutz et al. 2020; Larson et al. 2022), especially following the 2012-2016 drought in the southern Sierra Nevada which contributed substantially to surface fuel loading (Reed et al. 2023; Vilanova et al. 2023; Northrop et al. 2024). Ultimately, we suspect that the fully restored post-fire structures observed in our study, characterized by lower canopy cover, reduced ladder fuels, and increased clump complexity, represent improved structural conditions compared to their unburned counterparts (*i.e.,* control sites) (Agee and Skinner 2005; Larson and Churchill 2012; Ritter et al. 2020). However, additional work may be needed to evaluate the extent to which first-entry wildfires have shifted species distributions and surface fuel loads toward desired conditions (Knapp and Keeley 2006; Cansler et al. 2019; Lutz et al. 2020; Hankin et al. 2024).

2.5.3. DRIVERS OF RESTORATIVE FIRE EFFECTS

Our results suggest that landscapes characterized by a mosaic of past wildfires were most likely to experience restorative fire effects across the entirety of the landscape during subsequent fires. Past work has demonstrated that fires occurring *within* recently burned areas tend to have low- to moderate-severity effects (Parks et al. 2015; Stevens-Rumann et al. 2016; Prichard et al. 2017). Our results suggest that these beneficial effects of past fires (*i.e.,* mostly low- to moderate-severity effects) may extend *beyond* an individual fire's footprint, for upwards of 1 km. The effect of past fire proximity may also indicate that fire boundaries were often located at places on the landscape where fuels were already sparse (*e.g.,* rocky ridgetops) or where fire suppression operations were more likely to be successful (*e.g.,* major roads) (O'Connor et al. 2017; Gannon et al. 2023). It is also likely that National Parks (representing 14% of our sample) had higher densities of past fires, considering their long-standing prescribed and natural fire programs (van Wagtendonk 2007; Hankin et al. 2024). Forests within National Parks are often characterized by higher proportions of older, more fire-resistant trees due to the relative lack of early century logging, which likely contributed to increased probability of restorative fire effects (Kane et al. 2023).

Modeled flame lengths of approximately 1-2 m (burning index 50-55) were most successful at producing post-fire structures within NRV in our analyses, suggesting that moderate-intensity wildfire is necessary to produce desired structural conditions in fire-suppressed YPMC forests. Our results were similar to Schmidt et al. (2006) who found that late-season prescribed burns in the Sierra Nevada with flame lengths of ~1-2.5 m were most successful at producing tree density and clumping patterns matching historical conditions. Lydersen et al. (2016) also found that flame lengths < 2.4 m (burning index < 75) were most likely to produce moderate severity fire effects within the 2013 Rim Fire, yet higher flame lengths generally resulted in high severity effects. As such, our results provide additional evidence, spanning a broad geographic extent and biophysical

setting in Sierra Nevada YPMC forests, that relatively specific fire intensities may be required in fire-suppressed forests to have the best chances of achieving restored post-fire structures (Knapp and Keeley 2006; Schmidt et al. 2006; Greenler et al. 2023). Importantly, while areas that burned under less intense fire weather may have failed to fully restore canopy structures, lower severity effects are always favorable over high severity; once overstory trees are lost, reestablishing forest cover becomes far more costly and challenging (North et al. 2019; Larson et al. 2022).

We observed complex (and likely interacting) relationships between several environmental factors and the probability of restorative fire effects. For example, we found that sites at lower elevations and with higher mean annual precipitation (*i.e.,* lower elevations in the northern Sierra Nevada), and sites with more exposed topographic positions tended to exhibit less restorative effects. To an extent, these trends may be driven by variations in species composition across the YPMC zone, in which lower elevation sites and ridges would support higher proportions of oak and incense cedar, which may have contributed to increased pre-fire ladder fuel densities and thus less restorative fire effects (Zald et al. 2008; Collins et al. 2015; Stevens et al. 2020; Cansler et al. 2020). It is also possible that underlying edaphic conditions may have contributed to increased restorative fire effects in the southern Sierra Nevada, which is generally characterized by steeper terrain and more exposed bedrock compared to the northern parts of the range (Safford and Stevens 2017). These edaphic conditions may have served as physical barriers to extreme fire spread at the landscape scale (Safford and Stevens 2017), facilitating more beneficial fire effects. Edaphic conditions in the southern Sierra Nevada may have also supported more complex pre-fire structures (*i.e.,* higher diameter diversity index) which were associated with higher probability of restored post-fire structures in our analyses (Meyer et al. 2007b; Fry et al. 2014). Lastly, it is possible that the lower elevations in the northern Sierra Nevada represented sites within closer proximity to industrially

managed forests, which can increase the incidence of high severity fire effects on adjacent public lands (Levine et al. 2022).

We found that a relatively high portion (58%) of the Sierra Nevada YPMC zone would be likely to benefit from future first-entry wildfires that burn under mild fire weather conditions (~1 m flame lengths), and a reasonable proportion (48%) could even benefit under moderate fire weather conditions (~2 m flame lengths). Regions with large, contiguous areas of likely restorative effects under both weather scenarios were observed primarily in Yosemite National Park, Sequoia National Park, and the upper elevation regions of several National Forests (Eldorado National Forest in particular). In Yosemite and Sequoia National Parks, this was likely due to their long-established prescribed and natural fire program which, over the past several decades, have created extensive patchworks of previously burned areas (Collins and Stephens 2007; van Wagtendonk 2007; Hankin et al. 2024). Our maps also show a large contiguous region that was unlikely to experience restorative effects across the lower elevations of Stanislaus, Eldorado, and Tahoe National Forests. In these sites, increased incense cedar and oak presence, lack of topographic barriers to fire spread, and closer proximity to industrial forests lands may contribute to less restorative fire effects. Importantly, we note that several large fires burned within the Sierra Nevada in 2021 and 2022; future research can evaluate the extent to which our predictions of restorative effects held true during these large fires.

2.5.4. MANAGEMENT IMPLICATIONS

The lidar-based restoration indices described in this study (or the raw topo-climatic NRV ranges provided in Table 2.A.2) could greatly inform post-fire management assessments and decision-making (Meyer et al. 2021; Stevens et al. 2021; Larson et al. 2022). Managers could delineate areas that met the full restoration target and deprioritize these sites for immediate intervention. In areas of partial restoration, additional fires will likely be necessary; but, since these sites already

exhibit reduced canopy and ladder fuel loads, they may be fairly resistant to even moderate-intensity summer-season fires in the near future (Knapp et al. 2005; Knapp and Keeley 2006; Schwilk et al. 2006). Additionally, areas that only met canopy cover targets, where ladder fuel densities remained relatively high, could be considered for more careful application of fire, perhaps via prescribed burning or beneficial wildfire use during cooler months (Knapp et al. 2005; Knapp and Keeley 2006; Schwilk et al. 2006). Lastly, first-entry burned areas that failed to meet any of the restoration targets may require mechanical thinning, prescribed burning, or planting, depending on whether post-fire structures fell above or below NRV (North et al. 2019; 2021; Meyer et al. 2021). Some post-fire sites with high residual canopy cover and ladder fuel densities may be delineated for lower intensity treatments that focus on improving wildlife habitat for key species like California spotted owl (*Strix occidentalis occidentalis*) and fisher (*Pekania pennanti*) (North et al. 2017; Kramer et al. 2021; Steel et al. 2023). Importantly, while our restoration indices can provide useful guidance for post-fire management, we note that these indices only quantify upper canopy structural conditions. As discussed above, many of these first-entry burn areas likely exhibit increased surface fuel loads and potentially misaligned species distributions (May et al. 2022; Zald et al. 2024; Cansler et al. 2019; Lutz et al. 2020), which may require field-based assessments and/or more careful application, or management, of subsequent fires and treatments (Hankin et al. 2024).

Managers can use our modeling results to better define the envelope of conditions within which restorative fire effects will be most likely to occur in future fires in the Sierra Nevada YPMC zone. To aid in this process, mapped predictions of restorative fire effects have been archived as raster layers in a publicly available Zenodo Digital Repository (https://doi.org/10.5281/zenodo.12802224). Notably, landscapes currently characterized by a mosaic of past fires (*i.e.,* National Parks and portions of several National Forests) are likely to support mostly restorative fire effects in the future (Meyer 2015). We also found a higher likelihood

of restorative effects at higher elevations, especially in the northern portion of the YPMC zone. Considering the operational challenges of treating higher elevation sites in the Sierra Nevada, and their relative distance from the wildland urban interface, these areas may be particularly suitable for resource objective wildfires and/or designation as Strategic Fire Zones (North et al. 2021; North et al. 2024). In contrast, lower elevation sites within Stanislaus, Eldorado, and Tahoe National Forests are less likely to experience restorative first-entry effects and may best be prioritized for mechanical treatment or prescribed burning (Krofcheck et al. 2018), particularly since such areas are closer to the wildland urban interface (North et al. 2021). Lastly, we note a distinct range of flame lengths during which restorative fire effects will be most probable (~1-2 m). This range of fire intensity can provide general guidance for conducting prescribed burns or for considering naturally ignited fires for resource objectives (North et al. 2021).

2.6. CONCLUSION

Climate change is expected to cause major shifts in vegetation dynamics and disturbance regimes across forested landscapes of western North America (Fettig et al. 2013; Schoennagel et al. 2017). If recent trends are a harbinger for the future, wildfires will continue to increase in size, frequency, and severity, especially in fire-suppressed forests that are most susceptible to extreme fire behavior (Abatzoglou et al. 2019; Williams et al. 2019; Safford et al. 2020). Fire-intact ecosystems, for which historical datasets and contemporary reference sites offer reliable proxies, are those in which fire plays a critical role in regulating vegetation dynamics and increasing resilience to future disturbances and climate change (Collins et al. 2016; Hagmann et al. 2021; Chamberlain et al. 2023a). If our goal is to ensure the persistence of dry forest ecosystems and the values they provide, increasing the extent of fire-intact, rather than fire-suppressed, forest ecosystems will be imperative over the next few decades (Prichard et al. 2021; Hessburg et al. 2021; North et al. 2024). Achieving

the structural and compositional conditions associated with fire-intact ecosystems will require (1) access to datasets and knowledge that support comprehensive and ecologically-based post-fire planning and operations (North et al. 2019; Meyer et al. 2021; Stevens et al. 2021; Larson et al. 2022) and (2) more nuanced pre- and active-fire management strategies that integrate both western science and Indigenous knowledge sources to encourage restorative and beneficial fire effects (Hessburg et al. 2021; North et al. 2021;2024; Lake et al. 2017). We believe that the results from our study, and the maps and data layers provided, will assist managers and policy makers in moving contemporary dry forest landscapes toward these desired conditions associated with fire-intact ecosystems.

2.7. APPENDIX B

Table 2.A.1. Statistics for 35 analysis fires in the Sierra Nevada ecoregion, California, USA.

Fire name	Fire year	Total fire area (ha)	First-entry, untreated area (ha)	% FE/U low severity	% FE/U moderate severity	% FE/U high severity
Freds	2004	3058	841	9	37	54
Hetchy	2004	784	603	52	41	7
Meadow WFU	2004	2036	265	46	49	5
Moke	2004	143	138	69	20	10
Power	2004	6873	4255	21	46	33
Bassetts	2006	849	686	34	31	35
Frog	2006	2440	209	45	55	0
Middle T Suppression	2006	139	110	58	36	6
Jack	2007	457	434	80	20	0
Moonlight	2007	26288	1142	9	29	62
Cold	2008	2266	1907	10	47	43
Complex BTU Lightning	2008	21731	13507	23	49	27
Complex Canyon Hartman	2008	134	114	78	22	0
Complex Canyon Little	2008	566	565	88	12	1
Complex Canyon Scotch	2008	5264	5188	54	41	4
Complex Canyon South-Frey	2008	5019	4619	59	33	7
Dome Rock	2008	371	371	47	38	15
Rich	2008	2473	561	6	36	58
Big Meadow	2009	3057	298	20	51	29
Knight	2009	2480	2274	55	35	11
Bar	2010	421	376	50	46	5
Slope	2010	692	642	77	22	0
Avalanche	2011	432	187	94	6	0
Blue II	2011	283	145	61	16	22
Long	2011	195	195	89	11	0
Punch	2011	205	107	100	0	0
Chips	2012	30898	10231	26	47	27
Ramsey	2012	460	459	30	48	22
Aspen	2013	9282	6587	26	56	18
Carstens	2013	691	319	3	51	45
Power	2013	435	411	22	47	31
Rim	2013	103671	27401	28	34	38
King	2014	39532	10932	28	32	40
Rough	2015	61329	24814	29	47	24
Willow	2015	2307	837	14	45	41
Row Summary		337263 (sum)	121730 (sum)	44 (mean)	35 (mean)	21 (mean)

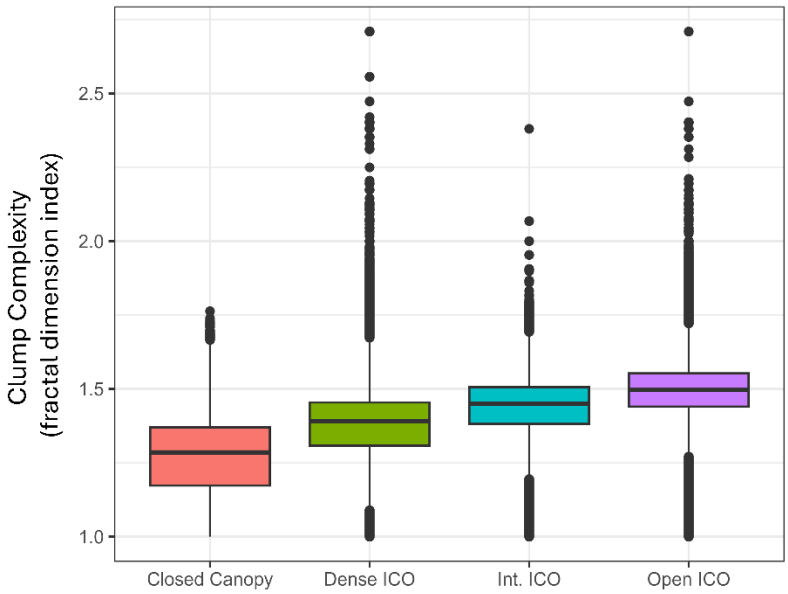

Figure 2.A.1. Comparing fractal dimension index to structure classes. We show the distribution of fractal dimension index values (our measure of clump complexity) within each of the four structure classes defined in Chamberlain et al. (2023). These structure classes represent statistically distinct clusters of 90-m structure metrics (identified using a hierarchical clustering approach) spanning the contemporary reference sites. Structure classes were defined using five structure metrics including % area gap, % canopy cover of individual tree approximate objects (TAOs), % canopy cover 2-4 TAO clumps, % canopy cover 5-9 TAO clumps, and % canopy cover 10+ TAO clumps. ICO refers to individual TAOs, clumps of TAOs, and open space. TAOs refer to airborne lidar segmented trees. Chamberlain et al. 2023a found that contemporary reference sites were characterized primarily by intermediate ICO and open ICO structure classes, which represent fractal dimension values of approximately 1.3-1.6. TAO: tree approximate object; ICO: individual TAOs, clumps of TAOs, open space.

Table 2.A.2. Natural range of variation (NRV), defined as the inner 68% of the distribution of values spanning the contemporary reference sites for each structure metric, split by climate class and topography (land management unit, LMU).

Climate Class	LMU	Canopy Cover	Ladder Fuel Density	Clump Complexity
Warm Dry Low Montane	Ridge	28.03 - 65.03	4.87 - 24.64	1.4 - 1.51
	SW Slope	25.2 - 64.74	4.41 - 22.12	1.39 - 1.53
	NE Slope	41.23 - 70.86	6.56 - 27.71	1.33 - 1.46
	Valley	40.44 - 74.27	10.18 - 34.66	1.3 - 1.48
Warm Mesic Low Montane	Ridge	28.39 - 64.23	3.95 - 22.72	1.39 - 1.5
	SW Slope	31.35 - 67.17	3.6 - 20.75	1.37 - 1.49
	NE Slope	36.01 - 68.37	3.91 - 23.08	1.36 - 1.49
	Valley	40.98 - 74.99	6.05 - 34.19	1.29 - 1.46
Cool Dry Mid Montane	Ridge	21.56 - 61.02	2.18 - 13.12	1.41 - 1.5
	SW Slope	20.73 - 62.4	2.45 - 13.99	1.4 - 1.51
	NE Slope	23.71 - 64.92	2.23 - 11.58	1.4 - 1.51
	Valley	28.23 - 65.86	2.92 - 15.45	1.4 - 1.51

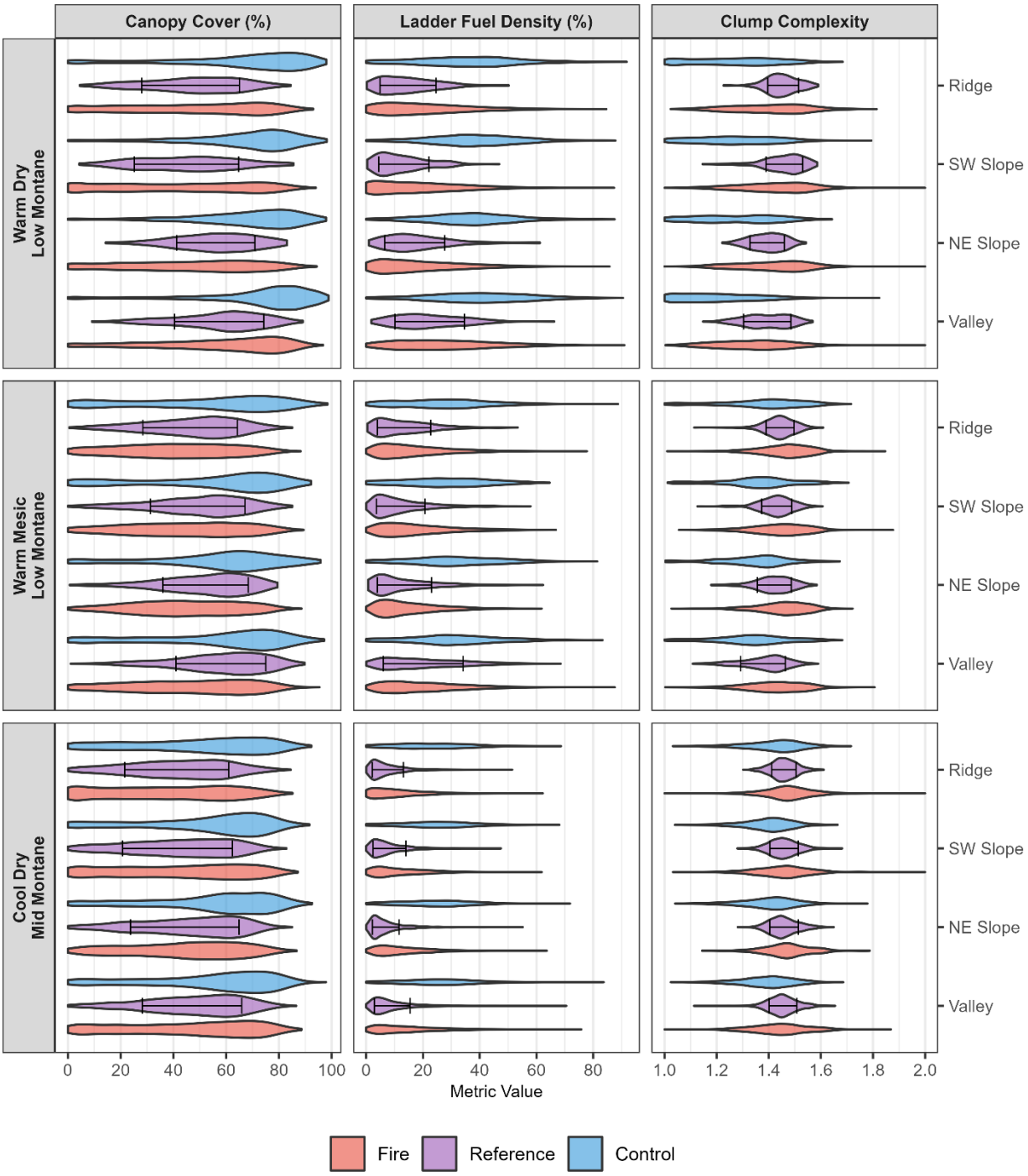

Figure 2.A.2. Raw distributions of each forest structure metric split by climate and topographic classes for first-entry wildfire sites (red), contemporary reference sites (purple), and unburned control sites (blue). Black error bar over the reference site distribution represents the natural range of variation (NRV), defined as the inner 68% of the distribution.

Supplemental Methods 2.A.1. Acquiring and deriving predictor variables.

We provide descriptions of the methods used to obtain and derive thirty-four predictor variables that were used in our study for modeling the drivers of restorative fire effects. From these variables, our variable reduction procedure identified 13 for inclusion in the final model, which are detailed in the main text of the manuscript. Our objective was to capture a range of pre- and active-fire conditions, including forest structure, fire weather, bioclimatic conditions, topography, and landscape context.

To consistently capture variability in pre-fire canopy fuels across each fire footprint, we utilized the Landscape Ecology, Modeling, Mapping & Analysis Gradient Nearest Neighbor dataset (GNN 2023). GNN data was obtained for the year preceding each fire, providing modeled forest structure variables at 30-m resolution corresponding with Landsat pixels. We selected a subset of the full set of GNN variables for our modeling procedure – basal area of live trees >= 2.5 cm diameter at breast height (DBH), volume of live trees >= 2.5 cm DBH, canopy cover of all live trees, and diameter diversity index (DDI), which corresponded with R^2 values of 0.63, 0.56, 0.48, and 0.50, respectively. Additionally, to provide metrics of pre-fire fuel conditions, we incorporated the snow disappearance date and snow cover frequency layers corresponding to the year of each fire, utilizing MODIS satellite methods developed by Crumley et al. (2020). These layers provide information about snow levels preceding each fire, and thus are related to pre-fire live fuel moisture and biophysical setting.

We produced day-of-burn fire weather metrics by linking GRIDMET data to MODIS-derived fire progression maps, generated using scripts from Parks (2014). The fire weather variables obtained from the GRIDMET website included maximum temperature, wind velocity, minimum relative humidity, energy release component, burning index, 100-hour fuel moisture, 1000-hour fuel moisture, and vapor pressure deficit (Abatzoglou 2013). These daily values were extracted to burn

progression rasters to produce fire weather metrics for each fire in our analyses.

To describe broad bioclimatic gradients across the Sierra Nevada yellow pine mixed conifer (YPMC) zone, we compiled a set of predictor variables from the Climate and Hydrology Basin Characterization Model website (Flint et al. 2021). These bioclimatic variables represent mean conditions across the years 1981-2010 and include actual evapotranspiration, April 1st snowpack, climatic water deficit, potential evapotranspiration, annual total precipitation, minimum annual temperature, and maximum annual temperature, all produced at 270-m resolution. Additionally, to describe fire-relevant gradients of forest type and species, we included the community fire resistance score (FRS) layer produced by Stevens et al. (2020).

Key topographic layers across each fire footprint were derived using the USGS 10-m resolution digital elevation model (DEM) downloaded from the National Map Viewer (USGS 2022). The terra package (Hijmans et al. 2023) in R (R Core Team 2023) was used to derive slope, aspect, and roughness layers from the DEM. We then used the spatialEco package (Evans and Murphy 2021) in R (R Core Team 2023) to derive the solar-radiation aspect index, topographic position index (TPI), and topographic ruggedness index (TRI) from the DEM. TPI was computed within 130-, 510-, and 2010-m windows to account for different scales of topography, while TRI was only computed within a 130-m window due to computational constraints.

Fire behavior and effects are influenced not only by local conditions, but also by the surrounding landscape within which an area burns. Landscape features like past fires, past treatments, roads, and water bodies can influence the physics of fire behavior, as well as active-fire management responses. To quantify landscape context, we produced layers including distance to past fire, distance to roads, distance to past treatment, and distance to rivers/streams/lakes. These layers were computed with a 90-m resolution raster using the terra package in R, with distance to the nearest feature (e.g., fire, treatment) measured in meters.

Table 2.A.3. Continuous predictor variables, prior to variable reduction, used to model restorative fire effects. DBH: diameter at breast height; AET: average annual actual evapotranspiration; AFSP: April first snow pack; CWD: average annual climatic water deficit; PET: average annual potential evapotranspiration; PPT: average annual precipitation; TMIN: average minimum annual temperature; TMAX: average maximum annual temperature; TPI: topographic position index; DEM: digital elevation model; USGS: United States Geological Survey.

Data Category	Variable Name	Variable Description	Resolution (m)	Units	References
Forest Structure	Basal Area Live Trees	Basal area of live trees >= 2.5 cm DBH	30	m^2/ha	GNN 2023
	Volume Live Trees	Volume of live trees >= 2.5 cm DBH	30	m^3/ha	GNN 2023
	Canopy Cover	Canopy cover of all live trees	30	percent	GNN 2023
	Diameter Diversity Index	"measure of the structural diversity of a forest stand, based on tree densities in different DBH classes"	30	continuous index	GNN 2023
Fuel Conditions	Snow Disappearance Date	Snow disappearance julian date	2000	Julian date	Crumley et al. 2020
	Snow Cover Frequency	Snow cover frequency measured as number of days with snow divided by 365 days	2000	percent	Crumley et al. 2020
Fire Weather	Maximum Temperature		30 (downscaled from 4000 m)	K	Abatzoglou 2013
	Wind Velocity	Wind velocity at 10 m	30 (downscaled from 32 km)	m/s	Abatzoglou 2013
	Minimum Relative Humidity	Minimum relative humidity	30 (downscaled from 4000 m)	percent	Abatzoglou 2013
	Energy Release Component	Energy release component	30 (downscaled from 4000 m)	continuous index	Abatzoglou 2013
	Burning Index	Burning index	30 (downscaled from 4000 m)	continuous index	Abatzoglou 2013
	100-hour Fuel Moisture	100-hour dead fuel moisture	30 (downscaled from 4000 m)	percent	Abatzoglou 2013
	1000-hour Fuel Moisture	1000-hour dead fuel moisture	30 (downscaled from 4000 m)	percent	Abatzoglou 2013
	Vapor Pressure Deficit	Mean vapor pressure deficit	30 (downscaled from 4000 m)	kPa	Abatzoglou 2013
Bioclimatic	Elevation	Elevation	10	m	USGS 2022
	AET 1981-2010	Mean actual evapotranspiration across years 1981-2010	270	mm	Flint et al. 2021

	AFSP 1981-2010	Mean April 1st snowpack across years 1981-2010			Flint et al. 2021
	CWD 1981-2010	Mean climatic water deficit across years 1981-2010	270	mm	Flint et al. 2021
	PET 1981-2010	Mean potential evapotranspiration across years 1981-2010	270	mm	Flint et al. 2021
	PRECIP 1981-2010	Mean annual total precipitation across years 1981-2010	270	mm	Flint et al. 2021
	TMIN 1981-2010	Mean minimum annual temperature across years 1981-2010	270	degrees Celsius	Flint et al. 2021
	TMAX 1981-2010	Mean maximum annual temperature across years 1981-2010	270	degrees Celsius	Flint et al. 2021
	Fire Resistance Score	Community fire resistance score	250	continuous numeric	Stevens et al. 2020
Topographic	Slope	Slope angle	10	degrees	USGS 2022; Hijmans et al. 2023
	Roughness	Local topographic roughness	10		USGS 2022; Hijmans et al. 2023
	Solar-radiation aspect index	Rotation of the circular slope aspect so that a value of 0 represents cooler, north-northeast facing slopes, and a value of 1 represents hotter, south-southwest facing slopes	10	continuous numeric	USGS 2022; Evans and Murphy 2023
	Topographic Position Index (TPI) 130-m	Topographic position index derived from USGS 10-m DEM using a 130-m window; lower values represent moderate-scale valleys and higher values represent moderate-scale ridges	10	unitless	USGS 2022; Evans and Murphy 2023
	Topographic Position Index (TPI) 510-m	Topographic position index derived from USGS 10-m DEM using a 510-m window; lower values represent moderate-scale valleys and higher values represent moderate-scale ridges	10	unitless	USGS 2022; Evans and Murphy 2023
	Topographic Position Index (TPI) 2010-m	Topographic position index derived from USGS 10-m DEM using a 2010-m window; lower values represent moderate-scale valleys and higher values represent moderate-scale ridges	10	unitless	USGS 2022; Evans and Murphy 2023

	Topographic Ruggedness Index	Topographic ruggedness index derived from USGS 10-m DEM using a 130-m window; 0-80 = level terrain; 81-116 = nearly level surface; 117-161 = slightly rugged surface; 162-239 = intermediately rugged surface; 240-497 = moderately rugged surface; 498+ = highly-extremely rugged surface	10	unitless	USGS 2022; Evans and Murphy 2023
Landscape Context	Distance to Past Fire	Distance to nearest previous fire	90	m	FRAP 2021; Hijmans et al. 2023
	Distance to Water	Distance to nearest river, stream, or lake	90	m	Hijmans et al. 2023
	Distance to Treatment	Distance to nearest prior treatment	90	m	Knight et al. 2022; Hijmans et al. 2023
	Distance to Roads	Distance to nearest national, state, or Forest Service road	90	m	Hijmans et al. 2023

Supplemental Methods 2.A.2. Variable reduction.

Prior to fitting final random forest models, we performed a variable reduction procedure to reduce multicollinearity among predictors. We performed variable reduction on the full set of 34 predictors. First, for each predictor, we identified all predictors for which Spearman's correlation coefficient was > 0.5. Then, for all pairs of correlated predictors, we fit logistic regression models predicting the full restoration response index, then discarded the predictor corresponding to the model with the highest Akaike Information Criterion (AIC). Following this process, we produced a final modeling dataframe with this subset of predictors and the full restoration index response. We used the *glm* function for fitting logistic regression models within the base R environment (R Core Team 2023).

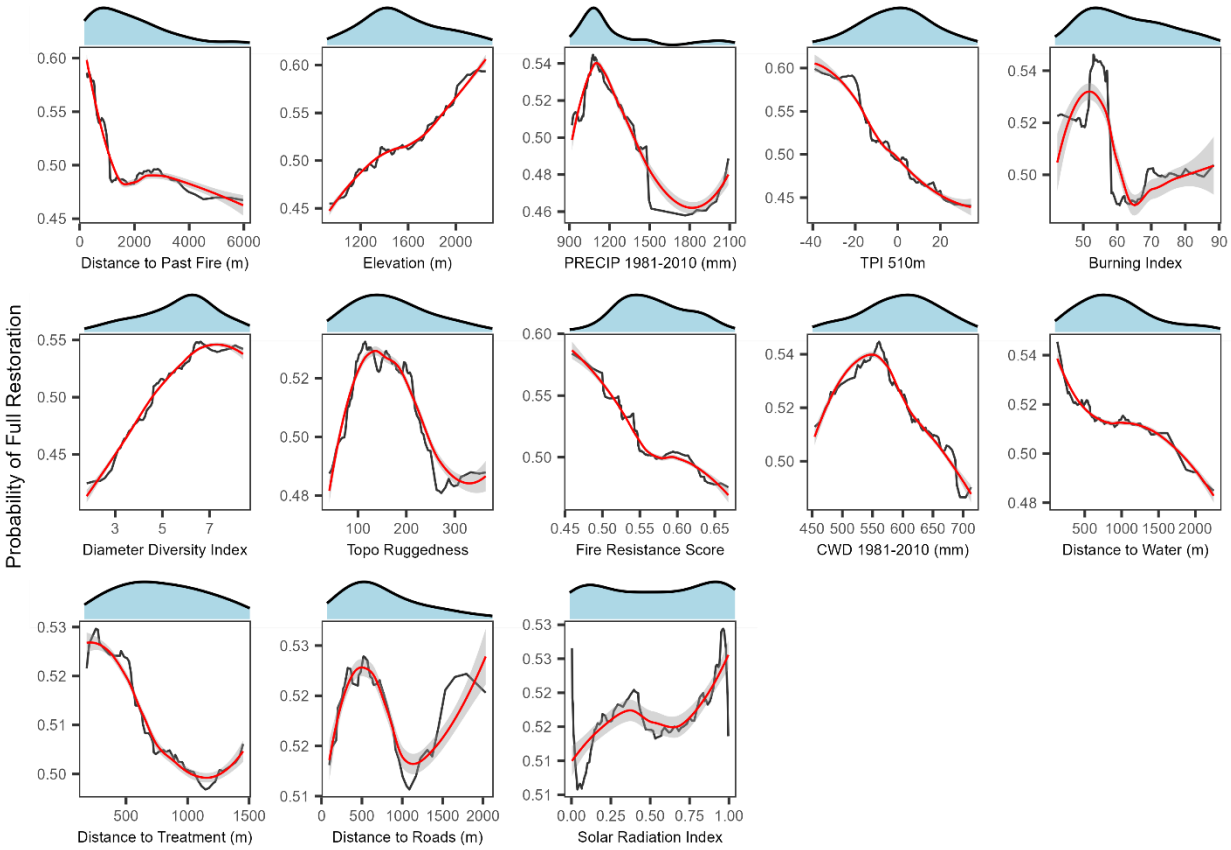

Figure 2.A.3. The full set of partial dependence plots (PDPs) for all 13 predictor variables included in the final random forest model predicting the full restoration index. Black line shows predictions, while red line shows loess smooth with standard error in grey. Density plots in blue show counts of observations across the range of values for each variable. PDPs were produced using the *DALEXtra* package (Maksymiuk et al. 2020) in R (R Core Team 2023). PRECIP: mean annual precipitation; TPI: topographic position index; CWD: average annual climatic water deficit.

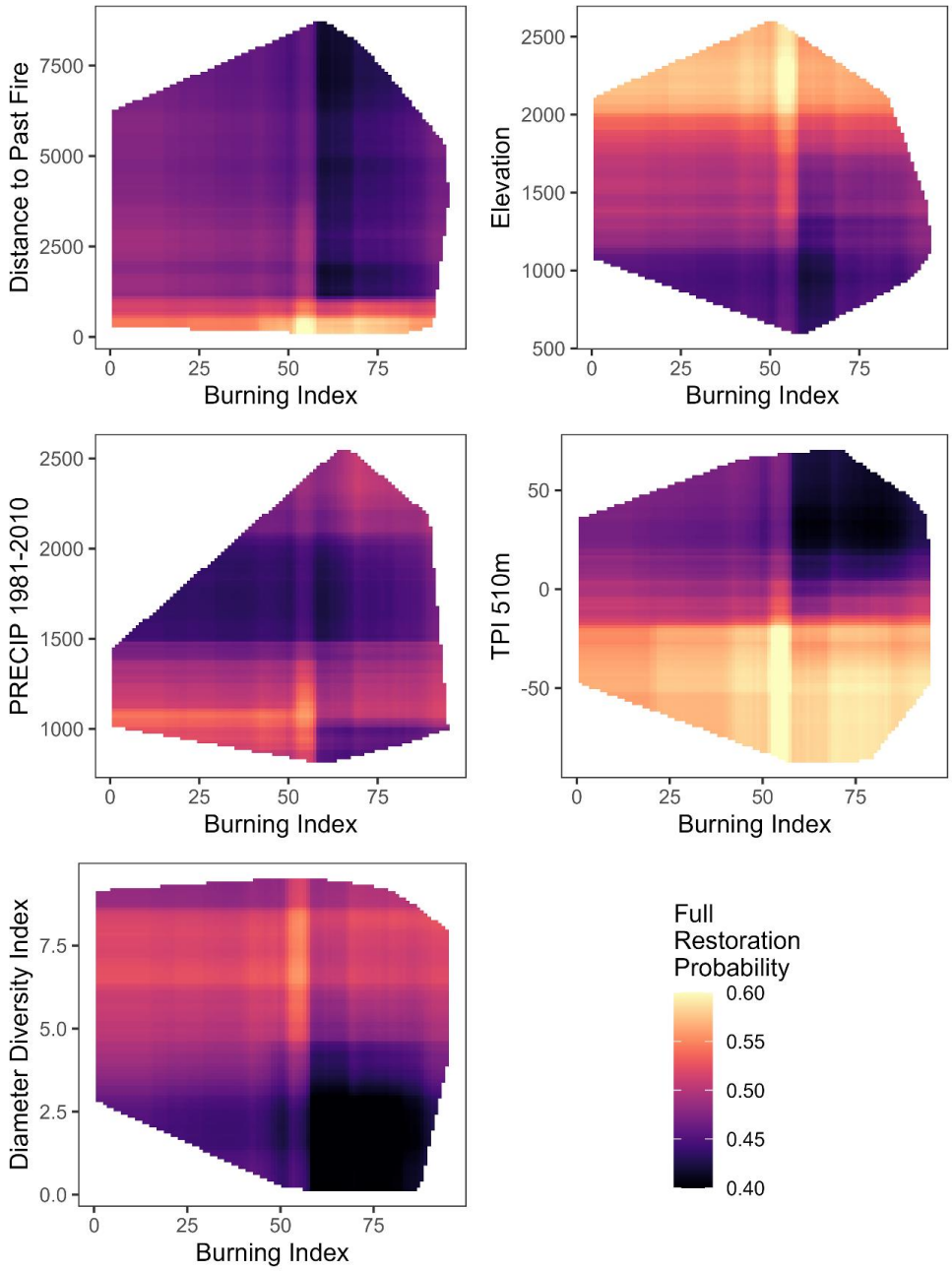

Figure 2.A.4. Two-variable partial dependence plots. We produced two-variable partial dependence plots from the final random forest model predicting the full restoration index. We show the interaction between burning index and the other top five predictors. Burning index is the variable that can best be controlled for during fire management (i.e., deciding to suppress or allow a fire to burn under given weather scenario); thus, it is valuable to show how the probability of restorative effects varies across this index in relation to other variables. We produced two-variable partial dependence plots using the *pdp* package (Greenwell 2017) in R (R Core Team 2023). TMIN: average minimum annual temperature; TPI: topographic position index.

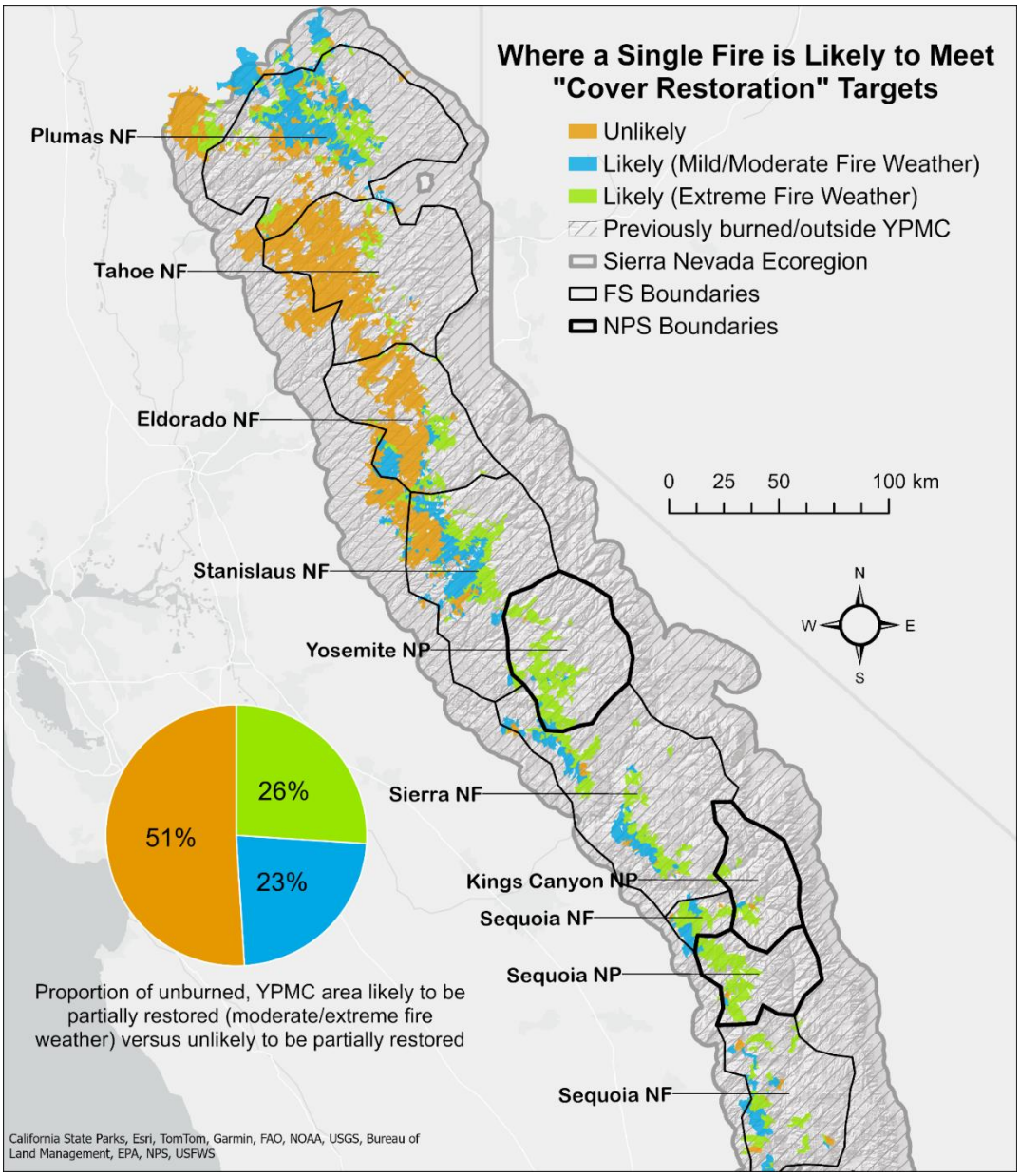

Figure 2.A.5. Model performance metrics and mapped predictions of the cover only restoration index. We used the same set of 13 predictors as described in the main text. The cover restoration model had an overall accuracy of 63.3%. When applied to yet unburned areas in the Sierra Nevada YPMC zone for year 2020, we found that 26% of total area was likely to experience restorative effects under moderate fire weather (burn index = 71), 23% under mild fire weather (burning index = 53), and 51% was not likely to experience restorative effects.

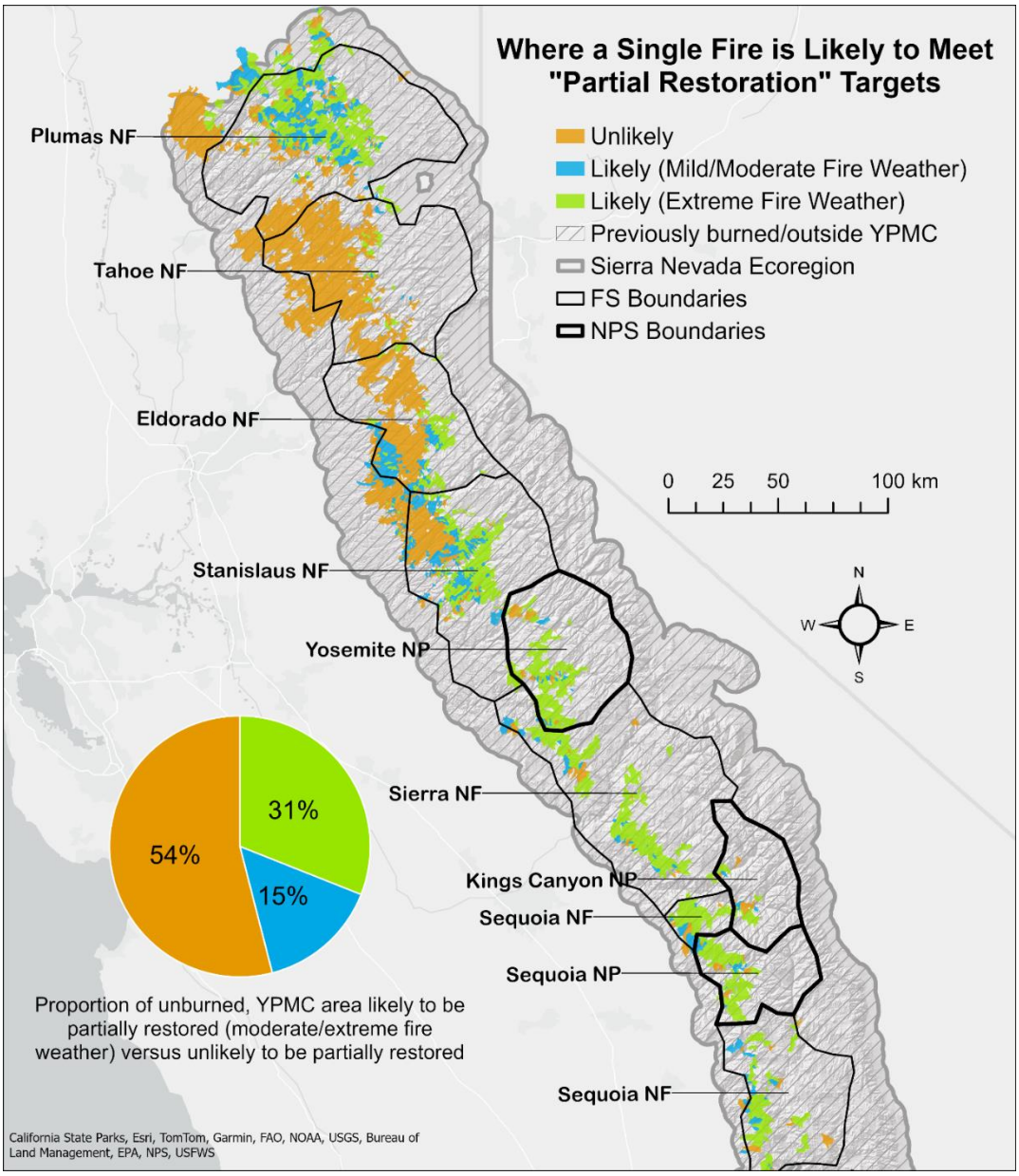

Figure 2.A.6. Model performance metrics and mapped predictions of the partial restoration index. We used the same set of 13 predictors as described in the main text. The partial restoration model had an overall accuracy of 61.8%. When applied to yet unburned areas in the Sierra Nevada YPMC zone for year 2020, we found that 31% total area was likely to experience restorative effects under moderate fire weather (burning index = 71), 15% under mild fire weather (burning index = 53), and 54% was not likely to experience restorative effects.

CHAPTER 3. ACTIVE-FIRE LANDSCAPES DEMONSTRATE STRUCTURAL RESISTANCE TO SUBSEQUENT FIRE AND DROUGHT

3.1. ABSTRACT

A key tenet of contemporary dry forest management in western North America is the reintroduction of fire, particularly frequent and lower severity fire, to fire-adapted forests. This objective is quickly being realized in many regions, both through the application of low-intensity prescribed burning and where recent wildfires have had primarily low- and moderate-severity effects. As partially-restored active-fire landscapes begin to establish in the modern era, it remains critical to evaluate the degree to which these landscapes demonstrate structural resistance under shifting climatic conditions and novel disturbance regimes. In this study, we used a bi-temporal airborne lidar dataset, spanning a region of partially-restored, active-fire landscapes in Yosemite National Park, to evaluate how tree densities, clumping patterns, and height distributions changed during a decade of moderate-intensity wildfire and high-intensity drought. We used regression models to identify patterns of resistance in a single disturbance (drought-only) and dual disturbance (drought-fire) context, and we used generalized additive models to evaluate how patterns of change varied across pre-disturbance gradients of fire history, forest structure, and biophysical conditions. Structural patterns in active-fire landscapes demonstrated near complete resistance during the 2012-2016 drought, with only slight loss of trees >32m (5% total reduction) and marked increases in 2-16m trees (33% total increase). In the drought-fire context, we observed higher magnitude structural changes compared to the drought-only context (25% total tree loss). Yet despite these changes, medium-sized (16-32m) and tall (>32m) trees, especially those belonging to 1-4 and 5-9 tree clumps, demonstrated a high degree of resistance. Structural changes in the drought-only context were primarily associated with cooler and wetter climatic conditions, whereas structural changes in the

drought-fire context occurred primarily in sites with higher pre-disturbance canopy cover (>40%), in more exposed topographic positions, and where time since past fire was longer (16+ years). Our results suggest that forest structures in contemporary active-fire landscapes exhibit high resistance to drought and moderate resistance to drought and wildfire, and that tall trees were most resistant when they belonged to small or medium-sized tree clumps. Policies and management practices that promote active-fire conditions in dry forest landscapes will contribute to the long-term sustainability of these forest ecosystems and potentially increase their adaptive capacity under climate change. Given that an important management objective is to conserve tall trees in the Sierra Nevada, we suggest that restoration efforts focus on creating or reinforcing fine-scale patterns of small and medium-sized tree clumps.

3.2. INTRODUCTION

Fires were excluded from most forest ecosystems of western North America for at least a century following Euro-American colonization (Marlon et al. 2012; Hagmann et al. 2021). However, recognizing the critical role of fire in fire-adapted forests (Falk et al. 2011; McLauchlan et al. 2020), national-level policies now promote prescribed burning and resource objective wildfires (as well as restoration thinning) across many federally managed landscapes (Stephens et al. 2016a; Huffman et al. 2020; North et al. 2024). Historically, frequent and low-severity fires promoted dry forest resistance (Hessburg et al. 2019); that is, the capacity of forest ecosystems to retain their intrinsic structures and compositions through subsequent disturbances and climatic variations (Walker et al. 2004; Falk et al. 2022). Yet as fires return to dry forest landscapes, uncertainties remain regarding the structural resistance of *contemporary* active-fire landscapes under shifting climatic conditions and novel disturbance regimes (Larson et al. 2013; Pawlikowski et al. 2019).

Wildfire, drought, and bark beetles are primary disturbance agents in dry forests, each having unique impacts on structures and compositions, and together defining complex and interacting disturbance regimes (Larson and Churchill 2012; Hessburg et al. 2019). Individual disturbances can mediate or amplify the likelihood, magnitude, and effects of subsequent disturbances, and multiple short-interval disturbances can have compounding effects on vegetation, sometimes exceeding the impacts of single disturbance events (Johnstone et al. 2016; Kane et al. 2017; Steel et al. 2023). With climate change likely to increase the interaction and compounding effects of disturbances in dry forests ecosystems (Buma 2015; Westerling 2016; Schoennagel et al. 2017), it is critical to understand the extent to which active-fire landscapes demonstrate resistance under these changing conditions.

Historically, fire-intact ecosystems contained both resistant and temporally dynamic structural features (Larson and Churchill 2012; Lloret et al. 2012). At fine spatial scales, large- and medium-sized fire-resistant pines, arranged primarily as single trees and small clumps of trees, were capable of persisting through multiple low-intensity disturbances (Keeley 2012; Falk et al. 2022). Intermixed within these resistant structural features were more dynamic structures including cohorts of small- and medium-sized trees, sometimes forming large contiguous tree clumps, that were more readily consumed by fires (Mast and Veblen 1999; Abella and Denton 2009; Larson and Churchill 2012). Droughts and associated bark beetle outbreaks could be widespread but typically had isolated effects on structures, occasionally killing mature trees within large clumps (Churchill et al. 2013; Das et al. 2016). Across broader spatial scales, vegetation dynamics varied by past disturbance intensity and underlying biophysical conditions creating heterogenous structural patterns across forest landscapes (Collins et al. 2007; Collins et al. 2015; Hessburg et al. 2015; Safford and Stevens 2017).

Dry forest ecosystems within California's Sierra Nevada have been impacted extensively by wildfires in recent decades (Cova et al. 2023; Williams et al. 2023). In some landscapes, where recent fires have had mostly low- and moderate-severity fire effects, active-fire conditions similar to the

historical fire regime of these forests have begun to reestablish (Collins et al. 2016; Jeronimo et al. 2019; Chamberlain et al. 2023a). Recent work indicates that structural patterns in these partially-restored active-fire landscapes resemble certain aspects of the resistant structures that historically characterized these forests, with relatively low tree densities, low and variable surface fuel loading (Collins et al. 2011a; Lydersen et al. 2014; Collins et al. 2016), and heterogenous structural patterns at multiple spatial scales (Kane et al. 2013; 2014; Jeronimo et al. 2019; Ng et al. 2020; Chamberlain et al. 2023a). Other work, however, suggests that these sites may still exhibit residual effects of fire-suppression with higher tree densities and fuel loading, and misaligned species distributions (Lydersen et al. 2014; May et al. 2023). Comparing structures and compositions between historical and contemporary active-fire landscapes provides key insight regarding the degree of departure of these sites, but it may ultimately be most informative to quantify the degree of resistance of these sites as they face novel conditions under climate change.

Numerous recent studies quantified patterns and mechanisms of tree-level mortality in active-fire landscapes during the 2012-2016 drought in the Sierra Nevada. Some work shows that pre-drought prescribed burning increased mortality rates during the drought, especially for large-diameter *Pinus* species (Knapp et al. 2021; Steel et al. 2021b), but other work showed that the density-reducing effects of prescribed burning eventually mediated subsequent mortality (Restaino et al. 2019; Furniss et al. 2022). Importantly, Boisramé et al. (2017) observed that landscapes in Yosemite National Park with over 40 years of managed wildfire (closely resembling the historical fire regime) experienced substantially lower mortality rates than adjacent fire-suppressed forests during the 2012-2016 drought, indicating a relatively high degree of tree-level resistance. Fewer studies have assessed how these tree-level mortality rates scale up to influence key structural patterns at stand- to landscape-scales (though see Young et al. (2020) and Furniss et al. (2022)).

Impacts from California's 2012-2016 drought were, or soon will be, proceeded by wildfire, resulting in instances of interacting disturbances and potential for compounding effects. Kane et al. (2015) and Lydersen et al. (2014) used satellite-derived burn severity indices to evaluate structural resistance following drought and fire in active-fire landscapes in the Sierra Nevada. Their results generally showed that active-fire landscapes burned primarily at low- and moderate-severity in subsequent fires (at least under non-extreme fire weather conditions), indicating moderate resistance of upper canopy cover. Hankin and Anderson (2022) used airborne lidar data to evaluate how vegetation height distributions varied by fire history characteristics in Yosemite National Park, finding that both upper and lower strata canopy structures tended to stabilize (i.e., demonstrate resistance) after two low-intensity fires. Furthermore, in the Ishi Wilderness in northern California, Pawlikowski et al. (2019) showed that large individual trees and small tree clumps demonstrated the greatest resistance during subsequent fires in a partially fire-restored landscape, though their analyses did not evaluate resistance under interacting drought and fire disturbances.

As fire is reintroduced to dry forest landscapes of western North America, it is critical to assess the degree to which contemporary active-fire landscapes demonstrate resistance during subsequent fires, droughts, and bark beetle disturbances. In this study we leveraged a 10,000 ha bi-temporal airborne lidar dataset to track changes in fine-scale tree spatial patterns and height distributions through contemporary disturbance regimes in an active-fire landscape in Yosemite National Park. We then assessed how structural changes varied across gradients of fire history and biophysical conditions. We focused our study on the historically fire-adapted yellow pine and mixed-conifer (YPMC) forests within the study area. We addressed two primary research questions:

1) How did total tree density, tree clumping patterns, and tree height distributions change in a single disturbance (drought-only) and dual disturbance (drought-wildfire) context?

2) How did pre-disturbance fire history, biophysical setting, and forest structural patterns influence structural changes in each disturbance context?

3.3. METHODS

We mapped drought-only and drought-fire settings across all YPMC forests in our study area. We used 2010 and 2019 airborne lidar acquisitions to quantify key neighborhood-level (90-m resolution) forest structure metrics including total tree density and the proportion of total density by tree clump size and height class. Linear models and generalized linear models (GLMs) were used to evaluate changes in forest structural conditions in each disturbance context, while holding key climatic and topographic factors constant (Objective 1). We then produced structural change metrics by differencing 2019 and 2010 conditions and used generalized additive models (GAMs) to identify relationships between these change metrics and key environmental variables including fire history, climate, topography, and pre-disturbance forest structure (Objective 2).

3.3.1. STUDY AREA

We defined our study area based on the overlapping footprints of the 2010 and 2019 airborne lidar acquisitions, representing a 10,631-ha region within Yosemite National Park in the central Sierra Nevada, California, USA (Figure 3.1). The study area is characterized by a Mediterranean climate. Mean annual precipitation ranges from 971-1,291 mm (Abatzoglou 2013) and elevation ranges from 1,287-2,545 m. Within our study area, we constrained our analyses to the historically fire-adapted YPMC forest types (using the FVEG Wildlife Habitat Relationship codes). Dominant tree species within YPMC forests include Jeffrey pine (*Pinus jeffreyi)*, ponderosa pine (*P. ponderosa)*, Douglas-fir (*Pseudotsuga menziesii*), sugar pine (*P. lambertiana*), incense-cedar (*Calocedrus decurrens*), and white fir (*Abies concolor*). At lower elevations, *Pinus* species are more common and often

intermix with California black oak (*Quercus kelloggii*), while higher elevations tend to have higher proportions of white fir and intermixing components of red fir (*Abies magnifica*) and lodgepole pine (*P. contorta*) (Safford and Stevens 2017).

Prior to Euro-American colonization, YPMC forests were characterized by a frequent and low-severity fire regime with an approximate mean fire return interval of 11-16 years (Safford and Stevens 2017). Wildfires and Indigenous burning practices were excluded from these landscapes for several decades beginning in the mid-1800s and extending to today (Taylor et al. 2016; Klimaszewski-Patterson et al. 2024). However, in Yosemite National Park, fire management policies began to support the reintroduction of low-severity fires as early as the 1960s (van Wagtendonk 2007; Collins and Stephens 2007), such that many landscapes within the park (including in our study area) have burned once and sometimes multiple times in recent history (Figure 3.1). Satellite-derived burn severity estimates revealed (Parks et al. 2019) that fires prior to 2010 in our study area burned primarily at low- and moderate severity, with only small patches of high severity effects, thus resembling the historical fire regime for these forest types (Safford and Stevens 2017).

3.3.2. DEFINING DISTURBANCE SEQUENCES

Forests within Yosemite National Park were impacted extensively by the intense 2012-2016 drought and subsequent bark beetle outbreaks. Recent studies indicated that this drought event was the most severe in at least the past 1,000 years for the region (Griffin and Anchukaitis 2014). Considering the pervasiveness of the drought across the region and the often coincident occurrence of drought and beetles, we ubiquitously classified *all* sites within our study region as a drought context, with this classification serving as an umbrella category to include the impacts of both drought and bark beetles.

Between 2010 and 2019, portions of our study area were impacted by several wildfires including the 2011 Bald and Tamarack Fires, the 2013 Rim Fire, the 2014 El Portal Fire, and the

2015 Middle Fire. We classified all burned sites within our study area as a drought-fire context. While portions of recent large fires in the Sierra Nevada (including the Rim Fire) have been characterized by extreme fire behavior and subsequent high severity effects on vegetation, we note that the portion of fires impacting our study area all burned under moderate fire weather conditions (i.e., burning index < 80; mapped using the GRIDMET dataset (Abatzoglou 2013) and the Parks (2014) burn progression layers). Burn indices below 80 are generally associated with flame lengths < 2.4 m and firefighters often use direct attack approaches under these conditions. Indeed, Lydersen et al. (2014) found that sites within the Rim Fire with burning index < 75 tended to have primarily moderate severity effects on vegetation.

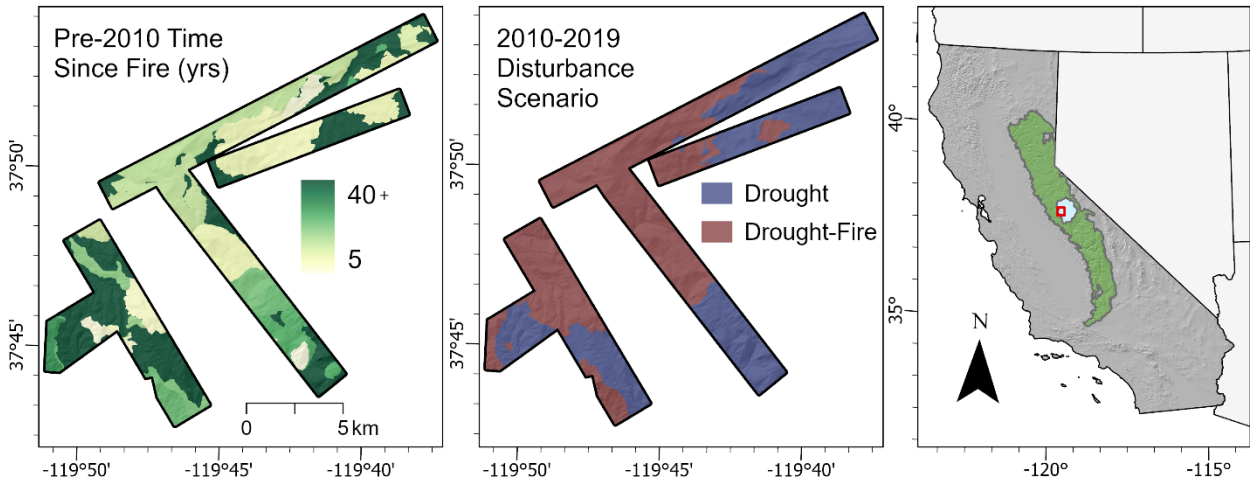

Figure 3.1. Study area representing the overlap of the 2010 and 2019 airborne lidar acquisitions within Yosemite National Park, California, USA. Left panel shows the time since pre-2010 fires for the year 2010, middle panel shows extent of the drought-only and drought-fire contexts, and the left panel shows the study area location in California (blue polygon is Yosemite National Park and green outline is Sierra Nevada ecoregion).

3.3.3. QUANTIFYING STRUCTURE WITH AIRBORNE LIDAR

We produced 90-m resolution live-canopy structure metrics from the 2010 and 2019 airborne lidar acquisitions. We used a 90-m resolution since past work indicates that fine-scale tree

clump and opening patterns tend to emerge at approximately this scale in frequent-fire forests under active fire conditions (Larson and Churchill 2012) and to align with related studies (Pawlikowski et al. 2019). Mean pulse density m^{-2} for 2010 and 2019 was 10.7 and 23.5, respectively, which meets the United States Geological Survey's Quality Level 1 standard, suitable for vegetation-related research (Mitchell et al. 2018). We acknowledge that the differences in pulse densities between the acquisitions may have influenced structure metrics; however, we note that past research found that tree segmentation algorithms performed similarly when pulse density exceeded 8 pulses m^{-2} (Kaartinen et al. 2012; Sparks et al. 2022)

We used the Forest Service's FUSION software to segment individual trees and to produce canopy height models (CHMs) and intensity rasters from each acquisition (McGaughey 2020). We refer to lidar-segmented trees as tree approximate objects (TAOs) to acknowledge that lidar-segmented trees often represent a single overstory tree and none to several subordinate trees (Jeronimo et al. 2018). Prior to segmenting TAOs and producing CHMs and intensity rasters, we normalized each point cloud so that Z coordinates measured vegetation height above ground. We produced 0.75-m canopy height models (smoothed using a 3x3-cell mean filter) from each acquisition and used the watershed algorithm to identify TAO high points. We also produced a corresponding 0.75-m intensity layer representing the mean near infrared reflectance of all points within each cell. We assumed circular crowns for each TAO, estimating the radius of each crown from the area of CHM cells corresponding to each high point.

We sought to quantify and evaluate *live* canopy structures in our analyses; thus, we developed TAO-level mortality models for each acquisition so that dead TAOs could be excluded prior to computing metrics of TAO density, clumping patterns, and height distributions (Khatri-Chhetri et al. 2024). To predict TAO-level mortality, we first produced training datasets for each acquisition comprised of 4,000 TAOs. The 4,000 TAOs were sampled from each acquisition using a stratified

random sampling design (stratified by recent disturbance history (Housman et al. 2022), clump size, and mean lidar intensity). Each of the 8,000 TAOs were manually labeled as live, dead, or unknown using (1) color imagery and (2) 0.75-m lidar intensity layers. We used 15-cm ortho imagery that was collected simultaneously with the lidar acquisition to label the 2010 TAOs and, for 2019 TAOs, we used 60-cm imagery from the National Agricultural Imagery Program that was collected in 2020. We considered a TAO as live if >50% of the crown appeared to be live in the aerial imagery. TAOs for which the imagery did not enable reliable labeling were marked as unknown and discarded from subsequent modeling (3.2% and 4.8% of the 2010 and 2019 training datasets, respectively). After labeling all TAOs in each acquisition, we extracted four intensity metrics from the 0.75-m intensity raster for each TAO (mean, minimum, maximum, and standard deviation) and also quantified each TAO's height to crown area ratio (as a way to differentiate tall snags with small, dead crowns). Each training dataset was then balanced (using random sampling) so that live and dead classes each had equivalent counts of observations. We fit RF models on each dataset using the *tidymodels* and *ranger* packages, including the four intensity metrics and the height to crown area ratio as predictors. We fit the models on 75% of the data and derived model fit statistics on the remaining 25% of the dataset (Table 3.A.1, Figure 3.A.1, Table 3.A.2, Figure 3.A.2). Finally, we used the RF models to predict TAO-level mortality across all TAOs in each acquisition and excluded all TAOs predicted as dead from subsequent analyses. Exploratory analyses revealed that mortality models in both acquisitions were biased toward live predictions in sites with recent fire activity (i.e., 2009, 2010, 2018, and 2019) where the majority of trees appeared to be in the "red phase" of mortality. Based on this observation, we decided to mask out all sites from our study area that burned within one year prior to the lidar acquisition to ensure the most reliable mortality mapping.

From the live TAOs in each acquisition, we produced 90-m resolution rasters representing total TAO ha^{-1} in 2010 and 2019, as well as metrics quantifying the proportion of total tree density

represented by different TAO clump sizes and height classes. Clumps of TAOs were identified based on overlapping TAO crowns and clump sizes were computed as the number of TAOs belonging to a given clump. We classified clumps as 1-4, 5-9, and 10-plus TAOs to support comparison with related studies (Lydersen et al. 2013; Kane et al. 2019). We also classified TAO heights using three height classes, 2-16 m, 16-32 m, and 32 m plus, where the 16 and 32 m thresholds corresponded approximately to the 33rd and 66th percentile of all TAO heights in our study. Lastly, we produced structural change metrics by differencing 2019 and 2010 layers for each structure metric.

3.3.4. MAPPING BIOPHYSICAL CONDITIONS AND FIRE HISTORY

We compiled a variety of datasets to describe environmental conditions in or prior to 2010 that were used as predictors in our modeling of structural change. To characterize the climatic setting of our study area we used layers from the Basin Characterization Model dataset describing long-term (1981-2010) mean annual actual evapotranspiration (AET) and climatic water deficit (CWD) (Flint et al. 2021). Past work suggests these metrics can reliably capture gradients of productivity (AET) and vegetation stress (CWD) in Sierra Nevada forests (Stephenson 1998). We used two metrics to capture topographic gradients in our analyses: topographic position index (TPI) and the solar radiation aspect index (SRI). TPI provides a continuous metric differentiating valleys, slopes, and ridges (Jenness 2007). We quantified TPI using a 510-m moving window since exploratory analyses suggested that this scale had the strongest relationship with our structural change metrics (compared to 130 m and 8010 m moving window sizes). SRI is a rotation of the circular slope aspect and provides a continuous index differentiating north- and northeast-facing slopes from south and southwest-facing slopes (Roberts and Cooper 1989). We also included two metrics to describe general gradients of canopy density across our study area in 2010 including (1)

90-m total canopy cover of live TAOs and (2) relative canopy cover in the 2-8 m height strata (as a proxy for ladder fuel density) (Hankin and Anderson 2022; Chamberlain et al. 2024).

We mapped pre-2010 fire history characteristics using fire perimeters from CALFIRE's Fire and Resource Assessment Program (FRAP) fire history dataset, which included all recorded wildfires and prescribed fires > 4 ha (FRAP 2021). To ensure reliability of the dataset, we also validated records in this dataset against Yosemite National Park fire records. We only included fires that burned 1985-2009 so that Landsat-8 imagery could be used to map burn severity. All areas with fire records prior to 1985 were masked out from subsequent analyses (8% of the total study area). We produced two fire history datasets: (1) time since most recent fire and (2) most recent burn severity. For the time since most recent fire metric, we set the "current" date as either the year of the fire that burned 2010-2019 or, in the drought-only context, as 2012 corresponding with the start of the 4-year drought. We classified this metric as 1-15, 16-30, or >31 years (these thresholds were selected as they ensured reasonable sample sizes under each category for both the drought-only and drought-fire context). To produce the most recent burn severity layer, we used the Google Earth Engine code described in Parks et al. (2019) to map the bias-corrected Composite Burn Index at 30-m resolution for all pre-2010 fires, then created a composite layer representing the most recent CBI value.

3.3.5. STATISTICAL ANALYSES

We first plotted TAO height distributions for all TAOs and for TAOs belonging to each clump size (1-4, 5-9, and 10 plus). We compared distributions between 2010 and 2019 under both the drought-only and drought-fire context to evaluate how these disturbance contexts impacted total TAO counts.

Next, prior to fitting models of structural change, we assessed predictor multicollinearity and model residual spatial autocorrelation (SA) to establish a standardized and robust modeling

workflow. To reduce multicollinearity, we computed Spearman's correlation coefficient among all continuous predictor variables. When correlation among variables exceeded 0.5, we selected the variable which produced the best fit generalized additive model (GAM) predicting change in total tree density as the response. We compared univariate models using the minimized generalized cross-validation (GCV) score, where lower GCV scores indicated a better model fit (Wood 2017). From this process, we identified CWD, TPI, SRI, and 2010 total canopy cover as the top predictors of structural change. We used these predictors, and the categorical time since fire metric, in subsequent modeling. To identify a minimum sampling distance within our study area, we assessed SA of model residuals using the Moran's I statistic. We fit a GAM model predicting total change in TPH as a function of the selected environmental variables. We then computed Moran's I of the model residuals at varying lag distances using the *ncf* package. We found that Moran's I values remained below 0.3 at lag distances greater than 410 m; thus, we conducted all additional modeling using a minimum among-sample distance of 450 m (i.e., the distance between 5, 90-m cells), which served to reduce the effects of SA while allowing sufficient sample sizes to make model-based inferences.

After reducing multicollinearity and subsampling to reduce SA, we fit two sets of final models. First, to quantify the magnitude and direction of change in each structure metric in each disturbance context (drought-only and drought-fire), we fit linear models and GLMs to predict each metric as a function of year, CWD, TPI, and SRI ("change models"). We fit linear models for the total TAO density metric, assuming a gaussian error distribution, and GLMs for each of the proportional metrics, assuming beta error distributions with a logit link (Faraway 2015). For proportion metrics, we reclassified all 0's as 0.001 and all 1's as 0.999 to meet the specifications of the beta distribution. From these models, we compared predicted means of each metric in each disturbance context and assessed 95% confidence intervals (CIs) around predictions, denoting a significant difference when CIs did not overlap. We also plotted the raw density curves of each

metric to visualize differences in metric distributions between the years in each disturbance context. We also compared distributions between 2010 and 2019 for absolute values of TPH by clump size and height class membership (as opposed to proportional metrics) in Figure 3.A.3 and Figure 3.A.4.

For our second set of models, we fit GAMs predicting the change in each metric in each disturbance context as a function of the biophysical, fire history, and 2010 forest structure conditions ("drivers of change models"). These models allowed us to quantify how structural changes varied linearly and non-linearly across environmental gradients within our study area (Wood 2017). For each GAM, we excluded samples in which 2010 structural conditions were 0 (i.e., no TAOs in 2010 or no TAOs belonging to a given clump or height class) so that instances of "no change" indicated no loss or gain of an existing structure. We assumed a gaussian error distribution for each GAM, which we validated by assessing post-hoc residual distributions. In all models, time since fire was fit as a linear predictor and each continuous predictor was fit using thin plate regression splines with a basis dimension of 5. We set select as "true" and used a gamma value of 1.4 to allow moderate penalization terms in each model, which allowed fitting of non-linear, linear, and 0 coefficients (Marra and Wood 2011; Wood 2017). Finally, to assess how patterns of structural change varied across environmental conditions in each disturbance context, we predicted the mean and 95% CIs of each metric across the full range of each environmental variable, while holding other variables at their means. For predictions of continuous variables, we set time since fire as 15-30 years to represent the mid-range of fire activity in our study area. We also provide modeled predictions across environmental variables for total change in TPH by clump size and height class membership (as opposed to proportional metrics) in Figure 3.A.5 and Figure 3.A.6.

3.4. RESULTS

3.4.1. CHANGES IN STRUCTURE THROUGH DROUGHT-ONLY AND DROUGHT-FIRE

In the drought-only context, we observed negligible changes in total TAO counts across all height classes (Figure 3.2). We observed 33% and 2% increases in the counts of short and medium-sized TAOs, respectively, and a 5% reduction in the count of tall TAOs. All clump sizes experienced similar changes in TAO counts across clump sizes, with slightly greater loss (5% reduction) of tall TAOs when they belonged to large clumps. In the drought-fire context, we observed a 25% reduction in the total count of all TAOs, corresponding to a 28% increase in the count of short TAOs and 50% and 35% reductions in the counts of medium-sized and tall TAOs, respectively (Figure 3.2). Across clump sizes, reductions in TAO counts were associated almost entirely with TAOs belonging to large clumps (74% and 62% reduction in total counts of medium-height and tall trees, respectively, belonging to large clumps). In contrast, medium-height and tall trees belonging to small and medium clumps demonstrated near complete stability (or slight increases) in total TAO counts in the drought-fire context (Figure 3.5).

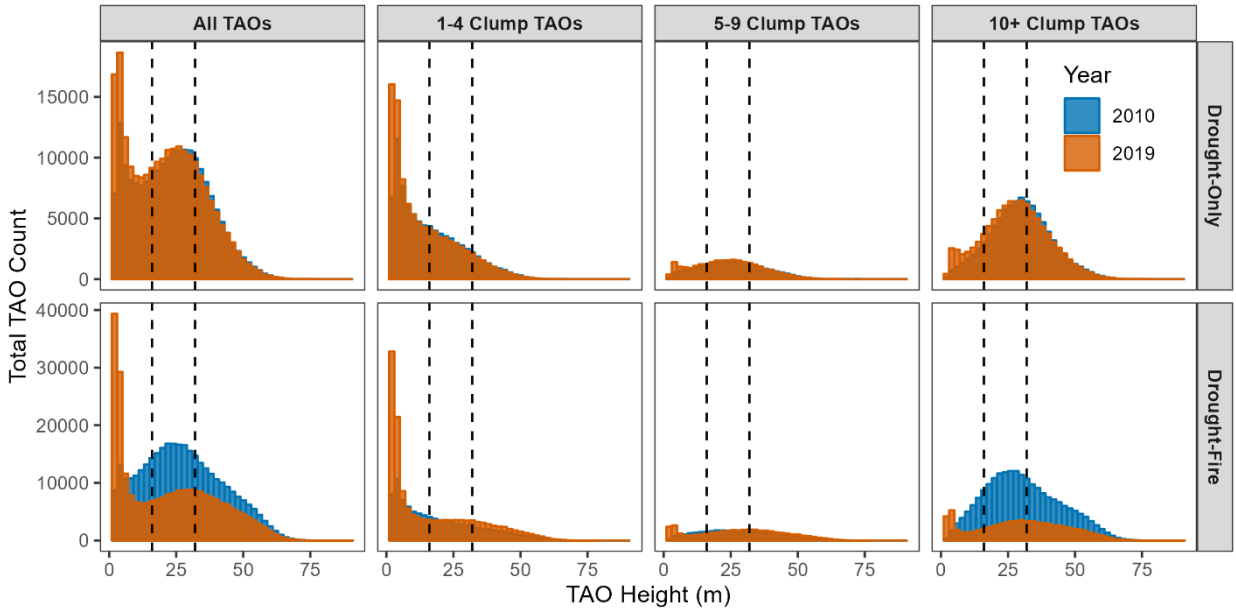

Figure 3.2. Changes from 2010 to 2019 in TAO height distributions by total TAO counts and TAO clump size membership for the drought-only and drought-fire contexts, in active-fire landscapes within Yosemite National Park, California, USA. Vertical dashed lines indicate 16 m and 32 m height thresholds. Each bar represents a 2-m height bin.

Our linear and generalized linear models (i.e., change models), which included year, CWD, TPI, and SRI to predict each forest structure metric, explained relatively low proportions of variance in both the drought-only and drought-fire contexts (Table 3.1). The variance explained by drought-only models ranged from 0.03 for the model predicting proportion medium clump (5-9 TAOs) membership to 0.27 for the model predicting proportion tall TAOs (>32m). For drought-fire models, variance explained ranged from 0.02 for the model predicting proportion medium clump membership to 0.21 for the model predicting large clump (10+ TAOs) membership. In both drought-only and drought-fire contexts, models predicting medium clump membership and proportion of medium-height TAOs (16-32m) had the weakest fits (Table 3.1).

Table 3.1. Descriptions and performance statistics for 14 change models and 14 drivers of change models. GLM: generalized linear model; CWD: climatic water deficit; TPI: topographic position index; SRI: solar radiation index; TAO: tree approximate object; TPH: TAOs per hectare; GAM: generalized additive model; CC: canopy cover; TSF: time since fire

Model Category	Model Type	Predictors	Error Distribution	Response	Drought-Only R^2	Drought-Fire R^2
Change	Linear GLM	Year, CWD, TPI, SRI	Gaussian Beta	Total TPH	0.18	0.14
				Prop. small clump	0.11	0.17
				Prop. medium clump	0.03	0.02
				Prop. large clump	0.15	0.21
				Prop. short TAOs	0.11	0.10
				Prop. medium TAOs	0.01	0.09
				Prop. tall TAOs	0.27	0.11
Drivers of Change	GAM	2010 CC, CWD, TPI, SRI, TSF (categorical)	Gaussian	Δ total TPH	0.50	0.41
				Δ prop. small clump	0.41	0.39
				Δ prop. med. clump	0.17	0.19
				Δ prop. large clump	0.45	0.40
				Δ prop. short TAOs	0.14	0.17
				Δ prop. med. TAOs	0.26	0.13
				Δ prop. tall TAOs	0.06	0.09

We observed no significant differences (in model-predicted means) between 2010 and 2019 for any structure metrics in the drought-only context (Figure 3.3). Mean total TPH increased non-significantly (from 86.0 in 2010 to 96.9 in 2019), which resulted in a slight but non-significant decrease in the proportion of small clump (1-4 TAOs) membership (0.01 lower in 2019 than 2010)

and a small but non-significant increase in the proportion of large clump membership (0.04 higher in 2019 than 2010). The increased TAO density also led to a slight but not significant increase in the proportion of short (2-16 m) TAOs (0.07 higher in 2019 than 2010) and a slight but non-significant decrease in the proportion of medium-height (16-32 m) and tall TAOs (0.03 and 0.02 lower in 2019 than 2010, respectively) (Figure 3.3). Distributional changes in structure metrics between 2010 and 2019 in the drought-only context generally followed similar patterns as model-predicted means, with moderate shifts toward higher total TAO densities reflected primarily as shifts toward higher proportions of large clump membership and short TAOs (Figure 3.3).

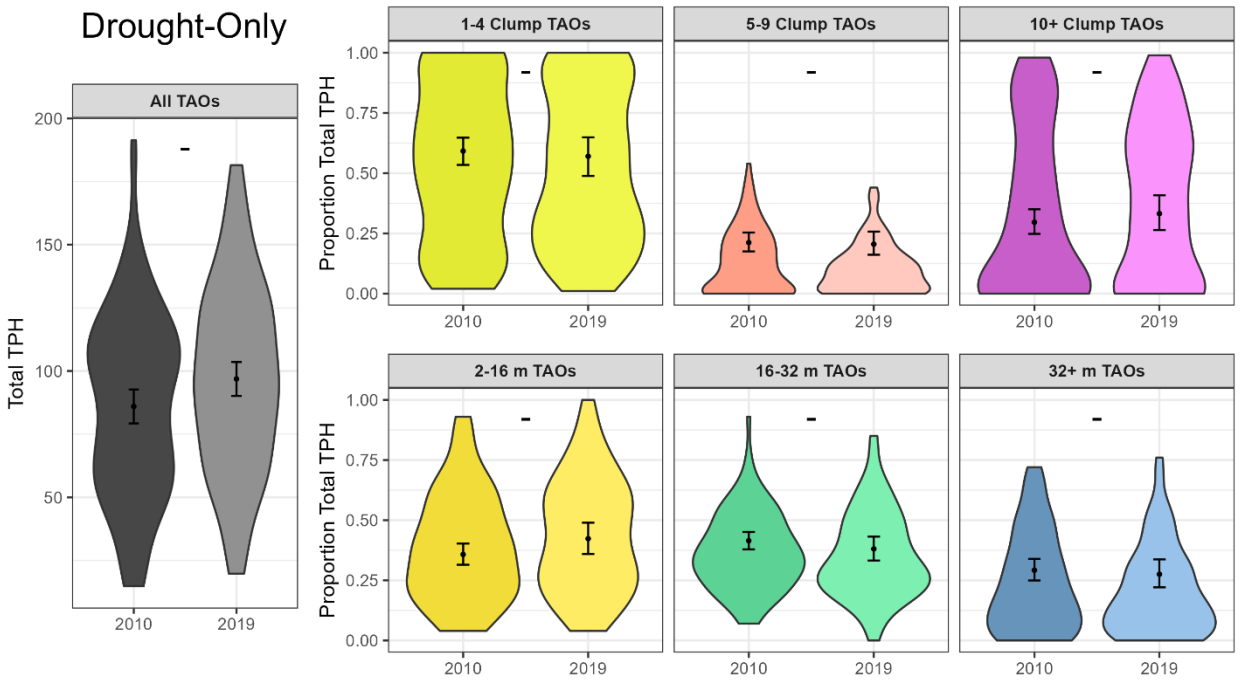

Figure 3.3. Differences between 2010 and 2019 for total TAO ha^{-1} (TPH), and proportion of TPH by TAO clump size and height class in the drought-only context, for active-fire landscapes within Yosemite National Park, California, USA. Density distributions represent all sample points. Points and error bars show model-predicted means and 95% confidence intervals, respectively, from linear models (All TAOs) and generalized linear models (clumping and height metrics). Asterisks (*) and dashes (-) indicate non-overlapping and overlapping confidence intervals, respectively.

Structural conditions changed considerably more in the drought-fire context compared to the drought-only context (Figure 3.3; Figure 3.4), with a general trend of decreasing TAO density a shift toward more open structural conditions. Indeed, we observed a significant mean reduction in total TPH from 2010 to 2019 (decreasing from 102.0 to 77.2). Distributional changes in total TPH also showed a shift toward lower post-disturbance densities, though most sites maintained TPH values > 25.0 (Figure 3.4). Regarding TAO clump membership, we observed a significant increase in the proportion of small clump membership (0.26 increase from 2010 to 2019) and a significant decrease in the proportion of large clump membership (0.23 decrease from 2010 to 2019), with a slight yet non-significant increase in the proportion of medium clump (5-9 TAOs) membership (Figure 3.4). Loss of total TPH in the drought-fire context was also reflected as a significant increase in the proportion of short TAOs (0.13 increase from 2010 to 2019) and a significant decrease in the proportion of medium-height TAOs (0.15 decrease from 2010 to 2019), with a slight but non-significant decrease in the proportion of tall TAOs (0.06 decrease from 2010 to 2019) (Figure 3.4). Shifts in structure metric distributions between 2010 and 2019 in the drought-fire context also show, generally, either increases or stability in small and medium clump membership and stability or slight loss of tall TAOs (Figure 3.4).

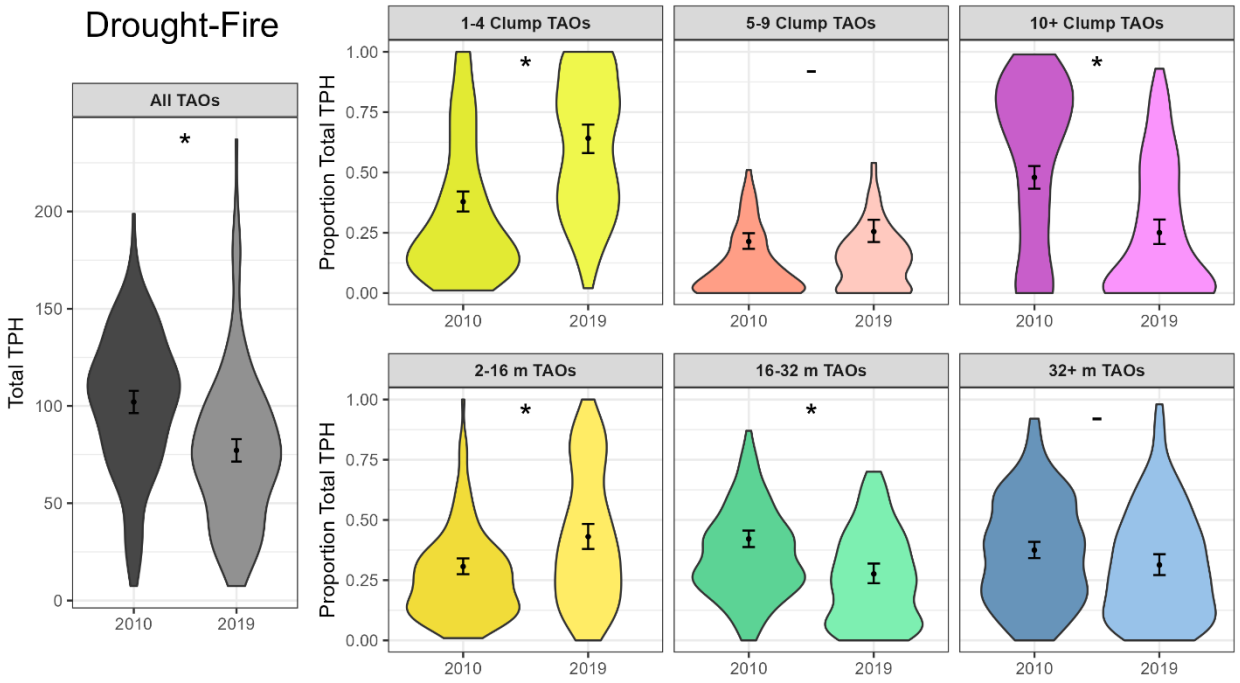

Figure 3.4. Differences between 2010 and 2019 for total TAO ha^{-1} (TPH), and proportion of TPH by TAO clump size and height class in the drought-fire context, for active-fire landscapes within Yosemite National Park, California, USA. Density distributions represent all sample points. Points and error bars show model-predicted means and 95% confidence intervals, respectively, from linear models (All TAOs) and generalized linear models (clumping and height metrics). Asterisks (*) and dashes (-) indicate non-overlapping and overlapping confidence intervals, respectively.

3.4.2. DRIVERS OF CHANGE DURING DROUGHT-ONLY AND DROUGHT-FIRE

Our GAMs (i.e., drivers of change models) predicting drivers of structural change as a function of pre-drought canopy cover biophysical metrics, and pre-2010 fire history explained low to moderate proportions of variance (Table 3.1). The drought-only and drought-fire models predicting absolute change in TPH exhibited relatively high variance explained, with R^2 values of 0.50 and 0.41, respectively. For both the drought-only and drought-fire context, models predicting change in the proportion of small and large TAO clump membership were relatively strong (R^2 for small clump = 0.41 (drought-only) and 0.39 (drought-fire) and R^2 for large clump = 0.45 (drought-

only) and 0.40 (drought-fire)). Models predicting change in the proportion of tall trees were weakest for both contexts (R^2 = 0.06 (drought-only) and 0.09 (drought-fire)).

Our drivers of change models showed that pre-drought canopy cover, biophysical setting, and pre-2010 fire history had minimal impact on patterns of structural change in the drought-only context (Figure 3.5). Model-predicted increases in total TPH were associated primarily with locations where 2010 canopy cover was lower (< approximately 60%) and in more moist climatic settings (CWD < 500 mm). Topographic conditions and fire history were less influential on changes in total TPH in the drought-only context, though less exposed topographic positions (TPI < 0) and sites that had experienced fire 16-30 years prior to the drought showed slight increases in model-predicted TPH (Figure 3.5). The most substantial changes in TAO clump size membership were observed at CWD values < 500 mm and, to lesser degree, when 2010 canopy cover was less than 20%. In these sites, a decrease of approximately 0.40 in the proportion small clump membership corresponded to an approximate 0.40 increase in the proportion large clump membership. Changes in TAO height distributions in the drought-only context showed only subtle trends across environmental gradients (Figure 3.5); irrespective of 2010 canopy cover and topographic positions, the proportion of short TAOs increased by approximately 0.10 while medium-height and tall TAOs decreased by approximately 0.10 and 0.05, respectively. A slight trend was observed across the CWD gradient such that the proportional loss of medium-height and tall TAOs was greater under more climatically stressed conditions (Figure 3.5).

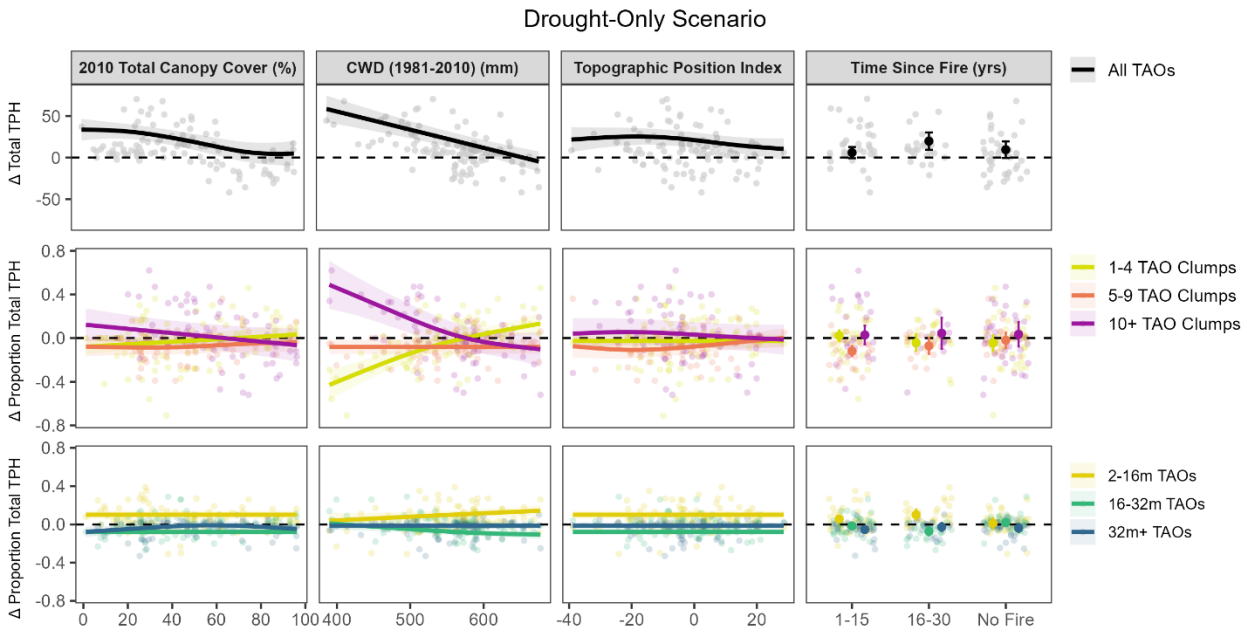

Figure 3.5. Model-predicted trends between environmental variables and structural change metrics for the drought-only context, in active-fire landscapes within Yosemite National Park, California, USA. In the left three columns, lines represent predicted means, and shaded regions represent 95% confidence intervals. In the rightmost column, full color points and error bars show model-predicted means and 95% confidence intervals, respectively. Transparent background points show the distributions of sample points in each model.

Changes in total TPH and TAO clumping patterns were influenced considerably by 2010 total canopy cover and TPI in the drought-fire context (Figure 3.6). As 2010 canopy cover increased and topographic position transitioned from valleys to ridges, the combined effects of drought and fire resulted in greater loss of total TPH. In terms of TAO clump membership, these reductions in total TPH corresponded almost exclusively with reductions in the proportion of large clump membership (up to 0.80) and increases in the proportion of small clump membership (up to 0.45) indicating a disaggregation of larger clumps into smaller clumps when 2010 canopy cover was higher and in more exposed topographic positions. While time since fire did not have a significant effect on change in total TPH in the drought-fire context (though a non-significant trend of increasing loss with longer time since fire was observed), fire history did have a significant effect on changes in

TAO clump membership. Specifically, we found that sites with no record of fire history showed a stronger signal of change from large clump to small clump membership, compared to sites that burned within the last 30 years. Changes in height distributions in the drought-fire context were less reflective of biophysical and fire history gradients in the drought-fire context (Figure 3.6). All sites exhibited an approximate increase of 0.20 in the proportion of short TAOs corresponding with an approximate 0.10 and 0.05 reduction in the proportion of medium-height and tall TAOs, respectively. This trend was accentuated slightly when 2010 canopy cover exceeded 80%, in topographic valleys, and when time since fire was 16-30 years (Figure 3.6).

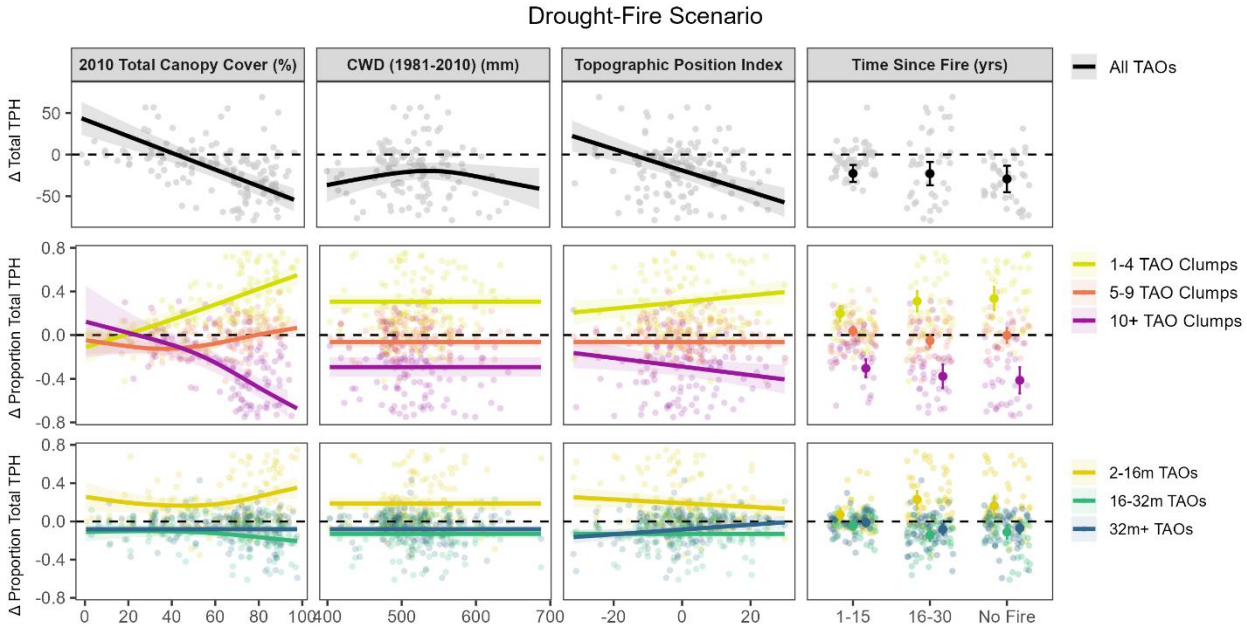

Figure 3.6. Model-predicted trends between environmental variables and structural change metrics for the drought-fire context, in active-fire landscapes within Yosemite National Park, California, USA. In the left three columns, lines represent predicted means, and shaded regions represent 95% confidence intervals. In the rightmost column, full color points and error bars show model-predicted means and 95% confidence intervals, respectively. Transparent background points show the distributions of sample points in each model.

3.5. DISCUSSION

Our results suggest that the reintroduction of frequent and low- to moderate-severity fire to fire-adapted forests can reinstate essential ecological processes that contribute to ecosystem function and resilience, which may help conserve valued forest resources during an era of rapid environmental change. We found that key structural features, including small TAO clumps and tall TAOs, demonstrated resistance during drought and fire disturbances in active-fire landscapes of California's Sierra Nevada. Tall TAOs were particularly resistant when they belonged to small- or medium-sized clumps. Across our study area, structural changes in the drought-fire context were moderated by pre-disturbance canopy cover, topographic position, and the timing of past fires, suggesting a reflection of the underlying biophysical template in patterns of structural change (Figure 3.7).

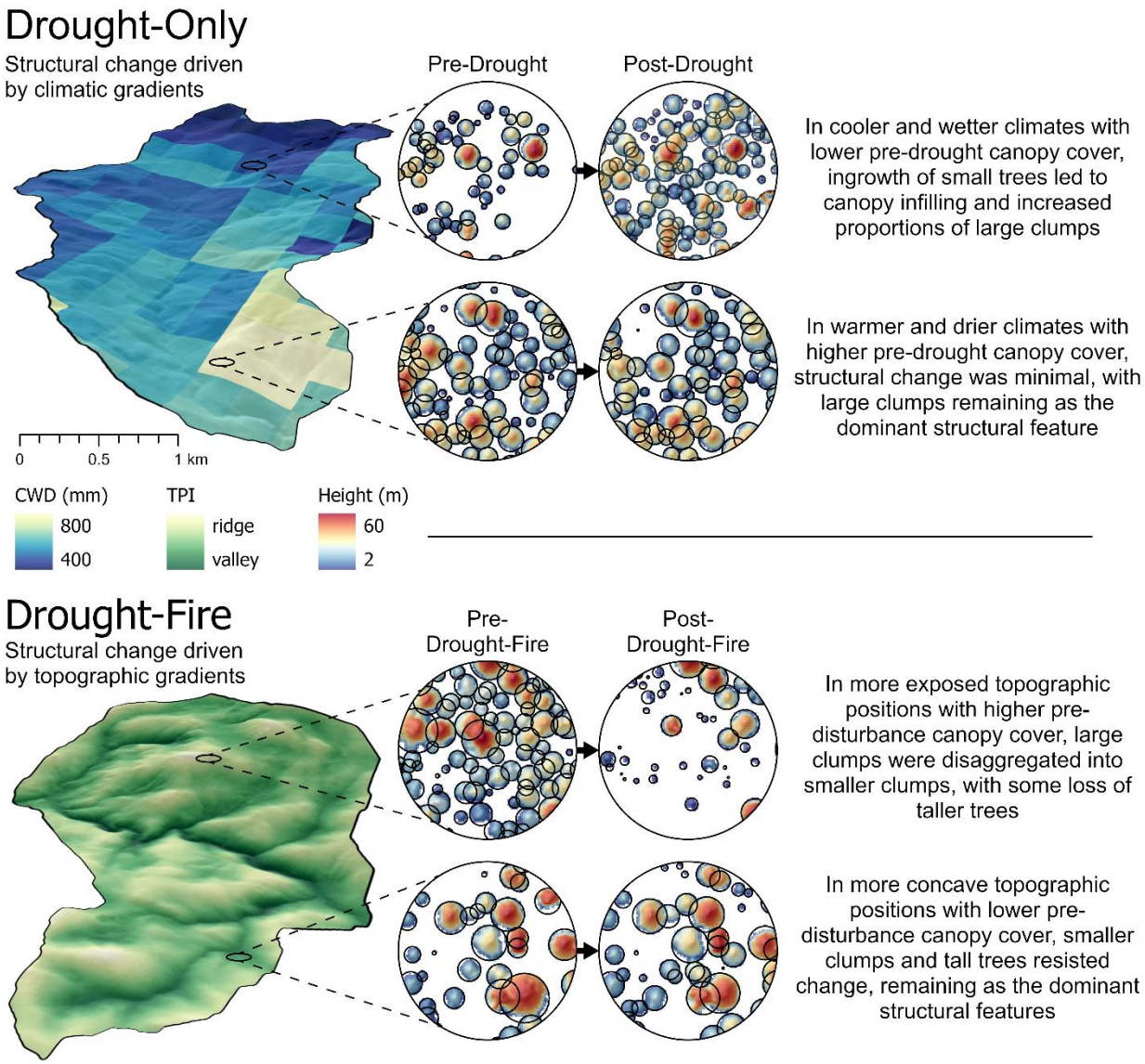

Figure 3.7. Conceptual diagram illustrating structural dynamics in an active-fire dry forest landscape under drought-only (top) and drought-fire (bottom) contexts. Circular insets show how shifts in TAO spatial patterns and height distributions from 2010 to 2019 vary across a gradient of climatic water deficit (top, drought-only context) and a gradient of topographic position index (bottom, drought-fire context).

3.5.1. ACTIVE-FIRE LANDSCAPES DEMONSTRATE RESISTANCE TO DROUGHT

Despite extensive research across the Sierra Nevada documenting widespread impacts of the 2012-2016 drought (Young et al. 2017; Fettig et al. 2019; Restaino et al. 2019), with some studies

reporting mortality rates as high as 48.9% (Fettig et al. 2019), we observed no significant reductions in TPH in our study area (Figure 3.3), and only a slight but non-statistically significant decrease in the total count and proportion of the tallest TAOs (>32m) (Figure 3.2). While changes in TPH and total TAO counts are not directly comparable to tree-level mortality rates, our findings were somewhat unexpected, especially considering the intensity of the 2012-2016 drought (Griffin and Anchukaitis 2014). We attribute the overall drought resistance in our study area to (1) the relatively higher elevations characterizing the majority of our study area and (2) our study area's partially-restored fire regime (Boisramé et al. 2017). Several studies have documented lower mortality rates during the 2012-2016 drought in higher elevation (and latitude) sites (Young et al. 2017; Fettig et al. 2019). Fettig et al. (2019) reported mean mortality rates of 54.4% and 46.1% for similar elevations as our study area, compared to the relatively higher 60.4% rate documented for lower elevation sites (<1200 m). However, structural changes in the drought-only context in our study still did not reflect anywhere close to a 46.1% loss of trees.

We suggest that the remaining discrepancy, and in fact an increase in TPH during drought, can be attributed to our study area's partially restored fire regime, which aligns with other assessments of drought resistance specifically in active-fire landscapes (Boisramé et al. 2017; Murphy et al. 2021). Some studies have shown that previous fire effects can increase mortality rates during drought and beetle outbreaks (Knapp et al. 2021; Steel et al. 2021b). However, other studies suggest that negative effects of past fire are short term (<7 years), and that reduced local tree density and competition can ultimately increase tree-level resistance (Hood et al. 2015; Restaino et al. 2019; Furniss et al. 2022). Indeed, much of our study area was characterized by relatively low-density stands and dominance of small TAO clumps prior to the drought, an outcome of recent low- and moderate-severity fire effects (Kane et al. 2014). We suggest that these low-density structural conditions contributed to healthier and more vigorous trees that were more capable of withstanding

the stress and beetle attacks of the 2012-2016 drought (Hood et al. 2015; Young et al. 2017; Furniss et al. 2022; Willson et al. 2024).

The drought-only affected portion of our study area was also characterized by relatively high variability in structural conditions in 2010 (*i.e.,* landscape-level heterogeneity) (Figure 3.3). We believe that this heterogeneity may have further enhanced neighborhood-level resistance of TAOs. Heterogeneous structural patterns are associated with more diverse species assemblages and more discontinuous canopies, both of which can inhibit the growth and spread of bark beetle populations and reduce subsequent severity (Fettig et al. 2007; Turner et al. 2013; Hessburg et al. 2019; Restaino et al. 2019; Koontz et al. 2021). In fact, a study that reported the highest mortality rates within prescribed burning treatments during the 2012-2016 drought indicated that a possible reason for such high mortality was the homogeneity of the broader fire-suppressed landscape in which the treatments had been implemented (Steel et al. 2021b). Our results provide evidence that the landscape heterogeneity produced by an active-fire regime (Collins et al. 2016; Chamberlain et al. 2023a) may contribute to increased tree- and neighborhood-level structural resistance during periods of intense drought.

3.5.2. TALL TREE AND SMALL CLUMP RESISTANCE DURING DROUGHT-FIRE

Compared to drought only, the combined impacts of drought and fire resulted in more significant and higher magnitude changes in structural conditions in our study area. Yet despite these changes, key structural features, those which define fine-scale structural patterns in dry forests (Larson and Churchill 2012; Lydersen et al. 2013), demonstrated a high degree of resistance to fire and drought. In particular, our results showed near complete stability of small- and medium-sized clumps and relatively high stability of the proportions and counts of the tallest TAOs, especially when they belonged to smaller clumps (Figure 3.2; Figure 3.4). The persistence of these backbone structural features will promote continued resistance, and likely resilience and adaptability, of these

forests under changing climatic conditions (Stephens, et al. 2008; Zald et al. 2008; Churchill et al. 2013; Koontz et al. 2020; Ziegler et al. 2021; Falk et al. 2022). Past work has primarily documented subsequent burn severity patterns in active-fire landscapes, showing a tendency toward lower burn severities (Lydersen et al. 2014; Kane et al. 2015a) and overall stability in burn severity proportions overtime (Collins et al. 2009). Our results provide additional insight at a much finer-spatial scale, showing that low- and moderate-severity fire effects in active-fire landscapes reflect stable patterns of primarily small and medium sized TAO clumps and relatively high proportions of tall TAOs.

Importantly, we note that the portions of fires that impacted our study area from 2010-2019 all burned under low and moderate fire weather conditions (burning index < 80). As such, our results only provide evidence of active-fire landscape resistance during these more moderate burning conditions. Fires burning under extreme conditions are increasing in frequency in western North America, due partly to more extreme fire weather and partly to a "suppression bias" that results in most of the largest fires being those that escape initial attack and burn during the hottest and driest months of the year (Williams et al. 2019; Moreira et al. 2020; Brown et al. 2023; Kreider et al. 2024). Our study highlights the beneficial role that fires can play during non-extreme burning conditions, and emphasizes an urgent need to diverge from suppression-focused policies so that more fires can burn under moderate weather conditions (North et al. 2021; North et al. 2024). Future research can build on existing work (e.g., Lydersen et al. 2014; Steel et al. 2021; 2023) to better define thresholds and tipping-points of structural resistance in active-fire landscapes under a wider range of fire weather scenarios.

Tall trees are critical backbones of forest structure in dry forest ecosystems and contribute disproportionately to carbon storage and regulation of ecological processes (Lutz et al. 2012; Hessburg et al. 2015). Tall trees are also important habitat features for the California Spotted Owl in the Sierra Nevada (North et al. 2017; Kramer et al. 2021). Recent work by Kane et al. (2023) showed

that a majority of the tall and very tall trees across the Sierra Nevada exist in locally-dense, closed-canopy forest conditions. Our results show that, even within the context of active-fire landscapes, tall trees were the most susceptible to loss during drought and fire when they belonged to large clumps (a 62% reduction of >32m TAOs that belonged to large TAO clumps in the drought-fire context) (Figure 3.2). If a management objective is to conserve tall trees in Sierra Nevada YPMC forests, we suggest that restoration efforts, including managed wildfire, prescribed burning, or restoration thinning, focus on creating or reinforcing fine-scale patterns of small and medium-sized clumps (Churchill et al. 2013; Kane et al. 2019).

Conceptual models of historically fire-intact dry forest ecosystems (Larson and Churchill 2012; Churchill et al. 2013; Lydersen et al. 2013; Clyatt et al. 2016), as well as recent advancements in fire behavior modeling (Pawlikowski et al. 2019; Ritter et al. 2020; Ziegler et al. 2021; Atchley et al. 2021), suggest that the structural properties of small tree clumps and their surroundings contribute to their increased fire resistance. Our study supports these past findings and provides empirical evidence of small clump resistance in contemporary active-fire landscapes (Figure 3.2; Figure 3.4). By definition, a small clump represents a group of trees that are surrounded, at least to a degree, by canopy openings. These canopy openings increase the probability that fires burning into small clumps are surface fires rather than crown fires, which can reduce within-clump tree mortality (Agee and Skinner 2005; Churchill et al. 2013). Additionally, fire behavior models suggest that individual trees and small tree clumps are less susceptible to crown fire due to (1) convective cooling around smaller clumps (Ritter et al. 2020) and (2) more variable surface wind patterns produced by heterogeneous fuel structures (Atchley et al. 2021), both of which can reduce fire intensity and thus mortality within small clumps. The structural properties of small clumps, and their influence on local fire behavior, likely contributed to our finding that small and medium clumps retained virtually all of their pre-fire medium and tall TAOs in the drought-fire context in our study.

3.5.3. BIOPHYSICAL DRIVERS OF STRUCTURAL CHANGE AND HETEROGENEITY

Our results suggest that biophysical gradients had a relatively strong influence on patterns of structural change in the drought-fire context (Figure 3.6). Across all biophysical gradients, we observed a disaggregation of larger clumps into smaller clumps, where fire and drought tended to consume entire portions of large clumps irrespective of TAO height (similar to findings from Kane et al. (2013; 2014)) (Figure 3.2). Importantly however, these patterns were accentuated in areas with higher pre-fire canopy cover, in more topographically exposed sites, and when time since fire was longer. Past work has documented that fine-scale forest structural patterns tend to align with topographic and resource gradients in the Sierra Nevada (*i.e.,* higher density conditions in valleys and more open-canopy conditions on ridges) (Lydersen and North 2012; Jeronimo et al. 2019; Ng et al. 2020). Our explicit tracking of structural conditions through time provides evidence that these topographically-mediated structural patterns are more than simply a reflection of topographic influences on resource gradients, but rather a reflection of how these resource gradients influence fire behavior (and drought effects) which in turn influence structural conditions and dynamics (Lydersen and North 2012; Kane et al. 2015b).

Landscape-level heterogeneity is a critical structural component in both historical and contemporary fire-intact ecosystems and contributes to increased resistance, resilience, and adaptability (Collins et al. 2015; Knapp et al. 2017; Hessburg et al. 2019; Chamberlain et al. 2023a; Francis et al. 2023). This heterogeneity is often characterized as high variability in tree densities, tree spatial patterns, and fuel loading across forested landscapes, and variability in physiognomic vegetation types (*e.g.,* forest, shrubland, grassland) across broader scales (Stephens et al. 2008; Collins et al. 2015; Safford and Stevens 2017; Hessburg et al. 2019). Our results demonstrate increasingly heterogeneous structural conditions following drought and fire in these active-fire landscapes (Figure 3.4), whereby patterns and fluctuations in heterogeneity are driven partly by stochastic fire

and drought effects and partly by the underlying topographic template (Meyer et al. 2007b; Lydersen and North 2012) (Figure 3.6). Our work corroborates recent analyses of active-fire landscapes (Chamberlain et al. 2023a) and provides additional evidence of a hierarchical multi-scale arrangement of structural patterns in these systems (Larson and Churchill 2012; Reynolds et al. 2013; Churchill et al. 2017).

3.5.4. IMPLICATIONS OF FIELD-BASED STUDIES

While airborne lidar affords many advantages in terms of quantifying and evaluating forest structural patterns, a key weakness is its capacity to identify and measure species (Jeronimo et al. 2018). Field-based studies on forest resistance in the Sierra Nevada have consistently emphasized the importance of tree species, both regarding how species distributions influence resistance and how fire and drought disturbances impact species distributions (Fettig et al. 2019; Restaino et al. 2019; Stephenson et al. 2019; Young et al. 2020; Das et al. 2022). Without coincident field-based stem mapping to corroborate our lidar assessments, we can, at best, summarize other work and apply inference to our results. First, most studies evaluating plot-level mortality rates during the 2012-2016 drought indicated much higher mortality rates for *Pinus* species (Fettig et al. 2019; Steel et al. 2021b; Das et al. 2022). Additionally, several studies showed that conspecific tree density had a strong positive influence on mortality rates for individual tree species (Restaino et al. 2019; Furniss et al. 2022; Germain and Lutz 2024). During drought in our study, we observed a slight but non-significant decrease in the proportion of large TAOs (Figure 3.3), and a slight reduction in the total counts of >32m TAOs belonging to large clumps (Figure 3.2). Inferring from field-based studies, we suspect that reported reductions in tall trees in our study primarily reflect losses of *Pinus* species, especially when they belonged to large clumps with high conspecific densities, which may suggest that post-drought tree densities are characterized by higher densities of shade-tolerant and possibly broadleaf species (Young et al. 2020).

Tree species compositions also have important implications for fire resistance and recovery in YPMC forests (Lydersen et al. 2014; Collins et al. 2018; Germain and Lutz 2024). Historically, more shade-tolerant species occurred in relatively lower proportions compared to the more shade-intolerant and fire-resistant pines (Scholl and Taylor 2010; Safford and Stevens 2017). However, following decades of fire-suppression, many studies have documented significant increases in total densities of shade-tolerant white fir and incense cedar in the Sierra Nevada (Scholl and Taylor 2010; Collins et al. 2011a; Knapp et al. 2013). Even following reintroduction of fire in these fire-suppressed forest, recent work suggests that proportions of fire-resistant pines do not align with historical estimates (May et al. 2023; Zald et al. 2024). With regard to our study, there is a chance that the small and medium clumps and tall TAOs that resisted drought and fire (Figure 3.2) may be characterized by relatively high proportions of white fir and incense cedar, especially since the drought led to greater loss of *Pinus* species. If this is the case, the active-fire landscapes in our study area may indeed lack the capacity to adapt and maintain resistance under warmer and drier future conditions (May et al. 2023; Zald et al. 2024). Future work can build on our structure-based study to better quantify and monitor species-level resistance in active-fire landscapes of the Sierra Nevada.

3.5.5. MANAGEMENT IMPLICATIONS

While the management history of Yosemite National Park is somewhat unique compared to adjacent State and Forest Service lands (i.e., relative lack of early century logging and early re-establishment of prescribed burning programs) (van Wagtendonk 2007; Kane et al. 2023), we argue that the active-fire conditions in Yosemite, and their demonstrated resistance, are achievable across other parts of the Sierra Nevada. We suggest that managers can increase the extent of active-fire landscapes by (1) continued implementation of mechanical thinning and prescribed burning programs (North et al. 2022; Davis et al. 2024) particularly in strategic locations that increase the scale of forest restoration (North et al. 2021) and where first-entry fires are least likely to achieve

restoration targets (Chamberlain et al. 2024), (2) shifting away from strict suppression-focused fire management to allow more low-intensity fires to burn during periods of less extreme weather (North et al. 2021; Kreider et al. 2024; North et al. 2024) particularly where first-entry fires are most likely to achieve forest restoration targets (Chamberlain et al. 2024), and (3) leveraging the beneficial work of recent fires by implementing ecologically-informed post-fire management strategies (Meyer et al. 2021; Stevens et al. 2021; Larson et al. 2022).

Our results highlight the importance of maintenance burning and/or mechanical treatments in active-fire landscapes. During drought, our results showed increases in total TPH between 2010 and 2019 with a marked increase in the shortest TAOs and a "closing in" of canopy conditions (Figure 3.3; Figure 3.5), suggesting reduced post-drought structural resistance (Furniss et al. 2022). As such, in drought-affected sites where fires have been absent for more than approximately 15 years, managers may need to prioritize near-term application of prescribed burning, restoration thinning, or managed wildfire to maintain lower tree densities and ensure continued resistance of key structural features. Restoring and maintaining active-fire landscapes is an ongoing process that will require continued input of financial and personnel resources to ensure continued occurrence of frequent and low-severity fires (North et al. 2021; Hessburg et al. 2021; North et al. 2024).

Our finding that topography influences patterns of structural change supports common dry forest restoration guidelines in the Sierra Nevada (North et al. 2009) and other dry forest ecosystems (Hessburg et al. 2015). Topography is a key driver of stand-level structural conditions in dry forest landscapes (Lydersen and North 2012; Ng et al. 2020). Thus, scientists recommend that restoration treatments mirror this underlying topographic template, which can promote landscape heterogeneity and increase the range of management objectives that restored dry forest landscapes achieve (i.e., reduced fire risk, biodiversity, wildlife habitat) (North et al. 2009; Hessburg et al. 2015). Our results extend this concept and provide evidence that topographic features also influence patterns of

drought- and fire-induced structural *change* in active-fire landscapes (Figure 3.6). As such, we suggest that topographic features continue to inform the design, placement, and prioritization of individual treatments (North et al. 2009) as well as the more comprehensive treatment programs which will dictate how forest ecosystems adapt and change over longer time periods (Hood et al. 2022).

Our results suggest that tall trees (>32 m) exhibited relatively high resistance to drought and fire when they belonged to small clumps and existed within a heterogeneous active-fire landscape. As such, if the objective is to conserve tall trees, management can work to restore fine-scale tree clump and opening patterns and landscape-level structural heterogeneity in dry forest ecosystems (North et al. 2009; Churchill et al. 2013; Hessburg et al. 2015). However, our results also suggest that losing some tall trees is an inevitable outcome of restoring fire to fire-adapted forests. This suggests a tradeoff in which the landscape benefits achieved by restoring active-fire conditions (e.g., increased resilience, adaptive capacity, wildlife habitat) may come with the cost of losing a proportion of tall trees (e.g., up to ~30%). We also found that topographically protected sites demonstrated high resistance during drought and fire. While these sites may currently lack high densities of tall trees due to past logging, their resistance to structural change should support tall tree development over time (Coop et al. 2019; Rodman et al. 2023). This suggests that while the re-establishment of active-fire conditions may result in loss of tall trees in some areas, it should ultimately promote higher densities of tall trees over longer time periods and at landscape scales.

3.6. CONCLUSION

California's YPMC forests, and other dry forests across western North America, face a potentially grave future under climate change (AghaKouchak et al. 2014; Westerling 2016; Liang et al. 2017; Schoennagel et al. 2017). With a strong legacy of fire suppression, fuel accumulation, and loss of keystone old trees (Knapp et al. 2013; Hagmann et al. 2021), coupled with an increasingly

warmer and drier climate and extended fire seasons (Westerling 2016; Pierce et al. 2018; Williams et al. 2019), there is no wonder why the majority of recent research on dry forest resistance and resilience portray a mostly dire situation (Coop et al. 2020). Indeed, the 2012-2016 drought resulted in significant mortality across the Sierra Nevada with a particularly strong impact on perhaps the most critical and fire-resistant trees (Fettig et al. 2019). Moreover, other studies document rapid increases in fire size, severity, and high-severity patch sizes in California over recent decades (Stevens et al. 2017; Steel et al. 2018; Cova et al. 2023), projecting similarly negative trends for future decades (Abatzoglou and Williams 2016; Williams et al. 2019). Undoubtedly, recent impacts from fire and drought are unprecedented and have serious implications for the sustainability of dry forest ecosystems and the suite of valued resources they provide (Coop et al. 2020; Steel et al. 2023).

Our study provides a degree of contrast against this largely negative environmental narrative. We demonstrate what could be achieved if intentional, ecologically-centered policies and management practices are adopted (Hessburg et al. 2021; Meyer et al. 2021; Prichard et al. 2021). For example, several recent studies have proposed landscape-level management plans which delineate large areas, generally far from the wildland urban interface, where more proactive fire management can be practiced (North et al. 2021; North et al. 2024). Indeed, North et al. (2024) show that large portions of existing dry forest landscapes across western North America are well positioned for this type of management and could be used to increase the total extent of active-fire landscapes. Our study suggests that proactive management strategies like these, focused on restoring the key process of fire to fire-adapted forests, can help bolster forest resistance and contribute to the long-term sustainability of dry forest ecosystems.

3.7. APPENDIX C

Table 3.A.1. Confusion matrix from the 2010 Random Forest mortality model predicting live vs. dead tree approximate object (TAO) status applied to the testing dataset. The model had an overall accuracy of 91.8%. The training dataset had 1,062 samples and testing dataset had 354 samples.

		Predicted	
		dead	live
Truth	dead	157	20
	live	9	168

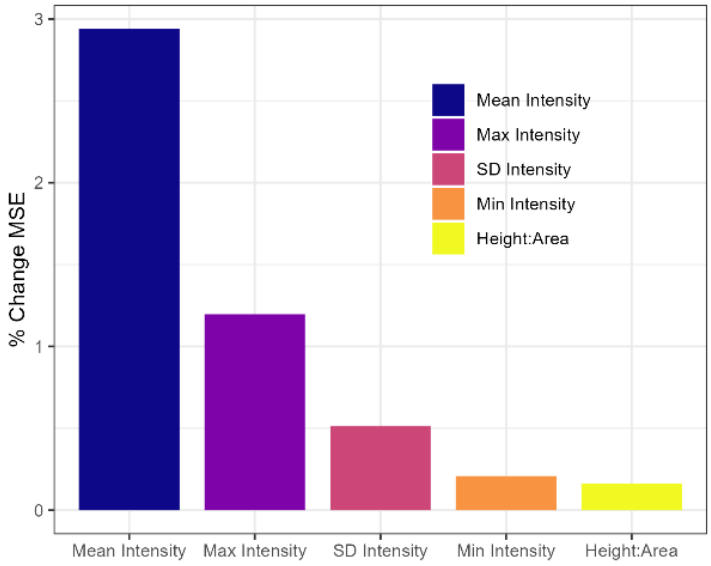

Figure 3.A.1. Variable importance plot from the Random Forest mortality model predicting live vs. dead tree approximate object (TAO) status for 2010.

Table 3.A.2. Confusion matrix from the 2019 Random Forest mortality model predicting live vs. dead tree approximate object (TAO) status applied to the testing dataset. The model had an overall accuracy of 93.6%. The training dataset had 1,464 samples and testing dataset had 488 samples.

		Predicted	
		dead	live
Truth	dead	227	17
	live	13	231

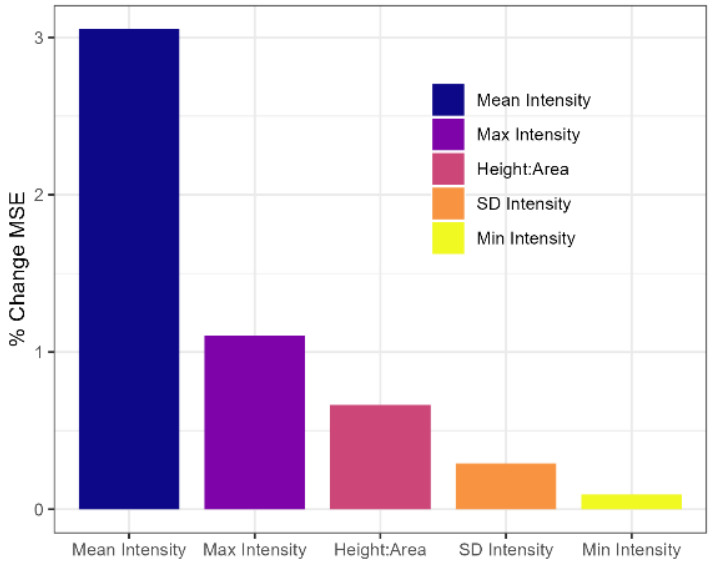

Figure 3.A.2. Variable importance plot from the Random Forest mortality model predicting live vs. dead tree approximate object (TAO) status for 2019.

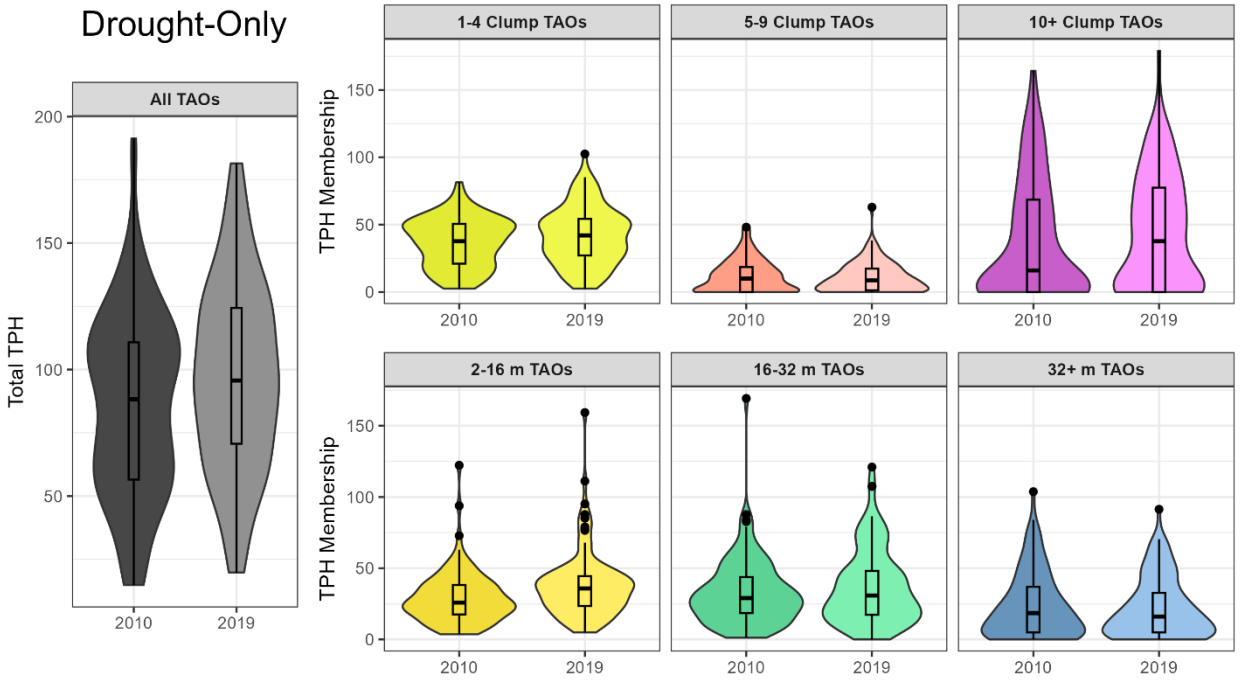

Figure 3.A.3. Distributions and boxplots of the total tree approximate objects (TAO) per hectare (TPH), and TPH by clump size and height class membership, for the drought-only context.

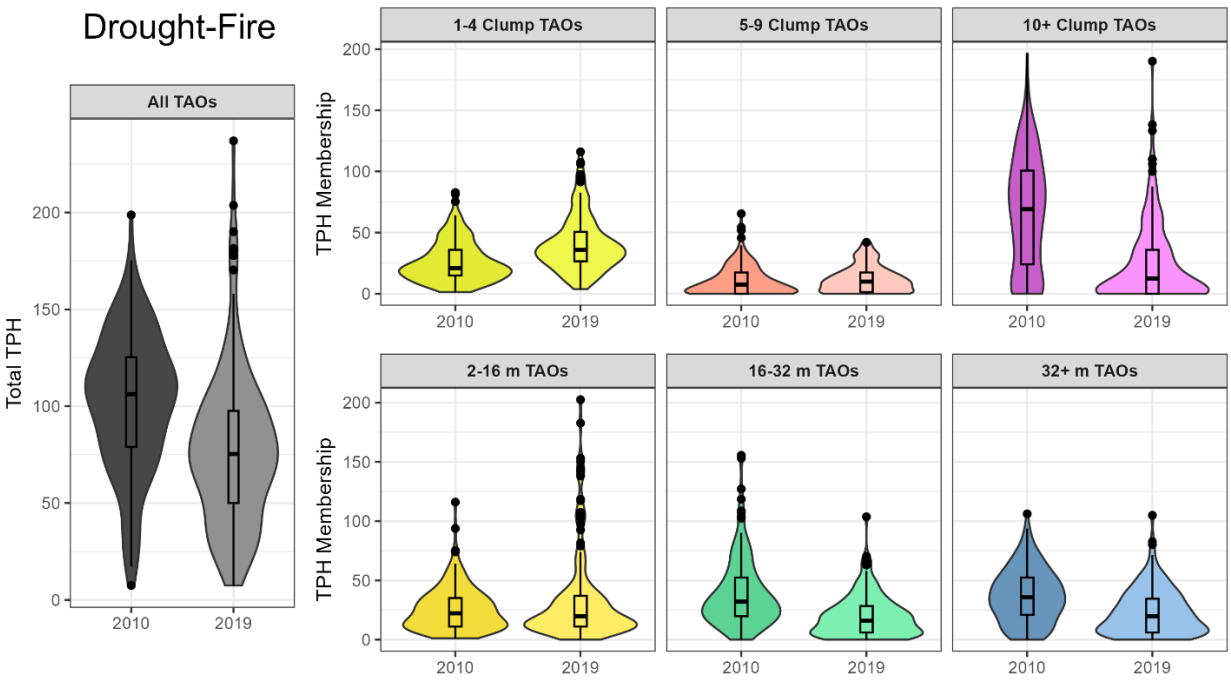

Figure 3.A.4. Distributions and boxplots of the total tree approximate objects (TAO) per hectare (TPH), and TPH by clump size and height class membership, for the drought-fire context.

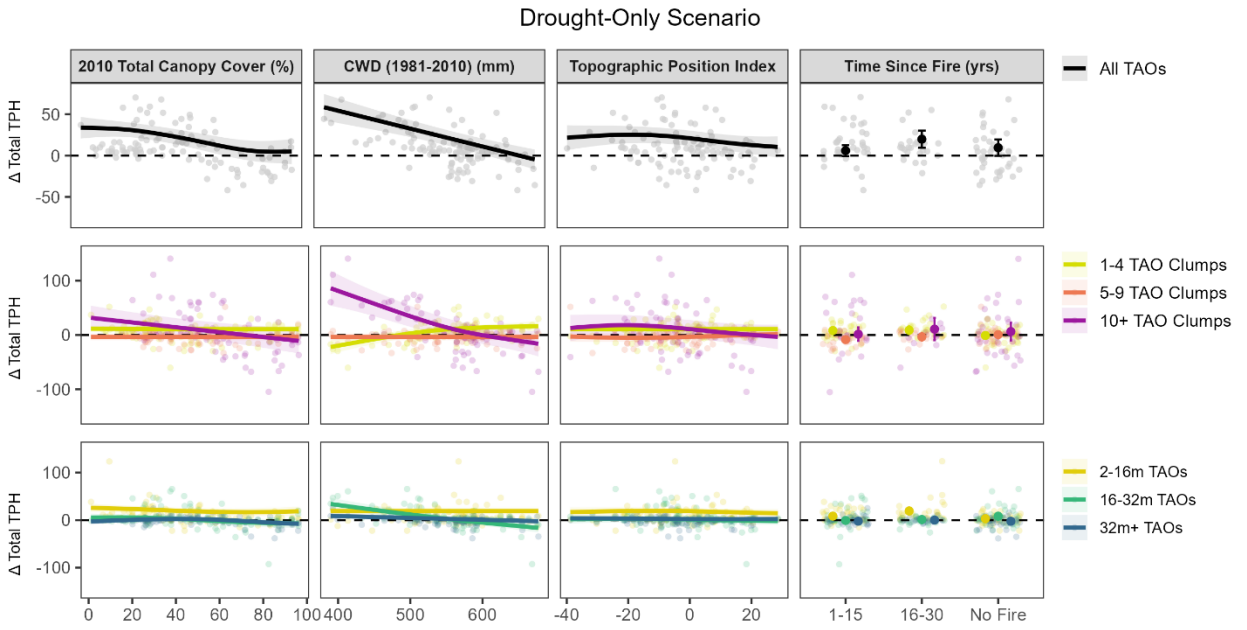

Figure 3.A.5. Model-predicted trends between environmental variables and absolute structural change metrics for the drought-only context, in active-fire landscapes within Yosemite National Park, California, USA. In the left three columns, lines represent predicted means, and shaded regions represent 95% confidence intervals. In the rightmost column, full color points and error bars show model-predicted means and 95% confidence intervals, respectively. Transparent background points show the distributions of sample points in each model.

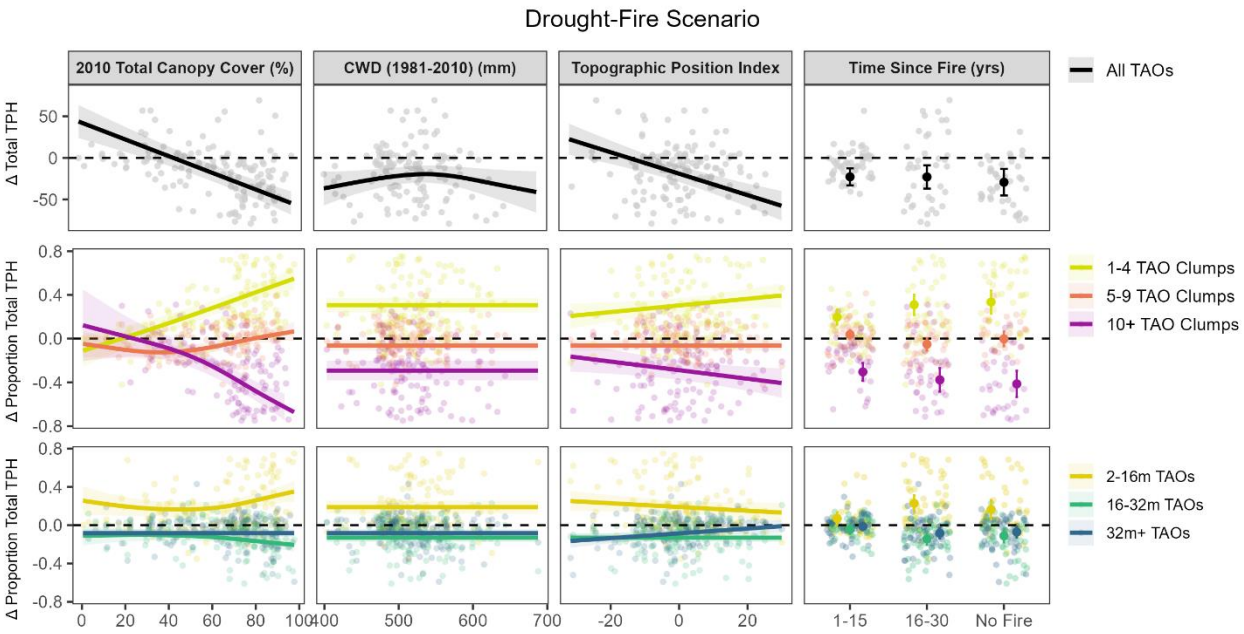

Figure 3.A.6. Model-predicted trends between environmental variables and absolute structural change metrics for the drought-fire context, in active-fire landscapes within Yosemite National Park, California, USA. In the left three columns, lines represent predicted means, and shaded regions represent 95% confidence intervals. In the rightmost column, full color points and error bars show model-predicted means and 95% confidence intervals, respectively. Transparent background points show the distributions of sample points in each model.

CONCLUSIONS

Fires can be both beneficial and detrimental to dry forest ecosystems in the 21st century. On one hand, the combined impacts of fire-exclusion and climate change are leading to increasingly severe fires which can degrade resilience and catalyze type conversions (Abatzoglou and Williams 2016; Coop et al. 2020); yet, these same fires, when their frequencies and intensities align with local plant adaptations, can serve as an essential ecological process that improves dry forest resilience and adaptive capacity (Hessburg et al. 2019; Cova et al. 2023). For my dissertation, I sought to better resolve this boundary between the beneficial and negative effects of contemporary fires. I focused my analyses on dry forests in California's Sierra Nevada where extensive coverage of recent airborne lidar acquisitions enabled inquiries at unprecedented spatial and temporal scales. In all three of my chapters, I offered practical suggestions for managers and policymakers regarding how and where fire can be effectively reestablished as an ecological process in the modern era, and I demonstrated the benefit of these reestablished fire regimes to contemporary dry forest resilience and conservation.

KEY FINDINGS

Results from my first chapter showed that, despite the pervasiveness of fire-exclusion in the Sierra Nevada, fire-intact landscapes that resemble those of historical conditions are beginning to reestablish in some regions (Chamberlain et al. 2023a). These fire-intact landscapes (i.e., contemporary reference sites) are characterized by distinct multi-scale structural patterns, with a high degree of heterogeneity at the neighborhood- and site-levels, and consistency of heterogeneity across broad landscape scales (Figure 4.1). A key finding from my first chapter is that frequent and low-severity fire represents a strong bottom-up control on forest structures, which can override top-down controls like fire weather and climate (Chamberlain et al. 2023a). This finding contrasts many

recent fires in the Sierra Nevada where warmer climatic conditions and extreme fire behavior have resulted in fires that homogenize forest structural patterns and degrade resilience (Stevens et al. 2017; Steel et al. 2018; Cova et al. 2023). Reestablishing frequent and low-severity fire regimes in dry forests may act as an essential counterweight to the intensifying climate and weather conditions of the 21st century (Abatzoglou et al. 2019; Coop et al. 2022), helping to stabilize and conserve dry forest ecosystems and the many values they provide.

In my second chapter, I found that *first-entry* wildfires in the Sierra Nevada were only sometimes capable of restoring key structural patterns associated with contemporary reference sites, highlighting the importance of reestablishing not just lower severity fires but *frequent* return intervals of these lower severity fires (Chamberlain et al. 2024). I also found that moderate severity first-entry effects – representing approximately 25-75% basal area loss – aligned most closely with reference conditions, suggesting that a relatively high level of overstory consumption was needed to achieve restorative fire effects in fire-excluded forests (Collins et al. 2011a; Kane et al. 2019). Achieving moderate severity effects can be challenging in practice, but predictive models from my second chapter provided key insight regarding when and where these restorative effects would be most likely to occur. Indeed, I found that, under mild fire weather conditions, up to 58% of previously unburned dry forests in the Sierra Nevada would be likely to experience restorative first-entry fire effects, demonstrating extensive regions where managers could consider more proactive managed wildfire strategies for reestablishing active-fire conditions (Stephens et al. 2016a; North et al. 2021; North et al. 2024).

For my third chapter, I explicitly tested the resistance of key structural features within fire-intact landscapes, revealing that tall trees and small tree clumps were highly resistant to high-intensity drought and moderate-intensity wildfire. These results provided empirical evidence of the conservation benefit of reestablishing active-fire conditions in the Sierra Nevada. My results offered

stark contrast to much of the literature documenting widespread tree mortality during the 2012-2016 drought in the Sierra Nevada (Young et al. 2017; Fettig et al. 2019) as well as recent work by Steel et al. (2023) who showed significant loss of mature conifer forests under compound drought and wildfire disturbances. I show that even partially-restored active-fire conditions can drastically alter these trajectories, enabling key structural features like tall trees and small tree clumps to persist through contemporary wildfire and drought disturbances, thus supporting the long-term sustainability of these valued forest ecosystems.

POLICY AND MANAGEMENT IMPLICATIONS

Results from all three of my chapters provided evidence that reestablishing frequent and low-severity fire regimes (i.e., active-fire conditions) in Sierra Nevada dry forests is likely to increase their resilience to climate change and shifting disturbance regimes. Other research across the western United States provides similar evidence (Hessburg et al. 2021; Prichard et al. 2021; Davis et al. 2023). However, managing for active-fire conditions can be politically and operationally challenging (North et al. 2015; Stephens et al. 2016a; Schultz et al. 2019; Franz et al. 2024). National- and state-level policies increasingly support prescribed fire, cultural burning, and management of resource objective wildfires (e.g., the National Cohesive Wildfire Strategy), but perceived risks of non-suppression approaches, competing management objectives, and lack of support from regional and national leadership can often thwart these efforts in practice (Franz et al. 2024). Because of this, suppression remains the primary management response to most fires in the western United States, which perpetuates the "suppression bias" and leads to the largest fires being those that escape initial control, burn during extreme fire weather, and thus have predominantly high severity effects (Parks et al. 2023; Kreider et al. 2024).

Frameworks continue to be presented in the scientific literature that offer pathways toward increasing active-fire conditions and beneficial fire effects. I argue these frameworks should be more

explicitly integrated into state and federal forest management plans in coming decades. In particular, North et al. (2024) describes a Strategic Fire Zone (SFZ) approach in which large portions of forest landscapes could be delineated where active-fire management is the default response rather than suppression (Stephens et al. 2016a). Results from my second chapter support this strategy and suggest that a high proportion (58%) of dry forests in the Sierra Nevada could be suitable for this non-suppression approach (Chamberlain et al. 2024). The Potential Operational Delineations (PODs) framework offers an important compliment to the SFZ approach and could be used to engage managers and other stakeholders in pre-fire planning so that more proactive, rather than reactive, decisions can be made when fires inevitably occur (Thompson et al. 2022). Lastly, several post-fire management frameworks have been developed in recent years, which are critical to ensuring that once-burned landscapes are strategically managed to better prepare forests, managers, and the public for subsequent fires (Meyer et al. 2021; Stevens et al. 2021; Larson et al. 2022). The structural targets derived from contemporary reference sites and partially-restored active-fire landscapes presented in all three of my chapters could be used to better guide and evaluate these post-fire management efforts.

A key implication emerging from my dissertation is the importance of multi-scale structural heterogeneity to dry forest ecosystems (Figure 4.1). Structural heterogeneity is both an outcome of frequent and low-severity fires and a key factor contributing to lower severity disturbances (Collins et al. 2015; Hessburg et al. 2019; Chamberlain et al. 2023a; Francis et al. 2023). While considerable work has documented *neighborhood-* and *stand-level* heterogeneity in active-fire landscapes (Larson and Churchill 2012; Lydersen et al. 2013; Jeronimo et al. 2019), I show that a fundamental characteristic of dry forest ecosystems is that this finer-scale heterogeneity scales up to produce heterogeneous patterns across broader spatial scales (i.e., site-level; ~100-1000 ha) (Figure 4.1) (Chamberlain et al. 2023a). My third chapter suggests that this site-level heterogeneity in active-fire dry forest

ecosystems is reflective of the underlying biophysical template, such that increased variability in topography and disturbance history leads to increased structural heterogeneity. Ultimately, results from my dissertation encourage management practices that promote multi-scale structural heterogeneity in dry forest landscapes. Achieving these structural targets may necessitate that managers deviate from stand-level prescriptions and planning and begin to adopt more cross-jurisdictional and multi-scaled management strategies (Hessburg et al. 2015; Hessburg et al. 2021).

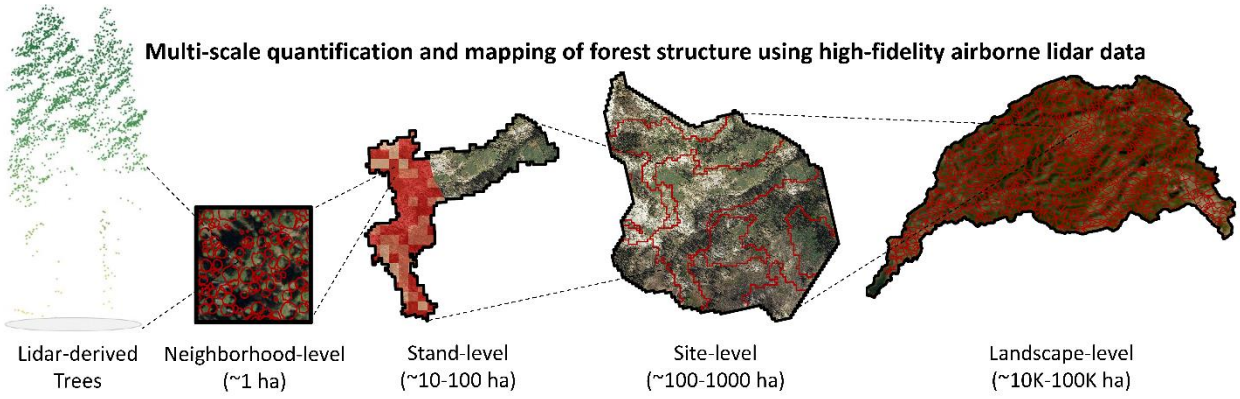

Figure 4.1 Conceptual diagram of key nested spatial scales in dry forest ecosystems.

FUTURE DIRECTIONS

Airborne lidar has clear limitations in terms of quantifying species, surface fuels, and understory conditions (Jeronimo et al. 2018; Beland et al. 2019), yet these factors remain critically important to dry forest resilience (Knapp et al. 2013; May et al. 2023). I recommend that future research not only continue to supplement lidar-based studies with field- and alternative remote sensing-based datasets, but that these datasets continue to be explicitly integrated to offer more comprehensive ecological assessments of changing forest conditions. For example, recent work has begun to couple high-resolution imagery datasets with lidar based products to quantify tree mortality trends (e.g., my third chapter, Khatri-Chhetri et al. 2024) and structure-composition classes (Su et al. 2016) in Sierra Nevada forests. Additionally, terrestrial laser scanning (TLS) systems are increasingly

used by field crews and provide robust information on subcanopy conditions, surface fuels, and understory species (Calders et al. 2020; Terryn et al. 2020; Hankin et al. 2024). Continued integration of these datasets with airborne lidar will provide more synoptic characterizations of dry forest ecosystems and, importantly, will enable more comprehensive ecological assessments of forest-disturbance interactions in the 21st century.

All fires and droughts analyzed in my dissertation occurred prior to 2020, yet fires impacting the Sierra Nevada since 2020 have been exceptionally large and impactful (Safford et al. 2020; Taylor et al. 2022; Cova et al. 2023; Turco et al. 2023). Future work could evaluate structural resistance under these increasingly intense burning conditions to identify thresholds and tipping points of resilience in active-fire dry forest landscapes. Additionally, while results from my third chapter provided empirical evidence of structural resistance in active-fire landscapes, caution should be taken when extrapolating these findings outside of Yosemite National Park, which has a unique fire and management history (van Wagtendonk 2007; Kane et al. 2023; Hankin et al. 2024). With new Sierra Nevada-wide lidar acquisitions collected in 2022, future work can extend these types of analyses across the entire region to understand structural resistance across a wider range of forest conditions and disturbance intensities. And lastly, structural resistance represents just one component of resilience (Walker et al. 2004; Falk et al. 2022); future work could more explicitly evaluate the capacity for recovery and adaptability of dry forest ecosystems under changing climate and disturbance regimes.

A wealth of research has emerged from the Sierra Nevada over recent decades that explores interactions between dry forests, disturbances, and climate change. While inferences can be made for other dry forest ecosystems across western North America, the Sierra Nevada has unique characteristics in terms of climate, topography, and human development (North et al. 2016). Fortunately, national-level efforts to increase the frequency and extent of airborne lidar acquisitions

are currently underway in the United States. Future research could extend the lidar-based ecological assessments presented in my dissertation (and other studies) to address similar questions in other dry forest regions in western North America, with potential to scale these types of analyses to multi-regional or even national levels.

Much of the research on dry forest ecosystems over the past several decades has centered on exploring disturbance effects in fire-excluded landscapes. While extensive forested areas still have yet to experience fire in the modern era, rapid increases in area burned and disturbance interactions are quickly altering this narrative (Prichard et al. 2017). As more fires and disturbances occur, overlap, and interact with climate change, forest ecosystems will become increasingly complex, straying further from historical or even contemporary analogs (Loehman et al. 2017; Loehman et al. 2020). These changes will necessitate increasingly complex study designs and research questions that capture comprehensive gradients of disturbance history, management, and biophysical gradients. Fortunately, improvements in remote sensing datasets, geospatial techniques, and statistical analyses are advancing almost as quickly as the climate is changing. These technological advancements will be essential to the ongoing study of increasingly complex forest ecosystems. However, while technologies advance, it remains critical that researchers of all disciplines maintain a keen focus on understanding and valuing, at their core, the ecological and social underpinnings that drive dry forest functions and processes.

REFERENCES

Abatzoglou JT. 2013. Development of gridded surface meteorological data for ecological applications and modelling. International Journal of Climatology. 33:121–131. doi:10.1002/joc.3413

Abatzoglou JT, Williams AP. 2016. Impact of anthropogenic climate change on wildfire across western US forests. Proceedings of the National Academy of Sciences. 113(42):11770–11775. doi:10.1073/pnas.1607171113

Abatzoglou JT, Williams AP, Barbero R. 2019. Global emergence of anthropogenic climate change in fire weather indices. Geophysical Research Letters. 46(1):326–336. doi:10.1029/2018GL080959

Abella SR, Denton CW. 2009. Spatial variation in reference conditions: historical tree density and pattern on a Pinus ponderosa landscape. Canadian Journal of Forest Research. 39(12):2391–2403. doi:10.1139/X09-146

ACWA. 2015. Improving the resiliency of California's headwaters: a framework. Association of California Water Agencies. https://www.acwa.com/resources/recommendations-for-californias-headwaters/

Agee JK, Skinner CN. 2005. Basic principles of forest fuel reduction treatments. Forest Ecology and Management. 211(1):83–96. doi:10.1016/j.foreco.2005.01.034

AghaKouchak A, Cheng L, Mazdiyasni O, Farahmand A. 2014. Global warming and changes in risk of concurrent climate extremes: insights from the 2014 California drought. Geophysical Research Letters. 41(24):8847–8852. doi:10.1002/2014GL062308

Akay AE, Oğuz H, Karas IR, Aruga K. 2009. Using LiDAR technology in forestry activities. Environmental Monitoring and Assessment. 151(1–4):117–125. doi:10.1007/s10661-008-0254-1

Allen CD, Breshears DD, McDowell NG. 2015. On underestimation of global vulnerability to tree mortality and forest die-off from hotter drought in the Anthropocene. Ecosphere. 6(8):art129. doi:10.1890/ES15-00203.1

Allen, I., Chhin, S., Zhang, J., 2019. Fire and forest management in montane forests of the northwestern states and California, USA. Fire 2(2), 17. doi:10.3390/fire2020017

Anderson, MK, Moratto MJ. 1996. Native American land-use practices and ecological impacts. In Sierra Nevada ecosystem project: final report to Congress. Davis, CA: University of California, Centers for Water and Wildland Resources Davis. 187-206.

Atchley AL, Linn R, Jonko A, Hoffman C, Hyman JD, Pimont F, Sieg C, Middleton RS, Atchley AL, Linn R, et al. 2021. Effects of fuel spatial distribution on wildland fire behaviour. International Journal of Wildland Fire. 30(3):179–189. doi:10.1071/WF20096

Barnett TP, Adam JC, Lettenmaier DP. 2005. Potential impacts of a warming climate on water availability in snow-dominated regions. Nature. 438(7066):303–309. doi:10.1038/nature04141

Beland M, Parker G, Sparrow B, Harding D, Chasmer L, Phinn S, Antonarakis A, Strahler A. 2019. On promoting the use of lidar systems in forest ecosystem research. Forest Ecology and Management. 450:117484. doi:10.1016/j.foreco.2019.117484

Bentz BJ, Régnière J, Fettig CJ, Hansen EM, Hayes JL, Hicke JA, Kelsey RG, Negrón JF, Seybold SJ. 2010. Climate change and bark beetles of the western United States and Canada: direct and indirect effects. BioScience. 60(8):602–613. doi:10.1525/bio.2010.60.8.6

Bernal, A.A., Stephens, S.L., Collins, B.M., Battles, J.J., 2022. Biomass stocks in California's fire-prone forests: mismatch in ecology and policy. Environmental Research Letters. 17(4), 044047. doi:10.1088/1748-9326/ac576a

Bigelow SW, North MP, Salk CF. 2011. Using light to predict fuels-reduction and group-selection effects on succession in Sierran mixed-conifer forest. Canadian Journal of Forest Research. 41(10), 2051–2063. doi:10.1139/x11-120

Bohlman GN, Safford HD, Skinner CN. 2021. Natural range of variation for yellow pine and mixed-conifer forests in northwestern California and southwestern Oregon. US Department of Agriculture, Forest Service, Pacific Southwest Research Station. PSW-GTR-273. 1-146. https://www.fs.usda.gov/psw/publications/documents/psw_gtr273/psw_gtr273.pdf

Boisramé G, Thompson S, Collins B, Stephens S. 2017. Managed wildfire effects on forest resilience and water in the Sierra Nevada. Ecosystems. 20(4):717–732. doi:10.1007/s10021-016-0048-1

Bone C, Moseley C, Vinyeta K, Bixler RP. 2016. Employing resilience in the United States Forest Service. Land Use Policy. 52:430–438. doi:10.1016/j.landusepol.2016.01.003

Bonnicksen TM, Stone EC. 1980. The giant sequoia—mixed conifer forest community characterized through pattern analysis as a mosaic of aggregations. Forest Ecology and Management. 3, 307–328. doi:10.1016/0378-1127(80)90031-6

Brown PT, Hanley H, Mahesh A, Reed C, Strenfel SJ, Davis SJ, Kochanski AK, Clements CB. 2023. Climate warming increases extreme daily wildfire growth risk in California. Nature. 621(7980):760–766. doi:10.1038/s41586-023-06444-3

Buma B. 2015. Disturbance interactions: characterization, prediction, and the potential for cascading effects. Ecosphere. 6(4):art70. doi:10.1890/ES15-00058.1

Calders K, Adams J, Armston J, Bartholomeus H, Bauwens S, Bentley LP, Chave J, Danson FM, Demol M, Disney M, et al. 2020. Terrestrial laser scanning in forest ecology: expanding the horizon. Remote Sensing of Environment. 251:112102. doi:10.1016/j.rse.2020.112102

Cansler CA, Hood SM, van Mantgem PJ, Varner JM. 2020. A large database supports the use of simple models of post-fire tree mortality for thick-barked conifers, with less support for other species. Fire Ecology. 16:25. doi:10.1186/s42408-020-00082-0

Cansler CA, Kane VR, Hessburg PF, Kane JT, Jeronimo SMA, Lutz JA, Povak NA, Churchill DJ, Larson AJ. 2022. Previous wildfires and management treatments moderate subsequent fire severity. Forest Ecology and Management. 504:119764. doi:10.1016/j.foreco.2021.119764.

Cansler CA, Swanson ME, Furniss TJ, Larson AJ, Lutz JA. 2019. Fuel dynamics after reintroduced fire in an old-growth Sierra Nevada mixed-conifer forest. Fire Ecology. 15(1):16. doi:10.1186/s42408-019-0035-y

Carpenter S, Walker B, Anderies JM, Abel N. 2001. From metaphor to measurement: resilience of what to what? Ecosystems 4: 765-781. doi:10.1007/s10021-001-0045-9

Chamberlain CP, Bartl-Geller BN, Cansler CA, North MP, Meyer MD, van Wagtendonk L, Redford HE, Kane VR. 2024. When do contemporary wildfires restore forest structures in the Sierra Nevada? Fire Ecology. 20(1):91. doi:10.1186/s42408-024-00324-5

Chamberlain CP, Cova GR, Cansler CA, North MP, Meyer MD, Jeronimo SMA, Kane VR. 2023a. Consistently heterogeneous structures observed at multiple spatial scales across fire-intact reference sites. Forest Ecology and Management. 550:121478. doi:10.1016/j.foreco.2023.121478

Chamberlain CP, Cova GR, Kane VR, Cansler CA, Bartl-Geller BN, Kane JT, Jeronimo SMA, Stine PA, North MP. 2023b. Sierra Nevada contemporary reference site boundaries and corresponding remote sensing-derived canopy structure rasters. Fort Collins, CO: Forest Service Research Data Archive. https://doi.org/10.2737/RDS-2023-0027

Chamberlain CP, Cova GR, Kane VR, Cansler CA, Kane JT, Bartl-Geller BN, van Wagtendonk L, Jeronimo SMA, Stine P, North MP. 2023c. Sierra Nevada reference conditions: a dataset of contemporary reference sites and corresponding remote sensing-derived forest structure

metrics for yellow pine and mixed-conifer forests. Data in Brief. 51:109807. doi:10.1016/j.dib.2023.109807
Churchill DJ, Carnwath GC, Larson AJ, Jeronimo SMA. 2017. Historical forest structure, composition, and spatial pattern in dry conifer forests of the western Blue Mountains, Oregon. US Department of Agriculture, Forest Service, Pacific Northwest Research Station. PNW-GTR-956. https://doi.org/10.2737/PNW-GTR-956
Churchill DJ, Jeronimo SMA, Hessburg PF, Cansler CA, Povak NA, Kane VR, Lutz JA, Larson AJ. 2022. Post-fire landscape evaluations in Eastern Washington, USA: assessing the work of contemporary wildfires. Forest Ecology and Management. 504:119796. doi:10.1016/j.foreco.2021.119796
Churchill DJ, Larson AJ, Dahlgreen MC, Franklin JF, Hessburg PF, Lutz JA. 2013. Restoring forest resilience: from reference spatial patterns to silvicultural prescriptions and monitoring. Forest Ecology and Management. 291, 442-457. doi:10.1016/j.foreco.2012.11.007
Clyatt KA, Crotteau JS, Schaedel MS, Wiggins HL, Kelley H, Churchill DJ, Larson AJ. 2016. Historical spatial patterns and contemporary tree mortality in dry mixed-conifer forests. Forest Ecology and Management. 361:23–37. doi:10.1016/j.foreco.2015.10.049
Collins BM, Everett RG, Stephens SL. 2011a. Impacts of fire exclusion and recent managed fire on forest structure in old growth Sierra Nevada mixed-conifer forests. Ecosphere. 2(4):art51. doi:10.1890/ES11-00026.1
Collins BM, Kelly M, van Wagtendonk JW, Stephens SL. 2007. Spatial patterns of large natural fires in Sierra Nevada wilderness areas. Landscape Ecology. 22(4):545–557. doi:10.1007/s10980-006-9047-5
Collins BM, Lydersen JM, Everett RG, Fry DL, Stephens SL. 2015. Novel characterization of landscape-level variability in historical vegetation structure. Ecological Applications 25(5), 1167-1174. doi:10.1890/14-1797.1
Collins BM, Lydersen JM, Everett RG, Stephens SL. 2018. How does forest recovery following moderate-severity fire influence effects of subsequent wildfire in mixed-conifer forests? Fire Ecology. 14(2):3. doi:10.1186/s42408-018-0004-x
Collins BM, Lydersen JM, Fry DL, Wilkin K, Moody T, Stephens SL. 2016. Variability in vegetation and surface fuels across mixed-conifer-dominated landscapes with over 40 years of natural fire. Forest Ecology and Management. 381, 74-83. doi:10.1016/j.foreco.2016.09.010
Collins BM, Miller JD, Thode AE, Kelly M, van Wagtendonk JW, Stephens SL. 2009. Interactions among wildland fires in a long-established Sierra Nevada natural fire area. Ecosystems 12(1), 114-128. doi:10.1007/s10021-008-9211-7
Collins BM, Stephens SL. 2007. Managing natural wildfires in Sierra Nevada wilderness areas. Frontiers in Ecology and the Environment. 5:523–527. Doi:10.1890/070007
Collins BM, Stephens SL, Roller GB, Battles JJ. 2011b. Simulating fire and forest dynamics for a landscape fuel treatment project in the Sierra Nevada. Forest Science. 57:77–88. doi:10.1093/forestscience/57.2.77
Coop JD, DeLory TJ, Downing WM, Haire SL, Krawchuk MA, Miller C, Parisien M-A, Walker RB. 2019. Contributions of fire refugia to resilient ponderosa pine and dry mixed-conifer forest landscapes. Ecosphere. 10(7):e02809. doi:10.1002/ecs2.2809
Coop JD, Parks SA, Stevens-Rumann CS, Crausbay SD, Higuera PE, Hurteau MD, Tepley A, Whitman E, Assal T, Collins BM, et al. 2020. Wildfire-driven forest conversion in western North American landscapes. BioScience. 70(8):659–673. doi:10.1093/biosci/biaa061
Coop JD, Parks SA, Stevens-Rumann CS, Ritter SM, Hoffman CM. 2022. Extreme fire spread events and area burned under recent and future climate in the western USA. Global Ecology and Biogeography. 31(10):1949–1959. doi:10.1111/geb.13496

Coppoletta M, Merriam KE, Collins BM. 2016. Post-fire vegetation and fuel development influences fire severity patterns in reburns. Ecological Applications. 26:686–699. doi:10.1890/15-0225
Coops NC, Tompalski P, Goodbody TRH, Queinnec M, Luther JE, Bolton DK, White JC, Wulder MA, van Lier OR, Hermosilla T. 2021. Modelling lidar-derived estimates of forest attributes over space and time: A review of approaches and future trends. Remote Sensing of Environment. 260:112477. doi:10.1016/j.rse.2021.112477
Cova G, Kane VR, Prichard S, North M, Cansler CA. 2023. The outsized role of California's largest wildfires in changing forest burn patterns and coarsening ecosystem scale. Forest Ecology and Management. 528:120620. doi:10.1016/j.foreco.2022.120620
Covington WW, Moore MM. 1994. Southwestern ponderosa forest structure: changes since Euro-American settlement. Journal of Forestry. 92:39–47.
Crompton, O.V., Boisrame, G.F.S., Rakhmatulina, E., Stephens, S.L., Thompson, S.E., 2022. Fire return intervals explain different vegetation cover responses to wildfire restoration in two Sierra Nevada basins. Forest Ecology and Management. 521, 120429. doi:10.1016/j.foreco.2022.120429
Crumley RL, Palomaki RT, Nolin AW, et al (2020) SnowCloudMetrics: snow information for everyone. Remote Sensing 12:3341. doi:10.3390/rs12203341
Cushman SA, McGarigal K, Neel MC. 2008. Parsimony in landscape metrics: strength, universality, and consistency. Ecological Indicators. 8(5), 691–703. doi:10.1016/j.ecolind.2007.12.002
Cutler DR, Edwards JTC, Beard KH, Cutler A, Hess KT, Gibson J, Lawler JJ. 2007. Random Forests for classification in ecology. Ecology. 88(11), 2783–2792. doi:10.1890/07-0539.1
Das AJ, Slaton MR, Mallory J, Asner GP, Martin RE, Hardwick P. 2022. Empirically validated drought vulnerability mapping in the mixed conifer forests of the Sierra Nevada. Ecological Applications. 32(2):e2514. doi:10.1002/eap.2514
Das AJ, Stephenson NL, Davis KP. 2016. Why do trees die? Characterizing the drivers of background tree mortality. Ecology. 97(10):2616–2627. doi:10.1002/ecy.1497
Davis FW, Synes NW, Fricker GA, McCullough IM, Serra-Diaz JM, Franklin J, Flint AL. 2019. LiDAR-derived topography and forest structure predict fine-scale variation in daily surface temperatures in oak savanna and conifer forest landscapes. Agricultural and Forest Meteorology. 269–270, 192–202. doi:10.1016/j.agrformet.2019.02.015
Davis KT, Peeler J, Fargione J, Haugo RD, Metlen KL, Robles MD, Woolley T. 2024. Tamm review: A meta-analysis of thinning, prescribed fire, and wildfire effects on subsequent wildfire severity in conifer dominated forests of the Western US. Forest Ecology and Management. 561:121885. doi:10.1016/j.foreco.2024.121885
Davis KT, Robles MD, Kemp KB, Higuera PE, Chapman T, Metlen KL, Peeler JL, Rodman KC, Woolley T, Addington RN, et al. 2023. Reduced fire severity offers near-term buffer to climate-driven declines in conifer resilience across the western United States. Proceedings of the National Academy of Sciences USA. 120(11):e2208120120. doi:10.1073/pnas.2208120120
De Frenne P, Rodríguez-Sánchez F, Coomes DA, Baeten L, Verstraeten G, Vellend M, Bernhardt-Römermann M, Brown, CD, Brunet J, Cornelis J, et al. 2013. Microclimate moderates plant responses to macroclimate warming. Proceedings of the National Academy of Sciences. 110(46), 18561–18565. https://doi.org/10.1073/pnas.1311190110
DeRose RJ, Long JN. 2014. Resistance and resilience: a conceptual framework for silviculture. Forest Science. 60: 1205-1212. https://doi.org/10.5849/forsci.13-507
Dobrowski SZ. 2011. A climatic basis for microrefugia: the influence of terrain on climate. Global Change Biology. 17, 1022–1035. doi:10.1111/j.1365-2486.2010.02263.x

Dudney J, Hobbs, RJ, Heilmayr R, Battles JJ, Suding KN. 2018. Navigating novelty and risk in resilience management. Trends in Ecology and Evolution. 33, 863–873. doi:10.1016/j.tree.2018.08.012

ESRI. 2021. Environmental Systems Research Institute. World Imagery. [accessed September 2021]. https://www.arcgis.com/home/item.html?id=c03a526d94704bfb839445e80de95495

Evans JS, Murphy MA. 2021. spatialEco. R package version 1.3-6. https://github.com/jeffreyevans/spatialEco

Falk DA, Heyerdahl EK, Brown PM, Farris C, Fulé PZ, McKenzie D, Swetnam TW, Taylor AH, van Horne ML. 2011. Multi-scale controls of historical forest-fire regimes: new insights from fire-scar networks. Frontiers in Ecology and the Environment. 9(8):446–454. doi:10.1890/100052

Falk DA, van Mantgem PJ, Keeley JE, Gregg RM, Guiterman CH, Tepley AJ, JN Young D, Marshall LA. 2022. Mechanisms of forest resilience. Forest Ecology and Management. 512:120129. doi:10.1016/j.foreco.2022.120129

Falk DA, Watts AC, Thode AE. 2019. Scaling ecological resilience. Frontiers in Ecology and Evolution. doi:10.3389/fevo.2019.00275

Faraway JJ. 2015. Linear Models with R, 2nd ed. Chapman and Hall/CRC Texts in Statistical Science, New York.

Fettig CJ, Klepzig KD, Billings RF, Munson AS, Nebeker TE, Negrón JF, Nowak JT. 2007. The effectiveness of vegetation management practices for prevention and control of bark beetle infestations in coniferous forests of the western and southern United States. Forest Ecology and Management. 238(1), 24–53. doi:10.1016/j.foreco.2006.10.011

Fettig CJ, Mortenson LA, Bulaon BM, Foulk PB. 2019. Tree mortality following drought in the central and southern Sierra Nevada, California, U.S. Forest Ecology and Management. 432:164–178. doi:10.1016/j.foreco.2018.09.006

Fettig CJ, Reid ML, Bentz BJ, Sevanto S, Spittlehouse DL, Wang T. 2013. Changing climates, changing forests: a western North American perspective. Journal of Forestry. 111(3):214–228. doi:10.5849/jof.12-085

Flint LE, Flint AL, Stern MA. 2021. The basin characterization model—A regional water balance software package. Reston, VA: U.S. Geological Survey Techniques and Methods Report No.: 6-H1. [accessed 2022 Dec 8]. http://pubs.er.usgs.gov/publication/tm6H1

Forest Management Task Force. 2021. California's Wildfire and Forest Resilience Action Plan. https://wildfiretaskforce.org/action-plan/

Franklin AB, Anderson DR, Gutiérrez RJ, Burnham KP. 2000. Climate, habitat quality, and fitness in northern spotted wwl populations in Northwestern California. Ecological Monographs. 70(4):539–590. doi:10.1890/0012-9615(2000)070[0539:CHQAFI]2.0.CO;2

FRAP. 2021. California Department of Forestry and Fire Protection's Fire and Resource Assessment Program. [accessed July 2021]. https://frap.fire.ca.gov/mapping/gis-data/

Francis EJ, Pourmohammadi P, Steel ZL, Collins BM, Hurteau MD. 2023. Proportion of forest area burned at high-severity increases with increasing forest cover and connectivity in western US watersheds. Landscape Ecology. 1-18. doi:10.1007/s10980-023-01710-1

Franz ST, Colavito MM, Edgeley CM. 2024. From flexibility to feasibility: identifying the policy conditions that support the management of wildfire for objectives other than full suppression. International Journal of Wildland Fire. 33(8). doi:10.1071/WF24031

Fry DL, Stephens SL, Collins BM, North MP, Franco-Vizcaíno E, Gill SJ. 2014. Contrasting spatial patterns in active-fire and fire-suppressed Mediterranean climate old-growth mixed conifer forests. PLOS ONE. 9(2), e88985. doi:10.1371/journal.pone.0088985

Fulé PZ, Covington WW, Moore MM. 1997. Determining reference conditions for ecosystem management of southwestern ponderosa pine forests. Ecological Applications. 7: 895–908. doi:10.1890/1051-0761(1997)007[0895:DRCFEM]2.0.CO;2
Furniss TJ, Das AJ, van Mantgem PJ, Stephenson NL, Lutz JA. 2022. Crowding, climate, and the case for social distancing among trees. Ecological Applications. 32(2):e2507. doi:10.1002/eap.2507
FVEG. 2015. California Department of Forestry and Fire Protection's Fire and Resource Assessment Program. [accessed July 2021]. https://map.dfg.ca.gov/metadata/ds1327.html
Gannon B, Wei Y, Belval E, Young J, Thompson M, O'Connor C, Calkin D, Dunn C. 2023. A quantitative analysis of fuel break effectiveness drivers in southern California National Forests. Fire. 6(3):104. doi:10.3390/fire6030104
Gatziolis D, Andersen HE. 2008. A guide to LIDAR data acquisition and processing for the forests of the Pacific Northwest. US Department of Agriculture, Forest Service, Pacific Northwest Research Station. PNW-GTR-768. https://www.fs.usda.gov/treesearch/pubs/30652
Germain SJ, Lutz JA. 2024. Stand diversity increases pine resistance and resilience to compound disturbance. Fire Ecology. 20(1):53. doi:10.1186/s42408-024-00283-x
GNN. 2023. Landscape ecology, modeling, mapping & analysis. [accessed September 2023]. https://lemma.forestry.oregonstate.edu/data/structure-maps
Gotelli NJ, Ellison AM. 2018. A Primer of Ecological Statistics, 2nd Edition. Sunderland, MA: Sinauer Associates, Inc. Oxford University Press.
Goulden ML, Bales RC. 2019. California forest die-off linked to multi-year deep soil drying in 2012–2015 drought. Nature Geoscience. 12(8):632–637. doi:10.1038/s41561-019-0388-5
Greenler SM, Dunn CJ, Johnston JD, Reilly MJ, Merschel AG, Hagmann RK, Bailey JD. 2023. Too hot, too cold, or just right: can wildfire restore dry forests of the interior Pacific Northwest? PLOS ONE. 18(2):e0281927. doi:10.1371/journal.pone.0281927
Greenwell BM. 2017. pdp: an R package for constructing partial dependence plots. The R Journal 9:1. https://journal.r-project.org/archive/2017/RJ-2017-016/index.html
Greiner SM, Grimm KE, Waltz AEM. 2020. Managing for resilience? Examining management implications of resilience in southwestern National Forests. Journal of Forestry. 118(4), 433–443. doi:10.1093/jofore/fvaa006
Griffin D, Anchukaitis KJ. 2014. How unusual is the 2012–2014 California drought? Geophysical Research Letters. 41(24):9017–9023. doi:10.1002/2014GL062433
Gunderson LH. 2000. Ecological resilience—in theory and application. Annual Review of Ecology and Systematics. 31(1), 425–439. doi:10.1146/annurev.ecolsys.31.1.425
Hagmann RK, Hessburg PF, Prichard SJ, Povak NA, Brown PM, Fulé PZ, Keane RE, Knapp EE, Lydersen JM, Metlen KL, et al. 2021. Evidence for widespread changes in the structure, composition, and fire regimes of western North American forests. Ecological Applications 31(8): 24-. 31(8):1–34. doi:10.1002/eap.2431
Hankin LE, Anderson CT. 2022. Second-entry burns reduce mid-canopy fuels and create resilient forest structure in Yosemite National Park, California. Forests. 13(9):1512. doi:10.3390/f13091512
Hankin LE, Anderson CT, Dickman GJ, Bevington P, Stephens SL. 2023. How forest management changed the course of the Washburn fire and the fate of Yosemite's giant sequoias (Sequoiadendron giganteum). Fire Ecology. 19(1):40. doi:10.1186/s42408-023-00202-6
Hankin LE, Crumrine SA, Anderson CT. 2024. Impacts of mega drought in fire-prone montane forests and implications for forest management. Forest Ecology and Management. 564:122010. doi:10.1016/j.foreco.2024.122010

Hannah L, Flint L, Syphard AD, Moritz MA, Buckley LB, McCullough IM. 2014. Fine-grain modeling of species' response to climate change: holdouts, stepping-stones, and microrefugia. Trends in Ecology and Evolution. 29, 390–397. doi:10.1016/j.tree.2014.04.006
Harvey BJ, Buonanduci MS, Turner MG. 2023. Spatial interactions among short-interval fires reshape forest landscapes. Global Ecology and Biogeography. 32:586–602. doi:10.1111/geb.13634
Harvey BJ, Donato DC, Turner MG. 2016. Burn me twice, shame on who? Interactions between successive forest fires across a temperate mountain region. Ecology. 97(9), 2272–2282. doi:10.1002/ecy.1439
He HS, DeZonia BE, Mladenoff DJ. 2000. An aggregation index (AI) to quantify spatial patterns of landscapes. Landscape Ecology. 15(7), 591–601. doi:10.1023/A:1008102521322
Hessburg PF, Churchill DJ, Larson AJ, Haugo RD, Miller C, Spies TA, North MP, Povak NA, Belote RT, Singleton PH, et al. 2015. Restoring fire-prone Inland Pacific landscapes: seven core principles. Landscape Ecology. 30(10):1805–1835. doi:10.1007/s10980-015-0218-0
Hessburg PF, Miller CL, Parks SA, Povak NA, Taylor AH, Higuera PE, Prichard SJ, North MP, Collins BM, Hurteau MD, et al. 2019. Climate, environment, and disturbance history Govern resilience of western North American forests. Frontiers in Ecology and Evolution. 7. doi:10.3389/fevo.2019.00239
Hessburg PF, Prichard SJ, Hagmann RK, Povak NA, Lake FK. 2021. Wildfire and climate change adaptation of western North American forests: a case for intentional management. Ecological Applications. 31(8):e02432. doi:10.1002/eap.2432
Hessburg PF, Smith BG, Salter RB, Ottmar RD, Alvarado E. 2000. Recent changes (1930s–1990s) in spatial patterns of interior northwest forests, USA. Forest Ecology and Management. 136(1), 53–83. doi:10.1016/S0378-1127(99)00263-7
Hesselbarth MH, Sciaini M, With KA, Wiegand K, Nowosad J. 2019. landscapemetrics: an open-source R tool to calculate landscape metrics. R package version 1.5.5. Ecography, 42, 1648-1657. doi:doi.org/10.1111/ecog.04617
Hijmans RJ, Bivand R, Pebesma E, Sumner M. 2023. terra: Spatial Data Analysis. R package version 1.6.7. https://rspatial.org/index.html
Hood S, Sala A, Heyerdahl EK, Boutin M. 2015. Low-severity fire increases tree defense against bark beetle attacks. Ecology. 96(7), 1846–1855. doi:10.1890/14-0487.1
Hood SM, Varner JM, Jain TB, Kane JM. 2022. A framework for quantifying forest wildfire hazard and fuel treatment effectiveness from stands to landscapes. Fire Ecology. 18(1):33. doi:10.1186/s42408-022-00157-0
Housman I, Campbel L., Heyer J, Goetz W, Finco M, Pugh N. 2022. US Forest Service Landscape Change Monitoring System Methods. Version 2021.7.
Huffman DW, Roccaforte JP, Springer JD, Crouse JE. 2020. Restoration applications of resource objective wildfires in western US forests: a status of knowledge review. Fire Ecology. 16(1):18. doi:10.1186/s42408-020-00077-x
IPCC. 2023. In: Climate Change 2023: Synthesis Report. Contribution of Working Groups I, II and III to the Sixth Assessment Report of the Intergovernmental Panel on Climate Change [Core Writing Team, H. Lee and J. Romero (eds.)]. IPCC, Geneva, Switzerland, pp. 35-115, doi: 10.59327/IPCC/AR6-9789291691647
Jenness J. 2007. Some thoughts on analyzing topographic habitat characteristics. Jenness Enterprises, Flagstaff, AZ, USA, p 26.
Jeronimo SMA, Kane VR, Churchill DJ, Lutz JA, North MP, Asner GP, Franklin JF. 2019. Forest structure and pattern vary by climate and landform across active-fire landscapes in the

montane Sierra Nevada. Forest Ecology and Management. 437:70–86. doi:10.1016/j.foreco.2019.01.033
Jeronimo SMA, Kane VR, Churchill DJ, McGaughey RJ, Franklin JF. 2018. Applying LiDAR individual tree detection to management of structurally diverse forest landscapes. Journal of Forestry. 116(4):336–346. doi:10.1093/jofore/fvy023
Jeronimo SMA, Lutz JA, Kane VR, Larson AJ, Franklin JF. 2020. Burn weather and three-dimensional fuel structure determine post-fire tree mortality. Landscape Ecology. 35, 859–878. doi:10.1007/s10980-020-00983-0
Johnstone JF, Allen CD, Franklin JF, Frelich LE, Harvey BJ, Higuera PE, Mack MC, Meentemeyer RK, Metz MR, Perry GL, et al. 2016. Changing disturbance regimes, ecological memory, and forest resilience. Frontiers in Ecology and the Environment. 14(7):369–378. doi:10.1002/fee.1311
Kaartinen H, Hyyppä J, Yu X, Vastaranta M, Hyyppä H, Kukko A, Holopainen M, Heipke C, Hirschmugl M, Morsdorf F, et al. 2012. An international comparison of individual tree detection and extraction using airborne laser scanning. Remote Sensing. 4(4):950–974. doi:10.3390/rs4040950
Kalies EL, Yocom Kent LL. 2016. Tamm Review: Are fuel treatments effective at achieving ecological and social objectives? A systematic review. Forest Ecology and Management. 375:84–95. doi:10.1016/j.foreco.2016.05.021
Kane JM, Varner JM, Metz MR, van Mantgem PJ. 2017. Characterizing interactions between fire and other disturbances and their impacts on tree mortality in western U.S. Forests. Forest Ecology and Management. 405:188–199. doi:10.1016/j.foreco.2017.09.037
Kane VR, Bartl-Geller BN, Cova GR, Chamberlain CP, van Wagtendonk L, North MP. 2023. Where are the large trees? A census of Sierra Nevada large trees to determine their frequency and spatial distribution across three large landscapes. Forest Ecology and Management. 546:121351. doi:10.1016/j.foreco.2023.121351
Kane VR, Bartl-Geller BN, North MP, Kane JT, Lydersen JM, Jeronimo SMA, Collins BM, Monika Moskal L. 2019. First-entry wildfires can create opening and tree clump patterns characteristic of resilient forests. Forest Ecology and Management. 454:117659. doi:10.1016/j.foreco.2019.117659
Kane VR, Cansler CA, Povak NA, et al (2015a) Mixed severity fire effects within the Rim fire: Relative importance of local climate, fire weather, topography, and forest structure. Forest Ecol Manag 358:62–79. https://doi.org/10.1016/j.foreco.2015.09.001
Kane VR, Lutz JA, Cansler CA, Povak NA, Churchill DJ, Smith DF, Kane JT, North MP. 2015b. Water balance and topography predict fire and forest structure patterns. Forest Ecology and Management. 338, 1–13. doi:10.1016/j.foreco.2014.10.038
Kane VR, Lutz JA, Roberts SL, Smith DF, McGaughey RJ, Povak NA, Brooks ML. 2013. Landscape-scale effects of fire severity on mixed-conifer and red fir forest structure in Yosemite National Park. Forest Ecology and Management. 287, 17–31. doi:10.1016/j.foreco.2012.08.044
Kane VR, North MP, Lutz JA, Churchill DJ, Roberts SL, Smith DF, McGaughey RJ, Kane JT, Brooks ML. 2014. Assessing fire effects on forest spatial structure using a fusion of Landsat and airborne LiDAR data in Yosemite National Park. Remote Sensing of Environment. 151:89–101. doi:10.1016/j.rse.2013.07.041
Keane RE, Hessburg PF, Landres PB, Swanson FJ. 2009. The use of historical range and variability (HRV) in landscape management. Forest Ecology and Management. 258, 1025–1037. doi:10.1016/j.foreco.2009.05.035

Keeley JE. 2012. Ecology and evolution of pine life histories. Annals of Forest Science. 69(4):445–453. doi:10.1007/s13595-012-0201-8.
Kelly LT, Brotons L, McCarthy MA. 2017. Putting pyrodiversity to work for animal conservation. Conservation Biology. 31(4):952–955
Khatri-Chhetri P, van Wagtendonk L, Hendryx SM, Kane VR. 2024. Enhancing individual tree mortality mapping: the impact of models, data modalities, and classification taxonomy. Remote Sensing of Environment. 300:113914. doi:10.1016/j.rse.2023.113914
Klimaszewski-Patterson A, Dingemans T, Morgan CT, Mensing SA. 2024. Human influence on late Holocene fire history in a mixed-conifer forest, Sierra National Forest, California. Fire Ecology. 20:3. doi:10.1186/s42408-023-00245-9
Knapp EE, Bernal AA, Kane JM, Fettig CJ, North MP. 2021. Variable thinning and prescribed fire influence tree mortality and growth during and after a severe drought. Forest Ecology and Management. 479:118595. doi:10.1016/j.foreco.2020.118595
Knapp EE, Keeley JE. 2006. Heterogeneity in fire severity within early season and late season prescribed burns in a mixed-conifer forest. International Journal of Wildland Fire. 15:37–45. doi:10.1071/WF04068
Knapp EE, Keeley JE, Ballenger EA, Brennan TJ. 2005. Fuel reduction and coarse woody debris dynamics with early season and late season prescribed fire in a Sierra Nevada mixed conifer forest. Forest Ecology Management. 208:383–397. doi:10.1016/j.foreco.2005.01.016
Knapp EE, Lydersen JM, North MP, Collins BM. 2017. Efficacy of variable density thinning and prescribed fire for restoring forest heterogeneity to mixed-conifer forest in the central Sierra Nevada, CA. Forest Ecology and Management. 406, 228–241. doi:10.1016/j.foreco.2017.08.028
Knapp EE, Skinner CN, North MP, Estes BL. 2013. Long-term overstory and understory change following logging and fire exclusion in a Sierra Nevada mixed-conifer forest. Forest Ecology and Management. 310:903–914. doi:10.1016/j.foreco.2013.09.041
Knight CA, Tompkins RE, Wang JA, York R, Goulden ML, Battles JJ. 2022. Accurate tracking of forest activity key to multi-jurisdictional management goals: a case study in California. Journal of Environmental Management. 302, 114083. doi:10.1016/j.jenvman.2021.114083
Kolb TE, Fettig CJ, Ayres MP, Bentz BJ, Hicke JA, Mathiasen R, Stewart JE, Weed AS. 2016. Observed and anticipated impacts of drought on forest insects and diseases in the United States. Forest Ecology and Management. 380:321–334. doi:10.1016/j.foreco.2016.04.051
Koontz MJ, Latimer AM, Mortenson LA, Fettig CJ, North MP. 2021. Cross-scale interaction of host tree size and climatic water deficit governs bark beetle-induced tree mortality. Nature Communications. 12(1), 129. doi:10.1038/s41467-020-20455-y
Koontz MJ, North MP, Werner CM, Fick SE, Latimer AM. 2020. Local forest structure variability increases resilience to wildfire in dry western U.S. coniferous forests. Ecology Letters. 23(3), 483–494. doi:10.1111/ele.13447
Kramer HA, Collins BM, Kelly M, Stephens SL (2014) Quantifying ladder fuels: a new approach using LiDAR. Forests 5:1432–1453. https://doi.org/10.3390/f5061432
Kramer HA, Jones GM, Kane VR, Bartl-Geller B, Kane JT, Whitmore SA, Berigan WJ, Dotters BP, Roberts KN, Sawyer SC, Keane JJ, North MP, GutiÉrrez RJ, Peery MZ. 2021. Elevational gradients strongly mediate habitat selection patterns in a nocturnal predator. Ecosphere. 12, e03500. doi:10.1002/ecs2.3500
Kreider MR, Higuera PE, Parks SA, Rice WL, White N, Larson AJ. 2024. Fire suppression makes wildfires more severe and accentuates impacts of climate change and fuel accumulation. Nature Communications. 15(1):2412. doi:10.1038/s41467-024-46702-0

Krofcheck DJ, Hurteau MD, Scheller RM, Loudermilk EL. 2018. Prioritizing forest fuels treatments based on the probability of high-severity fire restores adaptive capacity in Sierran forests. Global Change Biology. 24:729–737. doi:10.1111/gcb.13913

Kuhn M. 2023. finetune: Additional Functions for Model Tuning. R package version 1.1.0, https://CRAN.R-project.org/package=finetune

Kuhn M, Wickham H. 2020. tidymodels: a collection of packages for modeling and machine learning using tidyverse principles. https://www.tidymodels.org

Lake FK, Wright V, Morgan P, McFadzen M, McWethy D, Stevens-Rumann C. 2017. Returning fire to the land: celebrating Traditional Knowledge and fire. Journal of Forestry. 115(5):343–353. doi:10.5849/jof.2016-043R2

Landres PB, Morgan P, Swanson FJ. 1999. Overview of the use of natural variability concepts in managing ecological systems. Ecological Applications. 9: 1179–88. doi:10.1890/1051-0761(1999)009[1179:OOTUON]2.0.CO;2

Larson AJ, Belote RT, Cansler CA, Parks SA, Dietz MS. 2013. Latent resilience in ponderosa pine forest: effects of resumed frequent fire. Ecological Applications. 23(6), 1243–1249. doi:10.1890/13-0066.1

Larson AJ, Churchill D. 2012. Tree spatial patterns in fire-frequent forests of western North America, including mechanisms of pattern formation and implications for designing fuel reduction and restoration treatments. Forest Ecology and Management. 267:74–92. doi:10.1016/j.foreco.2011.11.038

Larson AJ, Jeronimo SMA, Hessburg PF, Lutz JA, Povak NA, Cansler CA, Kane VR, Churchill DJ. 2022. Tamm Review: Ecological principles to guide post-fire forest landscape management in the Inland Pacific and Northern Rocky Mountain regions. Forest Ecology and Management. 504, 119680. doi:10.1016/j.foreco.2021.119680

LeFevre ME, Churchill DJ, Larson AJ, Jeronimo SMA, Bass J, Franklin JF, Kane VR. 2020. Evaluating restoration treatment effectiveness through a comparison of residual composition, structure, and spatial pattern with historical reference sites. Forest Science. 66(5), 578–588. doi:10.1093/forsci/fxaa014

EPA. 2023. Environmental Protection Agency. Level IV Ecoregions. [accessed March 2023]. https://www.epa.gov/eco-research/ecoregion-download-files-state-region-9#pane-04.

Levine JI, Collins BM, Steel ZL, de Valpine P, Stephens SL. 2022. Higher incidence of high-severity fire in and near industrially managed forests. Frontiers in Ecology and the Environment. 20(7):397–404. doi:10.1002/fee.2499

Liang S, Hurteau MD, Westerling AL. 2017. Response of Sierra Nevada forests to projected climate–wildfire interactions. Global Change Biology. 23(5), 2016–2030. doi:10.1111/gcb.13544

Liaw A, Wiener M. 2002. randomForest: Classification and regression. R package version 4.7-1.1. https://CRAN.R-project.org/doc/Rnews/

Lloret F, Escudero A, Iriondo JM, Martínez-Vilalta J, Valladares F. 2012. Extreme climatic events and vegetation: the role of stabilizing processes. Global Change Biology. 18(3):797–805. doi:10.1111/j.1365-2486.2011.02624.x

Loehman RA, Keane RE, Holsinger LM. 2020. Simulation modeling of complex climate, wildfire, and vegetation dynamics to address wicked problems in land management. Frontiers in Forests and Global Change. 3. doi:10.3389/ffgc.2020.00003

Loehman RA, Keane RE, Holsinger LM, Wu Z. 2017. Interactions of landscape disturbances and climate change dictate ecological pattern and process: spatial modeling of wildfire, insect, and disease dynamics under future climates. Landscape Ecology. 32(7), 1447–1459. doi:10.1007/s10980-016-0414-6

Loudermilk EL, O'Brien JJ, Goodrick SL, Linn RR, Skowronski NS, Hiers JK. 2022. Vegetation's influence on fire behavior goes beyond just being fuel. Fire Ecology. 18(1), 9. doi:10.1186/s42408-022-00132-9

Lutz JA, Larson AJ, Swanson ME, Freund JA. 2012. Ecological importance of large-diameter trees in a temperate mixed-conifer forest. PLOS ONE. 7(5):e36131. doi:10.1371/journal.pone.0036131

Lutz JA, Furniss TJ, Johnson DJ, Davies SJ, Allen D, Alonso A, Anderson-Teixeira KJ, Andrade A, Baltzer J, Becker KML, et al. 2018. Global importance of large-diameter trees. Global Ecology and Biogeography. 27(7):849–864. doi:10.1111/geb.12747

Lutz JA, Struckman S, Furniss TJ, Cansler CA, Germain SJ, Yocom LL, McAvoy DJ, Kolden CA, Smith AMS, Swanson ME, et al. 2020. Large-diameter trees dominate snag and surface biomass following reintroduced fire. Ecological Processes. 9(1):41. doi:10.1186/s13717-020-00243-8

Lydersen JM, North MP. 2012. Topographic variation in active-fire forest structure under current climate conditions. Ecosystems. 15: 1134-1146. doi:10.1007/s10021-012-9573-8

Lydersen JM, Collins BM, Miller JD, Fry DL, Stephens SL. 2016. Relating Fire-Caused Change in Forest Structure to Remotely Sensed Estimates of Fire Severity. Fire Ecology. 12(3):99–116. doi:10.4996/fireecology.1203099

Lydersen JM, North MP, Collins BM. 2014. Severity of an uncharacteristically large wildfire, the Rim Fire, in forests with relatively restored frequent fire regimes. Forest Ecology and Management. 328, 326–334. doi:10.1016/j.foreco.2014.06.005

Lydersen JM, North MP, Knapp EE, Collins BM. 2013. Quantifying spatial patterns of tree groups and gaps in mixed-conifer forests: reference conditions and long-term changes following fire suppression and logging. Forest Ecology and Management. 304:370–382. doi:10.1016/j.foreco.2013.05.023

Maksymiuk S, Alicja G, Przemyslaw B. 2020. DALEXtra: Landscape of R packages for eXplainable Artificial Intelligence. https://arxiv.org/abs/2009.13248

Manley P, Wilson K, Povak N. 2020. Framework for promoting socio-ecological resilience across forested landscapes in the Sierra Nevada. Sierra Nevada Conservancy.

Marlon JR, Bartlein PJ, Gavin DG, Long CJ, Anderson RS, Briles CE, Brown KJ, Colombaroli D, Hallett DJ, Power MJ, et al. 2012. Long-term perspective on wildfires in the western USA. Proceedings of the National Academy of Sciences. 109(9). doi:10.1073/pnas.1112839109

Marra G, Wood SN. 2011. Practical variable selection for generalized additive models. Computational Statistics & Data Analysis. 55(7):2372–2387. doi:10.1016/j.csda.2011.02.004

Marvin NW, Ziegler A. 2017. ranger: A Fast Implementation of Random Forests for High Dimensional Data in C++ and R. Journal of Statistical Software. 77:1-17. doi:10.18637/jss.v077.i01

Massip N. 2020. The 1964 Wilderness Act, from "wilderness idea" to governmental oversight and protection of wilderness. Miranda 20. doi:.4000/miranda.26787

Mast JN, Veblen TT. 1999. Tree spatial patterns and stand development along the pine-grassland ecotone in the Colorado Front Range. Canadian Journal of Forest Research. 29(5):575–584. doi:10.1139/x99-025

May CJ, Zald HSJ, North MP, Gray AN, Hurteau MD. 2023. Repeated burns fail to restore pine regeneration to the natural range of variability in a Sierra Nevada mixed-conifer forest, U.S.A. Restoration Ecology. 31(5):e13863. doi:10.1111/rec.13863

McCarley TR, Kolden CA, Vaillant NM, Hudak AT, Smith AMS, Wing BM, Kellogg BS, Kreitler J. 2017. Multi-temporal LiDAR and Landsat quantification of fire-induced changes to forest structure. Remote Sensing of Environment. 191:419–432. doi:10.1016/j.rse.2016.12.022

McGarigal K, Marks BJ. 1995. FRAGSTATS: spatial pattern analysis program for quantifying landscape structure. US Department of Agriculture, Forest Service, Pacific Southwest Research Station. PNW-GTR-351. https://www.fs.usda.gov/treesearch/pubs/3064

McGaughey RJ. 2020. FUSION/LDV: Software for LIDAR Data Analysis and Visualization: Version 4.00. USDA Forest Service Pacific Northwest Research Station, Seattle, WA. http://forsys.cfr.washington.edu/FUSION/fusion_overview.html

McLauchlan KK, Higuera PE, Miesel J, Rogers BM, Schweitzer J, Shuman JK, Tepley AJ, Varner JM, Veblen TT, Adalsteinsson SA, et al. 2020. Fire as a fundamental ecological process: research advances and frontiers. Journal of Ecology. 108(5):2047–2069. doi:10.1111/1365-2745.13403

Meigs GW, Case MJ, Churchill DJ, Hersey CM, Jeronimo SMA, Smith LAC. 2022. Drought, wildfire and forest transformation: characterizing trailing edge forests in the eastern Cascade Range, Washington, USA. Forestry. 1-15. doi:10.1093/forestry/cpac046

Meyer MD. 2015. Forest fire severity patterns of resource objective wildfires in the southern Sierra Nevada. Journal of Forestry. 113:49–56. doi:10.5849/jof.14-084

Meyer MD, Kelt D, North MP. 2007a. Microhabitat associations of northern flying squirrels in burned and thinned stands of the Sierra Nevada. The American Midland Naturalist. 157: 202-211.

Meyer MD, Long JW, Safford HD. 2021. Postfire restoration framework for national forests in California. US Department of Agriculture, Forest Service, Pacific Southwest Research Station. PSW-GTR-270. 1-204. https://www.fs.usda.gov/research/treesearch/61909

Meyer MD, North MP, Gray AN, Zald HSJ. 2007b. Influence of soil thickness on stand characteristics in a Sierra Nevada mixed-conifer forest. Plant Soil. 294(1), 113-123. doi:10.1007/s11104-007-9235-3

Millar CI, Stephenson NL. 2015. Temperate forest health in an era of emerging megadisturbance. Science. 349(6250):823–826. doi:10.1126/science.aaa9933

Millar CI, Stephenson NL, Stephens SL. 2007. Climate change and forests of the future: managing in the face of uncertainty. Ecological Applications. 17(8):2145–2151. doi:10.1890/06-1715.1

Miller JD, Thode AE. 2007. Quantifying burn severity in a heterogeneous landscape with a relative version of the delta Normalized Burn Ratio (dNBR). Remote Sensing of Environment. 109(1), 66-80. https://doi.org/10.1016/j.rse.2006.12.006

Mitchell B, Fisk H, Clark J, et al (2018) Lidar acquisition specifications for forestry applications. US Forest Service, Geospatial Technology & Applications Centre: Salt Lake City, UT, USA.

Moore MM, Covington WW, Fulé PZ. 1999. Reference conditions and ecological restoration: a southwestern ponderosa pine perspective. Ecological Applications. 9: 1266–77. doi:10.1890/1051-0761(1999)009[1266:RCAERA]2.0.CO;2

Moreira F, Ascoli D, Safford H, Adams MA, Moreno JM, Pereira JMC, Catry FX, Armesto J, Bond W, González ME, et al. 2020. Wildfire management in Mediterranean-type regions: paradigm change needed. Environ Research Letters. 15(1):011001. doi:10.1088/1748-9326/ab541e

Moritz MA, Hessburg PF, Povak NA. 2010. Native fire regimes and landscape resilience. The Landscape Ecology of Fire (pp. 51-86). Dordrecht: Springer Netherlands.

Murphy JS, York R, Rivera Huerta H, Stephens SL. 2021. Characteristics and metrics of resilient forests in the Sierra de San Pedro Martír, Mexico. Forest Ecology and Management. 482:118864. doi:10.1016/j.foreco.2020.118864

Newman EA, Kennedy MC, Falk DA, McKenzie D. 2019. Scaling and complexity in landscape ecology. Front in Ecology and Evolution. 7. doi:10.3389/fevo.2019.00293

Ng J, North MP, Arditti AJ, Cooper MR, Lutz JA. 2020. Topographic variation in tree group and gap structure in Sierra Nevada mixed-conifer forests with active fire regimes. Forest Ecology and Management. 472:118220. doi:10.1016/j.foreco.2020.118220
EPA. 2021. Environmental Protection Agency. NHDPlusV2 National Hydrography Dataset Plus. [accessed July 2021]. https://www.epa.gov/waterdata/nhdplus-national-data
North M. 2012. Managing Sierra Nevada forests. US Department of Agriculture, Forest Service, Pacific Southwest Research Station. PSW-GTR-237. https://www.fs.usda.gov/treesearch/pubs/40254
North MP, Bisbing SM, Hankins DL, Hessburg PF, Hurteau MD, Kobziar LN, Meyer MD, Rhea AE, Stephens SL, Stevens-Rumann CS. 2024. Strategic fire zones are essential to wildfire risk reduction in the Western United States. Fire Ecology. 20(1):50. doi:10.1186/s42408-024-00282-y
North M, Brough A, Long J, Collins B, Bowden P, Yasuda D, Miller J, Sugihara N. 2015. Constraints on mechanized treatment significantly limit mechanical fuels reduction extent in the Sierra Nevada. Journal of Forestry. 113(1):40–48. doi:10.5849/jof.14-058
North M, Chen J, Oakley B, Song B, Rudnicki M, Gray A, Innes J. 2004. Forest stand structure and pattern of old-growth western hemlock/Douglas-fir and mixed-conifer forests. Forest Science. 50(3):299–311. doi:10.1093/forestscience/50.3.299
North M, Collins BM, Safford H, Stephenson NL. 2016. Montane forests. Montane forests. In M. Harold & Z. Erika (Eds.) Ecosystems of California (pp. 553-577). Berkeley, CA: University of California Press.http://www.fs.usda.gov/treesearch/pubs/54829
North MP, Kane JT, Kane VR, Asner P., Berigan W, Churchill DJ, Conway S, Gutiérrez RJ, Jeronimo SMA, Keane J, Koltunov A, Mark T, Moskal LM, Munton T, Peery Z, Ramirez C, Sollmann R, White AM, Whitmore S. 2017. Cover of tall trees best predicts California spotted owl habitat. Forest Ecology and Management. 405, 166-178. doi:10.1016/j.foreco.2017.09.019
North MP, Stephens SL, Collins BM, Agee JK, Aplet G, Franklin JF, Fulé PZ. 2015. Reform forest fire management. Science. 349(6254):1280–1281. doi:10.1126/science.aab2356.
North MP, Stevens JT, Greene DF, et al (2019) Tamm Review: Reforestation for resilience in dry western U.S. forests. Forest Ecology and Management. 432:209–224. doi:10.1016/j.foreco.2018.09.007
North M, Stine P, O'Hara K, Zielinski W, Stephens S. 2009. An ecosystem management strategy for Sierran mixed-conifer forests. US Department of Agriculture, Forest Service, Pacific Southwest Research Station. PSW-GTR-2020. http://www.fs.usda.gov/treesearch/pubs/32916
North MP, Tompkins RE, Bernal AA, Collins BM, Stephens SL, York RA. 2022. Operational resilience in western US frequent-fire forests. Forest Ecology and Management. 507:120004. doi:10.1016/j.foreco.2021.120004
North MP, York RA, Collins BM, Hurteau MD, Jones GM, Knapp EE, Kobziar L, McCann H, Meyer MD, Stephens SL, et al. 2021. Pyrosilviculture needed for landscape resilience of dry western United States forests. Journal of Forestry. 119(5):520–544. doi:10.1093/jofore/fvab026
Northrop H, Axelson JN, Das AJ, Stephenson NL, Vilanova E, Stephens SL, Battles JJ. 2024. Snag dynamics and surface fuel loads in the Sierra Nevada: Predicting the impact of the 2012–2016 drought. Forest Ecology and Management. 551:121521. doi:10.1016/j.foreco.2023.121521
O'Connor CD, Calkin DE, Thompson MP, Calkin DE, Thompson MP. 2017. An empirical machine learning method for predicting potential fire control locations for pre-fire planning

and operational fire management. International Journal of Wildland Fire. 26(7):587–597. doi:10.1071/WF16135
Oksanen J, Simpson G, Blanchet F, Kindt R, Legendre P, Minchin P, O'Hara R, Solymos P, Stevens M, Szoecs E, et al., 2022. vegan: Community Ecology Package. R package version 2.6-4. https://CRAN.R-project.org/package=vegan
Pan Y, Birdsey RA, Phillips OL, Jackson RB. 2013. The structure, distribution, and biomass of the world's forests. Annual Review of Ecology, Evolution, and Systematics. 44:593–622. doi:10.1146/annurev-ecolsys-110512-135914
Parks SA. 2014. Mapping day-of-burning with coarse-resolution satellite fire-detection data. International Journal of Wildland Fire. 23:215–223. doi:10.1071/WF13138
Parks SA, Abatzoglou JT. 2020. Warmer and drier fire seasons contribute to increases in area burned at high severity in Western US forests from 1985 to 2017. Geophysical Research Letters. 47(22):e2020GL089858. doi:10.1029/2020GL089858
Parks SA, Holsinger LM, Blankenship K, Dillon GK, Goeking SA, Swaty R. 2023. Contemporary wildfires are more severe compared to the historical reference period in western US dry conifer forests. Forest Ecology and Management. 544:121232. doi:10.1016/j.foreco.2023.121232
Parks SA, Holsinger LM, Koontz MJ, Collins L, Whitman E, Parisien MA, Loehman RA, Barnes JL, Bourdon JF, Boucher J, et al. 2019. Giving ecological meaning to satellite-derived fire severity metrics across North American forests. Remote Sensing. 11(14), 14. doi:10.3390/rs11141735
Parks SA, Holsinger LM, Miller C, Nelson CR. 2015. Wildland fire as a self-regulating mechanism: the role of previous burns and weather in limiting fire progression. Ecological Applications. 25:1478–1492. doi:10.1890/14-1430.1
Parks SA, Holsinger LM, Panunto MH, Jolly WM, Dobrowski SZ, Dillon GK. 2018. High-severity fire: evaluating its key drivers and mapping its probability across western US forests. Environmental Research Letters. 13(4):044037. doi:10.1088/1748-9326/aab791
Parsons RA, Linn RR, Pimont F, Hoffman C, Sauer J, Winterkamp J, Sieg CH, Jolly WM. 2017. Numerical investigation of aggregated fuel spatial pattern impacts on fire behavior. Land, 6(2), 43. doi:10.3390/land6020043
Pawlikowski NC, Coppoletta M, Knapp E, Taylor AH. 2019. Spatial dynamics of tree group and gap structure in an old-growth ponderosa pine-California black oak forest burned by repeated wildfires. Forest Ecology and Management. 434, 289–302. doi:10.1016/j.foreco.2018.12.016
Peterson G, Allen CR, Holling CS. 1998. Ecological resilience, biodiversity, and scale. Ecosystems 1, 6–18. doi:10.1007/s100219900002
Pierce DW, Kalansky JF, Cayan DR. 2018. California's Fourth Climate Change Assessment. https://www.climateassessment.ca.gov/
Pile LS, Meyer MD, Rojas R, Roe O, Smith MT. 2019. Drought impacts and compounding mortality on forest trees in the southern Sierra Nevada. Forests, 10(3), 237. doi:10.3390/f10030237
Pimont F, Dupuy JL, Caraglio Y, Morvan D. 2009. Effect of vegetation heterogeneity on radiative transfer in forest fires. International Journal of Wildland Fire. 18(5), 536–553. doi:10.1071/WF07115
Povak NA, Kane VR, Collins BM, Lydersen JM, Kane JT. 2020. Multi-scaled drivers of severity patterns vary across land ownerships for the 2013 Rim Fire, California. Landscape Ecology. 35(2):293–318. doi:10.1007/s10980-019-00947-z
Prichard SJ, Hessburg PF, Hagmann RK, Povak NA, Dobrowski SZ, Hurteau MD, Kane VR, Keane RE, Kobziar LN, Kolden CA, et al. 2021. Adapting western North American forests

to climate change and wildfires: 10 common questions. Ecological Applications. 31(8):e02433. doi:10.1002/eap.2433
Prichard SJ, Stevens-Rumann CS, Hessburg PF. 2017. Tamm Review: Shifting global fire regimes: lessons from reburns and research needs. Forest Ecology and Management. 396:217–233. doi:10.1016/j.foreco.2017.03.035
R Core Team. 2023. R version 4.2.2. R: a language and environment for statistical computing. R Foundation for Statistical Computing, Vienna, Austria. www.R-project.org
Reed CC, Hood SM, Cluck DR, Smith SL. 2023. Fuels change quickly after California drought and bark beetle outbreaks with implications for potential fire behavior and emissions. Fire Ecology 19:16. doi:10.1186/s42408-023-00175-6
Restaino C, Young DJN, Estes B, Gross S, Wuenschel A, Meyer M, Safford H. 2019. Forest structure and climate mediate drought-induced tree mortality in forests of the Sierra Nevada, USA. Ecological Applications. 29(4), e01902. doi:10.1002/eap.1902
Reynolds RT, Sánchez Meador AJ, Youtz JA, Nicolet T, Matonis MS, Jackson PL, DeLorenzo DG, Graves AD. 2013. Restoring composition and structure in Southwestern frequent-fire forests: a science-based framework for improving ecosystem resiliency. US Department of Agriculture, Forest Service, Rocky Mountain Research Station. Gen. Tech. Rep. RMRS-GTR-310. http://www.fs.usda.gov/treesearch/pubs/44885
Richardson JJ, Moskal LM. 2011. Strengths and limitations of assessing forest density and spatial configuration with aerial LiDAR. Remote Sensing of Environment. 115(10), 2640–2651. doi:10.1016/j.rse.2011.05.020
Ritter SM, Hoffman CM, Battaglia MA, Stevens-Rumann CS, Mell WE. 2020. Fine-scale fire patterns mediate forest structure in frequent-fire ecosystems. Ecosphere. 11(7):e03177. doi:10.1002/ecs2.3177
Roberts DW, Cooper SV. 1989. Concepts and techniques of vegetation mapping. In Land Classifications Based on Vegetation: Applications for Resource Management. US Department of Agriculture, Forest Service. GTR INT-257. 90-96
Rodman KC, Davis KT, Parks SA, Chapman TB, Coop JD, Iniguez JM, Roccaforte JP, Sánchez Meador AJ, Springer JD, Stevens-Rumann CS, et al. 2023. Refuge-yeah or refuge-nah? Predicting locations of forest resistance and recruitment in a fiery world. Global Change Biology. doi:10.1111/gcb.16939
Safford HD, Paulson AK, Steel ZL, Young DJN, Wayman RB. 2022. The 2020 California fire season: A year like no other, a return to the past or a harbinger of the future? Global Ecology and Biogeography. 31(10):2005–2025. doi:10.1111/geb.13498
Safford HD, Stevens JT. 2017. Natural range of variation for yellow pine and mixed-conifer forests in the Sierra Nevada, southern Cascades, and Modoc and Inyo National Forests, California, USA. Forests. US Department of Agriculture, Forest Service, Pacific Southwest Research Station. Gen. Tech. Rep. PSW-GTR-256. http://www.fs.usda.gov/treesearch/pubs/55393
Safford HD, Stevens JT, Merriam K, Meyer MD, Latimer AM. 2012. Fuel treatment effectiveness in California yellow pine and mixed conifer forests. Forest Ecology and Management. 274:17–28. doi:10.1016/j.foreco.2012.02.013
Schoennagel T, Balch JK, Brenkert-Smith H, Dennison PE, Harvey BJ, Krawchuk MA, Mietkiewicz N, Morgan P, Moritz MA, Rasker R, et al. 2017. Adapt to more wildfire in western North American forests as climate changes. Proceedings of the National Academy of Sciences. 114(18):4582–4590. doi:10.1073/pnas.1617464114
Scholl AE, Taylor AH. 2010. Fire regimes, forest change, and self-organization in an old-growth mixed-conifer forest, Yosemite National Park, USA. Ecological Applications. 20(2):362–380. doi:10.1890/08-2324.1

Schmidt L, Hille MG, Stephens SL. 2006. Restoring northern Sierra Nevada mixed conifer forest composition and structure with prescribed fires of varying intensities. Fire Ecology. 2:20–33. doi:10.4996/fireecology.0202020
Schultz CA, McCaffrey SM, Huber-Stearns HR. 2019. Policy barriers and opportunities for prescribed fire application in the western United States. International Journal of Wildland Fire. 28(11):874–884. doi:10.1071/WF19040
Schulze SS, Fischer EC, Hamideh S, Mahmoud H. 2020. Wildfire impacts on schools and hospitals following the 2018 California Camp Fire. Natural Hazards. 104(1), 901–925. doi:10.1007/s11069-020-04197-0
Schwilk DW, Knapp EE, Ferrenberg SM, Keeley JE, Caprio AC. 2006. Tree mortality from fire and bark beetles following early and late season prescribed fires in a Sierra Nevada mixed-conifer forest. Forest Ecology and Management. 232(1):36–45. doi:10.1016/j.foreco.2006.05.036
Seidl R, Rammer W, Scheller RM, Spies TA. 2012. An individual-based process model to simulate landscape-scale forest ecosystem dynamics. Ecological Modeling. 231, 87–100. doi:10.1016/j.ecolmodel.2012.02.015
Singleton MP, Thode AE, Sánchez Meador AJ, Iniguez JM. 2019. Increasing trends in high-severity fire in the southwestern USA from 1984 to 2015. Forest Ecology and Management. 433, 709–719. doi:10.1016/j.foreco.2018.11.039
Sparks AM, Corrao MV, Smith AMS. 2022. Cross-comparison of individual tree detection methods using low and high pulse density airborne laser scanning data. Remote Sensing. 14(14):3480. doi:10.3390/rs14143480
Steel ZL, Foster D, Coppoletta M, Lydersen JM, Stephens SL, Paudel A, Markwith SH, Merriam K, Collins BM. 2021a. Ecological resilience and vegetation transition in the face of two successive large wildfires. Journal of Ecology. 109(9):3340–3355. doi:10.1111/1365-2745.13764
Steel ZL, Goodwin MJ, Meyer MD, Fricker GA, Zald HSJ, Hurteau MD, North MP. 2021a. Do forest fuel reduction treatments confer resistance to beetle infestation and drought mortality? Ecosphere. 12(1):e03344. doi:10.1002/ecs2.3344
Steel ZL, Jones GM, Collins BM, Green R, Koltunov A, Purcell KL, Sawyer SC, Slaton MR, Stephens SL, Stine P, et al. 2023. Mega-disturbances cause rapid decline of mature conifer forest habitat in California. Ecological Applications. 33(2):e2763. doi:10.1002/eap.2763
Steel ZL, Koontz MJ, Safford HD. 2018. The changing landscape of wildfire: burn pattern trends and implications for California's yellow pine and mixed conifer forests. Landscape Ecology. 33(7):1159–1176. doi:10.1007/s10980-018-0665-5
Steel ZL, Safford HD, Viers JH. 2015. The fire frequency-severity relationship and the legacy of fire suppression in California forests. Ecosphere. 6(1), art8. doi:10.1890/ES14-00224.1
Stephens SL, Battaglia MA, Churchill DJ, Collins BM, Coppoletta M, Hoffman CM, Lydersen JM, North MP, Parsons RA, Ritter SM, et al. 2021. Forest restoration and fuels reduction: convergent or divergent? BioScience. 71(1):85–101. doi:10.1093/biosci/biaa134
Stephens SL, Collins BM, Biber E, Fulé PZ. 2016a. U.S. federal fire and forest policy: emphasizing resilience in dry forests. Ecosphere. 7(11), e01584. doi:doi.org/10.1002/ecs2.1584
Stephens SL, Foster DE, Battles JJ, Bernal AA, Collins BM, Hedges R, Moghaddas JJ, Roughton AT, York RA. 2023. Forest restoration and fuels reduction work: different pathways for achieving success in the Sierra Nevada. Ecological Applications.:e2932. doi:10.1002/eap.2932
Stephens SL, Fry DL, Franco-Vizcaíno E. 2008. Wildfire and spatial patterns in forests in northwestern Mexico: the United States wishes it had similar fire problems. Ecology and Society. 13(2). https://www.jstor.org/stable/26267961

Stephens SL, Lydersen JM, Collins BM, Fry DL, Meyer MD. 2015. Historical and current landscape-scale ponderosa pine and mixed conifer forest structure in the Southern Sierra Nevada. Ecosphere. 6(5), art79. doi:10.1890/ES14-00379.1

Stephens SL, Millar CI, Collins BM. 2010. Operational approaches to managing forests of the future in Mediterranean regions within a context of changing climates. Environmental Research Letters. 5(2), 024003. doi:10.1088/1748-9326/5/2/024003

Stephens SL, Miller JD, Collins BM, North MP, Keane JJ, Roberts SL. 2016b. Wildfire impacts on California spotted owl nesting habitat in the Sierra Nevada. Ecosphere. 7(11):e01478. doi:10.1002/ecs2.1478

Stephenson N. 1998. Actual evapotranspiration and deficit: biologically meaningful correlates of vegetation distribution across spatial scales. Journal of Biogeography. 25(5):855–870. doi:10.1046/j.1365-2699.1998.00233.x

Stephenson NL, Das AJ, Ampersee NJ, Bulaon BM, Yee JL. 2019. Which trees die during drought? The key role of insect host-tree selection. Journal of Ecology. 107(5):2383–2401. doi:10.1111/1365-2745.13176

Stevens JT, Collins BM, Miller JD, North MP, Stephens SL. 2017. Changing spatial patterns of stand-replacing fire in California conifer forests. Forest Ecology and Management. 406:28–36. doi:10.1016/j.foreco.2017.08.051

Stevens JT, Haffey CM, Coop JD, Fornwalt PJ, Yocom L, Allen CD, Bradley A, Burney OT, Carril D, Chambers ME, et al. 2021. Tamm Review: Postfire landscape management in frequent-fire conifer forests of the southwestern United States. Forest Ecology and Management. 502:119678. doi:10.1016/j.foreco.2021.119678

Stevens JT, Kling MM, Schwilk DW, Varner JM, Kane JM. 2020. Biogeography of fire regimes in western U.S. conifer forests: A trait-based approach. Global Ecology and Biogeography. 29(5):944–955. doi:10.1111/geb.13079

Stevens-Rumann CS, Kemp KB, Higuera PE, Harvey BJ, Rother MT, Donato DC, Morgan P, Veblen TT. 2018. Evidence for declining forest resilience to wildfires under climate change. Ecology Letters. 21(2):243–252. doi:10.1111/ele.12889

Stevens-Rumann CS, Prichard SJ, Strand EK, Morgan P. 2016. Prior wildfires influence burn severity of subsequent large fires. Canadian Journal of Forest Research. 46:1375–1385. doi:10.1139/cjfr-2016-0185

Strassburg BBN, Iribarrem A, Beyer HL, Cordeiro CL, Crouzeilles R, Jakovac CC, Braga Junqueira A, Lacerda E, Latawiec AE, Balmford A, et al. 2020. Global priority areas for ecosystem restoration. Nature. 586(7831):724–729. doi:10.1038/s41586-020-2784-9

Sullivan AL. 2017. Inside the inferno: fundamental processes of wildland fire behavior. Current Forestry Reports. 3(2), 132-149. doi:10.1007/s40725-017-0057-0

Su Y, Guo Q, Fry DL, Collins BM, Kelly M, Flanagan JP, Battles JJ. 2016. A vegetation mapping strategy for conifer forests by combining airborne LiDAR data and aerial imagery. Canadian Journal of Remote Sensing. 42(1):1–15. doi:10.1080/07038992.2016.1131114

Swingland IR, Bettelheim EC, Grace J, Prance GT, Saunders LS, Malhi Y, Meir P, Brown S. 2002. Forests, carbon and global climate. Philosophical Transactions of the Royal Society of London Series A: Mathematical, Physical and Engineering Sciences. 360(1797):1567–1591. doi:10.1098/rsta.2002.1020

Tague C, Dugger AL. 2010. Ecohydrology and climate change in the mountains of the western USA – a review of research and opportunities. Geography Compass. 4(11):1648–1663. doi:10.1111/j.1749-8198.2010.00400.x

Taylor AH, Harris LB, Skinner CN. 2022. Severity patterns of the 2021 Dixie Fire exemplify the need to increase low-severity fire treatments in California's forests. Environmental Research Letters. 17(7):071002. doi:10.1088/1748-9326/ac7735

Taylor AH, Trouet V, Skinner CN, Stephens S. 2016. Socioecological transitions trigger fire regime shifts and modulate fire–climate interactions in the Sierra Nevada, USA, 1600–2015 CE. Proceedings of the National Academy of Sciences. 113(48):13684–13689. doi:10.1073/pnas.1609775113

Terryn L, Calders K, Disney M, Origo N, Malhi Y, Newnham G, Raumonen P, Å kerblom M, Verbeeck H. 2020. Tree species classification using structural features derived from terrestrial laser scanning. ISPRS Journal of Photogrammetry and Remote Sensing. 168:170–181. doi:10.1016/j.isprsjprs.2020.08.009

Thompson MP, O'Connor CD, Gannon BM, Caggiano MD, Dunn CJ, Schultz CA, Calkin DE, Pietruszka B, Greiner SM, Stratton R, et al. 2022. Potential operational delineations: new horizons for proactive, risk-informed strategic land and fire management. Fire Ecology. (1):17. doi:10.1186/s42408-022-00139-2

Tingley MW, Ruiz-Gutiérrez V, Wilkerson RL, Howell CA, Siegel RB. 2016. Pyrodiversity promotes avian diversity over the decade following forest fire. Proceedings of the Royal Society B: Biological Sciences. 283(1840):20161703. doi:10.1098/rspb.2016.1703

Turco M, Abatzoglou JT, Herrera S, Zhuang Y, Jerez S, Lucas DD, AghaKouchak A, Cvijanovic I. 2023. Anthropogenic climate change impacts exacerbate summer forest fires in California. Proceedings of the National Academy of Sciences. 120(25):e2213815120. doi:10.1073/pnas.2213815120

Turner MG, Donato DC, Romme WH. 2013. Consequences of spatial heterogeneity for ecosystem services in changing forest landscapes: priorities for future research. Landscape Ecology. 28(6):1081–1097. doi:10.1007/s10980-012-9741-4

Turner MG, Romme WH. 1994. Landscape dynamics in crown fire ecosystems. Landscape Ecology. 9(1), 59-77. doi:10.1007/BF00135079

Underwood EC, Viers JH, Quinn JF, North M. 2010. Using topography to meet wildlife and fuels treatment objectives in fire-suppressed landscapes. Environmental Management. 46:809–819. doi:10.1007/s00267-010-9556-5

USDA. 2021. US Department of Agriculture Forest Service Activity Tracking System. [accessed July 2021]. https://data.fs.usda.gov/geodata/edw/datasets.php

USGS. 2022. 1/3rd Arc Second. United States Geological Survey National Map Viewer. [accessed August 2022]. https://www.usgs.gov/tools/national-map-viewer

Vaillant NM, Reinhardt ED. 2017. An evaluation of the forest service hazardous fuels treatment program—are we treating enough to promote resiliency or reduce hazard? Journal of Forestry. 115(4):300–308. doi:10.5849/jof.16-067

van Mantgem PJ, Stephenson NL, Knapp E, Battles J, Keeley JE. 2011. Long-term effects of prescribed fire on mixed conifer forest structure in the Sierra Nevada, California. Forest Ecology and Management. 261, 989–994. doi:10.1016/j.foreco.2010.12.013

van Wagtendonk JW, Sugihara NG, Stephens SL, Thode AE, Shaffer KE, Fites-Kaufman J. 2018. Fire in California's ecosystems. Second edition. Oakland, California: University of California Press.

van Wagtendonk WJ. 2007. The history and evolution of wildland fire use. Fire Ecology. 3(2), 3–17. doi:10.4996/fireecology.0302003

Vilanova E, Mortenson LA, Cox LE, Bulaon BM, Lydersen JM, Fettig CJ, Battles JJ, Axelson JN. 2023. Characterizing ground and surface fuels across Sierra Nevada forests shortly after the

2012–2016 drought. Forest Ecology and Management. 537:120945. doi:10.1016/j.foreco.2023.120945
Vincent L. Soille P. 1991. Watersheds in digital spaces: an efficient algorithm based on immersion simulations. IEEE Transactions on Pattern Analysis & Machine Intelligence. 13(6), 583–598. doi:10.1109/34.87344
Walker B, Holling CS, Carpenter SR, Kinzig A. 2004. Resilience, adaptability and yransformability in social–ecological systems. Ecology and Society. 9(2). https://www.jstor.org/stable/26267673
Watson JEM, Evans T, Venter O, Williams B, Tulloch A, Stewart C, Thompson I, Ray JC, Murray K, Salazar A, et al. 2018. The exceptional value of intact forest ecosystems. Nature Ecology & Evolution. 2(4):599–610. doi:10.1038/s41559-018-0490-x
Weatherspoon CP, Skinner CN. 1995. An assessment of factors associated with damage to tree crowns from the 1987 wildfires in Northern California Forest Science. 41(3), 430-451.
Weed AS, Ayres MP, Hicke JA. 2013. Consequences of climate change for biotic disturbances in North American forests. Ecological Monographs. 83(4):441–470. doi:10.1890/13-0160.1
Weiskopf SR, Rubenstein MA, Crozier LG, Gaichas S, Griffis R, Halofsky JE, Hyde KJW, Morelli TL, Morisette JT, Muñoz RC, et al. 2020. Climate change effects on biodiversity, ecosystems, ecosystem services, and natural resource management in the United States. Science of The Total Environment. 733:137782. doi:10.1016/j.scitotenv.2020.137782
Westerling AL. 2016. Increasing western US forest wildfire activity: sensitivity to changes in the timing of spring. Philosophical Transactions of the Royal Society B: Biological Sciences. 371(1696):20150178. doi:10.1098/rstb.2015.0178
Westman WE. 1978. Measuring the inertia and resilience of ecosystems. BioScience 28: 705-710. doi:10.2307/1307321
White AM, Zipkin EF, Manley PN, Schlesinger MD. 2013. Conservation of avian diversity in the Sierra Nevada: moving beyond a single-species management focus. PLOS ONE 8, e63088. doi:10.1371/journal.pone.0063088
White AM, Zipkin EF, Manley PN, Schlesinger MD. 2013. Simulating avian species and foraging group responses to fuel reduction treatments in coniferous forests. Forest Ecology and Management. 304:261–274. doi:10.1016/j.foreco.2013.04.039
Wiggins HL, Nelson CR, Larson AJ, Safford HD. 2019. Using LiDAR to develop high-resolution reference models of forest structure and spatial pattern. Forest Ecology and Management. 434:318–330. doi:10.1016/j.foreco.2018.12.012
Williams AP, Abatzoglou JT, Gershunov A, Guzman-Morales J, Bishop DA, Balch JK, Lettenmaier DP. 2019. Observed impacts of anthropogenic climate change on wildfire in California. Earths Future. 7(8), 892–910. doi:10.1029/2019EF001210
Williams JN, Safford HD, Enstice N, Steel ZL, Paulson AK. 2023. High-severity burned area and proportion exceed historic conditions in Sierra Nevada, California, and adjacent ranges. Ecosphere. 14(1), e4397. doi:10.1002/ecs2.4397
Willson KG, Margolis EQ, Hurteau MD. 2024. Trees have similar growth responses to first-entry fires and reburns following long-term fire exclusion. Forest Ecology and Management. 571:122226. doi:10.1016/j.foreco.2024.122226
Wood SN. 2017. Generalized additive models: an introduction with R. chapman and hall/CRC.
Wood CM, Jones GM. 2019. Framing management of social-ecological systems in terms of the cost of failure: the Sierra Nevada, USA as a case study. Environmental Research Letters. 14(10), 105004. doi:10.1088/1748-9326/ab4033

Wright MN, Ziegler A. 2017. ranger: A Fast Implementation of Random Forests for High Dimensional Data in C++ and R. Journal of Statistical Software. 77(1), 1-17. doi:10.18637/jss.v077.i01

Young DJN, Meyer M, Estes B, Gross S, Wuenschel A, Restaino C, Safford HD. 2020. Forest recovery following extreme drought in California, USA: natural patterns and effects of pre-drought management. Ecological Applications. 30(1):e02002. doi:10.1002/eap.2002

Young DJN, Stevens JT, Earles JM, Moore J, Ellis A, Jirka AL, Latimer AM. 2017. Long-term climate and competition explain forest mortality patterns under extreme drought. Ecology Letters. 20(1):78–86. doi:10.1111/ele.12711

Zald HSJ, Gray AN, North M, Kern RA. 2008. Initial tree regeneration responses to fire and thinning treatments in a Sierra Nevada mixed-conifer forest, USA. Forest Ecology and Management. 256(1), 168–179. doi:10.1016/j.foreco.2008.04.022

Zald HSJ, May CJ, Gray AN, North MP, Hurteau MD. 2024. Thinning and prescribed burning increase shade-tolerant conifer regeneration in a fire excluded mixed-conifer forest. Forest Ecology and Management. 551:121531. doi:10.1016/j.foreco.2023.121531

Ziegler JP, Hoffman C, Battaglia M, Mell W. 2017. Spatially explicit measurements of forest structure and fire behavior following restoration treatments in dry forests. Forest Ecology and Management. 386, 1–12. doi:10.1016/j.foreco.2016.12.002

Ziegler JP, Hoffman CM, Collins BM, Knapp EE, Mell WR. 2021. Pyric tree spatial patterning interactions in historical and contemporary mixed conifer forests, California, USA. Ecology and Evolution. 11(2), 820–834. doi:10.1002/ece3.7084